NATIONAL AND KAPODISTRIAN UNIVERSITY OF ATHENS

SCHOOL OF SCIENCES

DEPARTMENT OF CHEMISTRY

DEPARTMENTAL POSTGRADUATE PROGRAMME IN "CHEMISTRY"
SPECIALIZATION "ANALYTICAL CHEMISTRY"

MASTER THESIS

Identification of transformation products of Citalopram during biodegradation batch experiments with activated sludge by Liquid Chromatography–Quadrupole-Time-of-Flight Mass Spectrometry (LC–QTOF-MS)

VASILIKI BERETSOU
CHEMIST

ATHENS

OCTOBER 2015

MASTER THESIS

Identification of transformation products of Citalopram during biodegradation batch experiments with activated sludge by Liquid Chromatography–Quadrupole-Time-of-Flight Mass Spectrometry (LC–QTOF-MS)

VASILIKI BERETSOU

Registration Number: 11302

SUPERVISING PROFESSOR:

Nikolaos Thomaidis, Assosiate Professor, NKUA

THREE-MEMBER EXAMINATION COMITTEE:

Antonios Calokerinos, Professor, NKUA

Michalis Koupparis, Professor, NKUA

Nikolaos Thomaidis, Assosiate Professor, NKUA

DEFENDING DATE 14/10/2015

ΕΡΕΥΝΗΤΙΚΗ ΕΡΓΑΣΙΑ ΔΙΠΛΩΜΑΤΟΣ ΕΙΔΙΚΕΥΣΗΣ

Ταυτοποίηση προϊόντων μετασχηματισμού του Citalopram κατά τη διάρκεια πειραμάτων βιοαποικοδόμησης σε συστήματα ενεργού ιλύος με LC–QTOF-MS

ΒΑΣΙΛΙΚΗ ΜΠΕΡΕΤΣΟΥ

Α.Μ.: 11302

ΕΠΙΒΛΕΠΩΝ ΚΑΘΗΓΗΤΗΣ:

Νικόλαος Θωμαΐδης**,** Αναπληρωτής Καθηγητής ΕΚΠΑ

ΤΡΙΜΕΛΗΣ ΕΞΕΤΑΣΤΙΚΗ ΕΠΙΤΡΟΠΗ:

Αντώνιος Καλοκαιρινός, Καθηγητής ΕΚΠΑ

Μιχαήλ Κουππάρης, Καθηγητής ΕΚΠΑ

Νικόλαος Θωμαΐδης**,** Αναπληρωτής Καθηγητής ΕΚΠΑ

ΗΜΕΡΟΜΗΝΙΑ ΕΞΕΤΑΣΗΣ 14/10/2015

ABSTRACT

Biodegradation is considered to be the key process for the elimination of the majority of pharmaceuticals in the environment. During wastewater treatment or once they are disposed in the aquatic environment, pharmaceuticals may be transformed to new, structurally-related compounds which are called transformation products (TPs). Since most of these compounds are unknown, their identification is essential not only to provide a comprehensive risk assessment on micropollutants in the environment, but also to design improved removal technologies for (pseudo)persistent trace contaminants.

In this study, batch reactors seeded with activated sludge from the wastewater-treatment plant (WWTP) of Athens were set up to assess biotic, abiotic and sorption losses of the drug, citalopram (CTR). TPs were identified by reversed-phase liquid chromatography quadrupole-time-of-flight mass spectrometry (RPLC-QTOF-MS). Hydrophilic interaction liquid chromatography (HILIC) was also used as a complementary, orthogonal, technique for the identified TPs. A workflow for suspect and non-target screening was developed. Structure elucidation of TPs was based on accurate mass and isotopic pattern measurements and interpretation of MS/MS spectra by the observed fragmentation pattern and literature data.

In total, fourteen TPs were identified and a transformation pathway based on the identified compounds was presented. Four out of them were confirmed by corresponding reference standards (N-desmethylCTR, CTR amide, CTR carboxylic acid and 3-oxo-CTR). A probable structure based on diagnostic evidence was proposed for the additional nine TPs, whereas only an unequivocal molecular formula was assigned to the last one. After the identification, the presence of the fourteen TPs was investigated in wastewater samples.

SUBJECT AREA: Environmental Analytical Chemistry

KEYWORDS: Citalopram, biodegradation, transformation products, RPLC-QTOF-MS, HILIC

ΠΕΡΙΛΗΨΗ

Η βιοαποικοδόμηση θεωρείται η διαδικασία-κλειδί για την απομάκρυνση των περισσότερων φαρμακευτικών ουσιών στο περιβάλλον. Κατά την επεξεργασία των λυμάτων ή αφού απορριφθούν στο υδάτινο περιβάλλον, τα φάρμακα ενδέχεται να μετατραπούν σε καινούριες, δομικά-συγγενείς ενώσεις που ονομάζονται προϊόντα μετασχηματισμού/μετατροπής. Εφόσον οι περισσότερες από αυτές τις ενώσεις είναι άγνωστες, η ταυτοποίηση τους είναι απαραίτητη όχι μόνο γιατί μπορούν να παρέχουν μια ολοκληρωμένη εκτίμηση κινδύνου, αλλά επιπλέον για να σχεδιαστούν βελτιωμένες τεχνολογίες απομάκρυνσης των «ψευδο» επίμονων υπολειμμάτων των ρύπων.

Σε αυτή την εργασία, χρησιμοποιήθηκαν βιοαντιδραστήρες με ενεργό ιλύ από το Κέντρο Επεξεργασίας Λυμμάτων της Αθήνας για να εξεταστούν οι βιοτικές και αβιοτικές διεργασίες καθώς και οι διεργασίες προσρόφησης του φαρμάκου Citalopram (CTR). Τα προϊόντα μετασχηματισμού ταυτοποιήθηκαν με υγρή χρωματογραφία αντίστροφης φάσης συζευγμένη με υβριδικό αναλυτή φασματομετρίας μάζας (reversed-phase liquid chromatography quadrupole-time-of-flight mass spectrometry, RPLC-QTOF-MS). Η υγρή χρωματογραφία υδρόφοβων αλληλεπιδράσεων (hydrophilic interaction liquid chromatography, HILIC) χρησιμοποιήθηκε επίσης ως μια συμπληρωματική, ορθογώνια τεχνική για τα ταυτοποιημένα προϊόντα μετατροπής. Για το σκοπό αυτό, αναπτύχθηκε ένα διάγραμμα ροής για υπόπτη και μη-στοχευμένη σάρωση. Η εξαγωγή της δομής των προϊόντων μετασχηματισμού βασίστηκε σε μετρήσεις ακριβούς μάζας και ισοτοπικού προφίλ αλλά και στην κατανόηση των φασμάτων μάζας μέσω του παρατηρούμενου προφίλ θραυσματοποίησης και της βιβλιογραφίας.

Συνολικά, ταυτοποιήθηκαν δεκατέσσερα προϊόντα μετασχηματισμού και παρουσιάστηκε ένα μονοπάτι μετασχηματισμού των ταυτοποιημένων ενώσεων. Η δομή των τεσσάρων από αυτές επιβεβαιώθηκε με το αντίστοιχο πρότυπο αναφοράς (N-desmethylCTR, CTR amide, CTR carboxylic acid and 3-oxo-CTR). Για τις υπόλοιπες εννέα ενώσεις προτάθηκε μια πιθανή δομή βασισμένη σε διαγνωστικά στοιχεία ενώ για μία αποδόθηκε μόνο μοριακός τύπος. Μετά την ταυτοποίηση, διερευνήθηκε η παρουσία των δεκατεσσάρων προϊόντων μετασχηματισμού σε πραγματικά δείγματα λυμάτων.

ΘΕΜΑΤΙΚΗ ΠΕΡΙΟΧΗ: Περιβαλλοντική Αναλυτική Χημεία

ΛΕΞΕΙΣ ΚΛΕΙΔΙΑ: Citalopram, βιοαποικοδόμηση,
προϊόντα μετασχηματισμού/μετατροπής, RPLC-QTOF-MS,
HILIC

CONTENTS

INDEX OF FIGURES

INDEX OF TABLES

PREFACE

This master thesis was conceived and performed at the Laboratory of Analytical Chemistry (Department of Chemistry, University of Athens, Greece) under the supervision of the Associate Professor, Nikolaos Thomaidis.

First of all, I would like to thank my supervisor, Dr. Nikolaos Thomaidis, for giving me the opportunity to become a member of his research group as well as for the cooperation regarding this master thesis, the valuable professional and personal advice. I would also like to thank the other two members of the examination committee, Professor Antonios Calokerinos and Professor Michalis Koupparis, for their insightful comments and remarks.

Furthermore, I am really thankful to Dr. Kathrin Fenner (Department of Environmental Chemistry, Eawag, Switzerland) for her contribution in the experimental setup and her substantive advice within the framework of the collaboration between our Laboratory and Eawag Institute.

A special thanks to all of my colleagues and friends in the Laboratory of Analytical Chemistry, for providing a great work environment and an enjoyable atmosphere in the lab and, in particular to Katerina Psoma, Anna Bletsou, Maristina Nika, Dimitris Damalas and Pablo Gago-Ferrero, for their constant guidance, assistance and cooperation.

Last but not least, I would like to express my deep gratitude to Christos, my brother, my parents and my friends for their enormous support of my decision to continue my studies for a master's degree and their encouragement throughout these two years and my life in general.

CHAPTER 1
Pharmaceuticals:
environmental contaminants of emerging concern

1.1 Introduction

Over the last few decades, the development of new and more sensitive analytical techniques has evidenced the presence of a large number of potentially dangerous compounds in the environment, globally known as emerging contaminants (ECs) or emerging pollutants (EPs) [1]. This term defines any chemical that was not included in national or international monitoring programs and not previously included in existing environmental-quality regulations, but is continually being introduced into the environment due to anthropogenic activities. These chemicals need not necessarily be new, although their environmental fate and (eco)toxicological study have not yet been evaluated, but potential threats to aquatic and terrestrial ecosystems and human health cannot be neglected [2].

ECs encompass a diverse group of compounds belonging to different chemical classes and with different applications, including pharmaceuticals, illicit drugs and drugs of abuse, personal-care products (PCPs), steroids, hormones and other endocrine disrupting compounds (EDCs), surfactants, perfluorinated compounds (PFCs), brominated and organophosphate flame retardants and plasticizers, industrial additives and agents, and gasoline additives, nanomaterials, disinfection by-products, polar pesticides, siloxanes as well as their transformation products (TPs) [3, 4].

Among ECs, pharmaceuticals belong to a group of increasing interest due to their pharmacological activity and rising consumption deriving from their use in human and veterinary medicine. Moreover, due to their ubiquitous presence in the environment arising from continual input into the aquatic compartment, they are considered as ‘‘pseudo’’ persistent pollutants [5, 6].

1.2 Occurrence, fate and transformation of pharmaceuticals in the environment

The continuous discharge of pharmaceuticals in effluents from production facilities, hospitals, and private households, improper disposal of unused drugs, and the direct discharge of veterinary medicines all lead to contamination of environmental waters, and wastewater-treatment plants (WWTPs) are considered to be a major source [7].

Before entering the environment, pharmaceuticals can be metabolized in living organisms to Phase I or Phase II metabolites. Phase I reactions are usually hydrolytic cleavages, along with oxidations (e.g., aliphatic hydroxylation, ring oxidation, epoxidation, N-oxidation), reductions (e.g., ketone reduction) alkylations (e.g., O-methylation) and dealkylations (e.g., O-demethylation). The second type refers to conjugation reactions with the most prominent to be glucuronidation, comprising transfer of glucuronic acid to phenols, aliphatic, hydroxyl, carboxyl, thiol, amine and hydroxyloamino groups [8].

Human pharmaceuticals enter aquatic systems after ingestion and subsequent excretion in the form of the non-metabolized drug or as polar metabolites through WWTPs. Once released into the environment, pharmaceuticals are subject to processes (e.g., biodegradation, and chemical and photochemical degradation) that contribute to their elimination [3, 8].

Biodegradation is considered to be the dominant process for eliminating the majority of xenobiotics, including pharmaceuticals. The biodegradation by metabolic pathways refers to the use of a chemical as a source of energy, carbon, nitrogen or other nutrients. Co-metabolism is the fortuitous breakdown of a contaminant by an enzyme or cofactor that is produced during microbial metabolism of another compound. Moreover, microbial communities are important degraders of organic matter and xenobiotics [9].

On the other hand, photodegradation represents an important degradation process in the environment whenever the rate of microbial conversion is low or negligible and it can be either direct or indirect. In the former, a compound is directly excited by absorbing energy from solar radiation, while indirect photolysis involves naturally occurring molecules such as nitrates which

generate strong reactive species e.g. singlet oxygen ($^1O_2$), hydroxyl radicals ($HO^{\cdot}$) or alkyl peroxyl radicals ($^{\cdot}OOR$) under solar radiation [10, 11].

Depending on the compartment in which pharmaceuticals are present in the environment (e.g., groundwater, surface water and sediment) or in the WWTPs and drinking-water facilities, different transformations can take place, sometimes producing TPs that, to some extent, differ in their environmental behaviour and ecotoxicological profile [3]. However, there remain significant gaps in our knowledge regarding such degradation mechanisms, the identity of TPs, and their origin, fate and effects on humans and other living organisms [12]. Thus, humans and aquatic ecosystems are exposed to a highly variable and unknown cocktail of chemicals. Although individual chemicals are typically present at low concentrations, they can interact with each other resulting in additive or potentially even synergistic mixture effects. The formation and environmental presence of TPs adds further complexity to chemical risk assessment because TPs may contribute significantly to the risk posed by the parent compound (a) if they are formed with a high yield; (b) if they are more persistent than the parent compounds; or (c) if they have a high toxicity [13].

Low comparability between human and environmental transformation processes, suggests that TPs are not structurally identical to human metabolites, underlining the need for further research in this field [14]. Therefore, since WWTPs provide the first, and possibly the only, opportunity for removal of pharmaceutical residues, it is of paramount importance to characterize their fate during WWT and investigate the potential formation of TPs [15].

1.3 Conventional wastewater treatment

Domestic wastewaters are generally subjected to a treatment sequence including preliminary treatments (screening, grit removal, and oil and grease removal), a primary gravity settling, secondary biological treatment (by activated sludge, fixed-film reactors, lagoon systems, and/or sedimentation) [16] and finally tertiary steps, including advanced oxidation processes (AOPs)

for disinfection and removal of micropollutants (chlorination, chloramination, ozonation, and advanced oxidation by UV/H_2O_2 treatment) [13].

For the secondary step, activated sludge treatment is that most extensively employed all over the world for processing both urban wastewaters from small and large communities and industrial effluents. This type of treatment was developed by two English researchers, Ardern and Lockett, in 1914, and since then, it has been implemented on a global scale. Activated sludge treatment consists mainly of flocculating microorganisms held in suspension and contact with wastewater in a mixed aerated tank. The so-called CAS (conventional activated sludge) system consists of a biological reactor (where activated sludge may develop and grow) followed by a secondary clarifier: The simplest diagram of this process is that shown in **Figure 1**, and subsequent configurations developed over the years are shown in **Figure 2**.

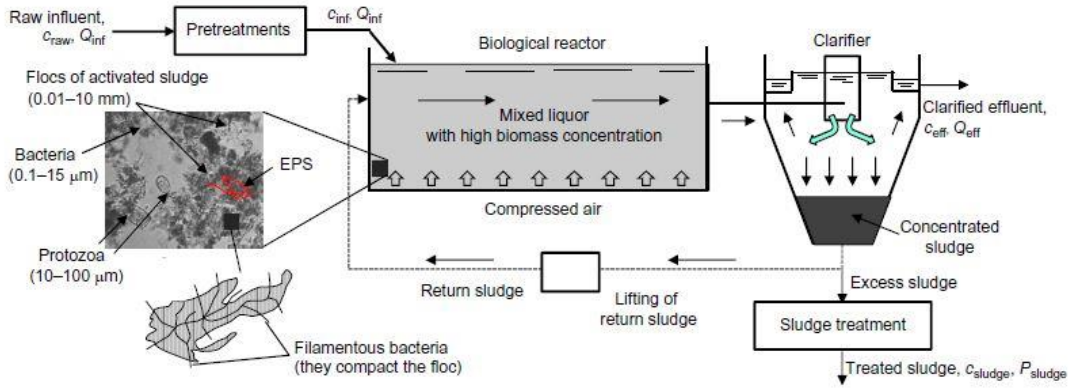

Figure 1: Simplified layout of the activated sludge process [16].

The biological reactor may consist of one **(Figures 1 and 2A)** or more compartments **(Figure 2B-F)**. Multiple compartments provide different operational conditions, namely, aerobic, anoxic, and anaerobic, and enable C, N, and P removal. Adsorption, absorption, flocculation, oxidation–reduction reactions, and sedimentation are the main physical and biochemical processes occurring within the activated sludge process. Biochemical reactions (anabolic, catabolic, and co-metabolic reactions) take place within the biological reactor and bring about the degradation of the organic compounds in the influent wastewater. The reactions are performed by the microorganisms suspended in the liquid, namely, bacteria, protozoa, rotifers, and fungi, which together form the biomass, which develops and grows as these reactions take place.

Organic compounds subject to biodegradation include not only lipids, proteins, and carbohydrates, which occur at the order of mg L^{-1}, but also micropollutants (i.e., pharmaceuticals and PCPs), occurring at concentrations of ng L^{-1} or mg L^{-1}.

After enough time for the appropriate biochemical reactions, the mixed liquor is transferred to a settling tank (secondary clarifier) to allow gravity separation of the suspended solids (in form of floc particles) from the treated effluent. Some of the settled solids are returned to the biological reactor in order to maintain the desired biomass concentration inside (about 3-4 g L^{-1}). The remainder is considered waste (the so-called excess sludge) and is subjected to thickening, by removing a portion of the liquid fraction in order to increase its solid content. Through the processes of stabilization, dewatering, drying, and combustion, both the water and organic fractions are considerably reduced, and the processed solids (treated or digested sludge) are suitable for reuse or disposal.

Over the years, different configurations of the activated sludge process were developed to promote nitrification, denitrification, and phosphorus removal. More recent evolutions in CAS include membrane bioreactors (MBRs) **(Figure 2E)** and moving bed biological reactors (MBBRs) **(Figure 2F)**. MBRs were developed with the primary aim not only to improve effluent quality but also to upgrade existing WWTPs by replacing the previous secondary settler with a membrane compartment able to better separate the solid from the liquid phase. MMBRs were designed to enhance biological processes by promoting the growth of both suspended and attached biomass, thereby increasing the biomass concentration in the aeration tank. One of the main advantages of the two new configurations is that they are able to treat a higher pollutant load in the “original” reactor volume. Although these two treatments are becoming more diffuse, CAS is still by far the most common in operation (and most studied) [16].

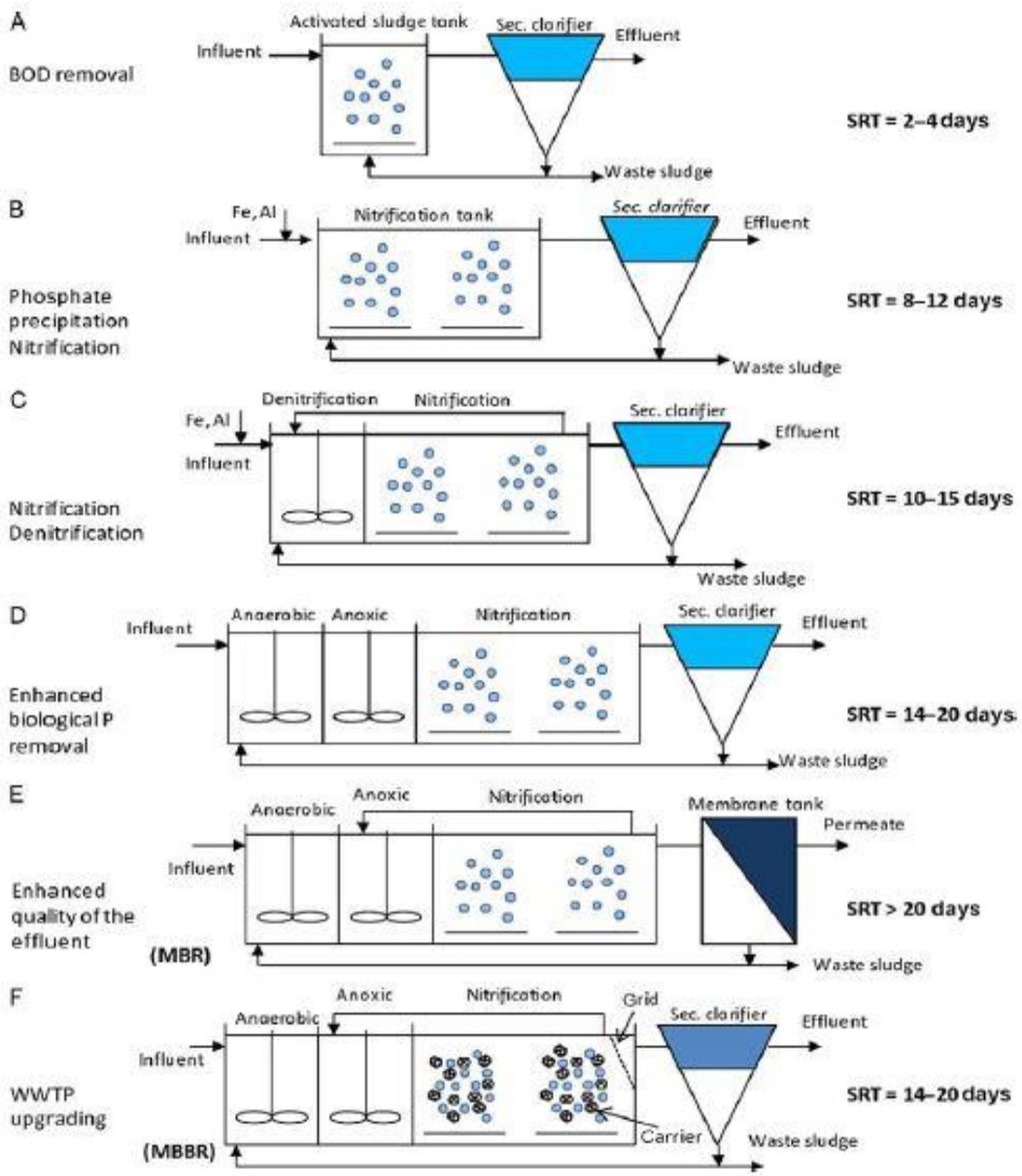

Figure 2: Historical development of activated sludge process: (A) BOD removal; (B) phosphate precipitation and nitrification; (C) nitrification and denitrification; (D) enhanced biological P removal; (E) MBR; (F) MBBR [16].

1.4 Removal of pharmaceuticals by conventional WWTPs

Whatever the configuration of the biological reactor, the main removal mechanisms invariably include biological degradation, sorption (adsorption and absorption), flocculation, and sedimentation. Chemical transformations may also occur within the biological reactor and generally consist of deconjugation of certain micropollutants, which is conversion back to their original compounds, but this is not a particularly influential occurrence.

The different removal mechanisms may be favored by different operational conditions (namely, redox, pH, temperature, sludge retention time (SRT), hydraulic retention time (HRT) and recirculation ratio) and different reactor configurations, as discussed in subchapter 1.3.

CAS processes are not able to efficiently remove all the different kinds of pharmaceuticals. In particular, pharmaceuticals are designed to be biologically stable, and their sorption tendency depends on the types and properties of both the suspended solids (sludge) and the compound molecule [16]. Moreover, both biotransformation and sorption could potentially lead to pH-dependent removal of micropollutants with ionizable functional groups. However, it was proved that elimination is more likely an effect of pH-dependent biotransformation but rather of pH-dependent sorption [17].

SRT seems to be the most critical influential operating parameter for activated sludge design, as it affects the treatment process performance, aeration tank volume, sludge production, and oxygen requirements. It has been proven that longer SRT improves the removal of most of the pharmaceuticals during sewage treatments. Indeed, WWTPs with high SRTs allow the enrichment of slowly growing bacteria and consequently the establishment of a more diverse biocoenosis with broader physiological capabilities (e.g., nitrification or the capacity for certain pathways) than WWTPs with low SRTs [16, 18].

CHAPTER 2

Approaches for the identification of transformation products – Literature review of Citalopram in the environment

2.1 Introduction

Identification of TPs of ECs is a challenging task and represents a higher grade of difficulty than the analysis of target pollutants, consequence of the unknown nature of these compounds, and the absence of analytical standards to confirm their identity. Analytical difficulties are mainly derived from the vast number of intermediates generated, their different physicochemical properties, the complexity and diversity of the matrices and the broad range of concentrations at which these TPs are produced. Additional problems arise from the formation of isomer compounds, difficult to differentiate, and the occurrence of co-elution of compounds with related structures. Therefore, identification of TPs requires the use of advanced analytical instrumentation and appropriate analysis strategies providing high selectivity, high sensitivity and, in particular, high capability for structure elucidation [19, 20].

2.1.1 Identification of TPs – Laboratory approaches

There are two different approaches to identify TPs: laboratory studies and environmental screening. These approaches are complementary and mutually enriching rather than the opposite of each other. Commonly, laboratory studies offer the advantage of simulating transformation processes under well-defined conditions with appropriate control that facilitates the establishment of differences in the samples that contain the compounds. However, the detection of at least a few of these compounds in the environment is the next necessary step [21].

The laboratory studies are focused on the different types of degradation mechanisms, biotic and abiotic, at relatively high concentrations of the parent ECs [19]. Samples can be provided directly from a WWTP [22] or a pilot-scale WWTP [23] or from natural waters [24].

Biodegradability is mostly evaluated in activated sludge batch experiments under different operational conditions: aerobic, anaerobic and anoxic [17, 22, 25-30]. For aerobic treatment, the sludge is aerated and mixed to suspend the microorganisms whereas N_2 stripping is applied at the beginning of the batch and after each sampling to establish anaerobic and anoxic conditions [27]. Temperature, pH, dissolved oxygen content, and content of total suspended solids are monitored and adjusted to allow direct comparison with environmental conditions [17, 27, 28, 30]. Spiked and non-spiked samples for background subtraction caused by natural sludge matrices, run in parallel, as do spiked autoclaved diluted sludge or autoclaved groundwater and ultrapure water in order to correct for abiotic transformation processes [25, 26]. Samples are collected periodically so that the reaction kinetics of the analytes can be determined sufficiently [28, 29].

Better simulation of the conditions in the full-scale system can be achieved by using alternative water treatment technologies such as MBRs. These MBRs are commonly fed with synthetic wastewater and inoculated with activated sludge from the full-scale WWTP [31].

Batch experiments have also been performed to establish biodegradation in soil [32] and water/river sediments [33, 34], where microorganisms play an important role in degradation.

The simulation of abiotic degradation occurs concurrently with engineered processes, such as oxidation reactions with chlorine, chlorine dioxide, or ozone and transformations by ultraviolet light [21]. There have also been a number of studies with laboratory-scale reactors reported in literature [11, 35-38]. Biotic and abiotic degradations occur together to transform ECs during the biological wastewater treatment [21].

When preliminary studies in batch experiments are completed, verification of the results should then be carried out using real environmental samples [19]. Those studies that correlate the identified TPs from batch experiments with detection in real matrices demonstrated that at least some of them are present in wastewaters and surface waters [22, 25, 27, 28, 35-37], pointing out the interest in small-scale simulation to increase knowledge of TPs [21].

To this end, there is a need for developing sensitive and selective analytical methods including the TPs expected to be present at low concentrations in the environment. Extraction procedures able to isolate and preconcentrate the analytes are extremely important, and conventional solid-phase extraction (SPE) is commonly used in the case of water. These procedures which sometimes also used in laboratory studies are not sophisticated, but are generic and robust since the physicochemical properties of the TPs are sometimes unknown [21]. To achieve sufficient enrichment for this broad range of compounds, Kern et al. used simultaneously four different SPE sorbents in one manually filled cartridge (weak anion, weak cation-exchange material, and nonpolar and hydrophilic-lipophilic interaction sorbents) [24]. Environmental screening studies of TPs are scarcer and some of them have focused on effluent wastewaters [39-41], while others have been performed in surface and natural waters [24, 42] or water sediments [43].

2.1.2 Identification of TPs – Analytical approaches

Chromatographic techniques coupled to MS have been far the most commonly applied analytical tools in TPs identification, especially with the introduction of the modern high-resolution mass spectrometric systems (HR-MS), such as time-of-flight (TOF), Fourier transform-ion cyclotron resonance (FT-ICR), Orbitrap, or new hybrid approaches [20]. Three major approaches for post-measurement processing were introduced by Krauss et al.; target analysis, suspect screening, and non-target screening **(Figure 3)**. Besides the classical quantitative target analysis approach (using reference standards), a qualitative suspect screening (exact mass as a priori information) approach or non-target screening (no previous information of the chemical available) can be pursued with HR-MS for the identification of TPs [44].

2.1.2.1 Chromatographic separation

A prerequisite for proper identification of TPs is the adequate separation of sample components. The parent compound and the TPs normally have part of the molecule in common, and the mass spectra have ions in common;

therefore, the separation is important [21]. Because of the *a priori* unknown nature of the TPs generated, it is not possible to optimize the chromatographic separation conditions. Liquid chromatography (LC) is commonly performed in reversed-phase (RP) mode using C18 columns. A linear mobile phase gradient covering a large variety of polarities is the preferred choice for TPs separation.

An interesting approach that can be useful in the identification of more polar TPs is hydrophilic interaction chromatography (HILIC). HILIC is a relatively recently introduced mode of liquid-phase separations that allows the separation of highly polar compounds by using a gradient of increasing aqueous content to elute analytes from a hydrophilic stationary phase. HILIC is becoming an attractive alternative or complementary approach to RP chromatography, due to the ability to separate hydrophilic compounds, which are poorly retained on RP columns [20]. On the other hand, HILIC coupled with electrospray ionization (ESI) potentially enables a higher sensitivity because the higher percentage of organic solvent in the HILIC mode contributes to more efficient desolvation during ESI [45].

2.1.2.2 Target analysis

In target analysis, as shown in **Figure 3**, TPs are already known and standards are available, so that they can be included within a defined MS method and be monitored in routine analysis. LC in combination with triple-quadrupole mass spectrometric detection (LC-QqQ MS/MS) dominates in target analysis. The QqQ analyzer permits application of MS/MS modes [e.g., production scan, precursor-ion scan, neutral-loss scan and selected reaction monitoring (SRM), which is the most predominant]. The SRM mode provides several advantages and interesting characteristics for target analysis, such as increased selectivity, reduced interferences and high sensitivity, which allows robust quantification. However, it focuses on a predefined list of compounds to be tested for, because the transitions must be preselected [19].

HR-MS for target analysis offers promising solutions to the limitations of SRM analysis. Virtually all compounds present in a sample can be determined simultaneously with HR-MS instruments operating in full scan mode, making it

unnecessary to pre-select compounds and associated SRM transitions [44]. Thus, information acquired is not analyte-specific, but general information contained in the full accurate-mass spectrum. The advantage of this post-target approach is the ability to detect and identify other compounds of interest without performing additional analyses (i.e., retrospective analysis) [39].Target compounds included in an accurate-mass database are screened in the sample based on retention time (t_R), isotopic pattern and MS/MS fragments [46]. Additionally, hybrid instruments offer the possibility of data-dependent MS/MS acquisition, where MS/MS analysis is triggered if a compound from a target-ion list is detected in the full scan [44, 47]. Their high mass resolving power allows enhancing the identification of isobaric compounds, thus providing reliable identification of target analytes in complex matrices or in presence of co-eluting compounds [48].

2.1.2.3 Suspect screening

In contrast to target analysis, the suspect screening approach **(Figure 3)** does not rely on reference standards for confirmation. These reference standards are currently not available for a large number of potential ECs, in particular TPs. However, compound-specific information for suspected molecules, such as molecular formula and structure, can be predicted and efficiently used in the identification and confirmation process of TPs [44].

Several commercially available or freely accessible programs are currently applied to predict microbial transformation pathways of xenobiotics and the structures of likely TPs. These tools include META, CATABOL, or the University of Minnesota Pathway Prediction System (UM-PPS, now exclusively provided from EAWAG as EAWAG-Biocatalysis/Biodegradation Database Pathway Prediction System, EAWAG-BBD PPS) and contain sets of transformation rules that predict likely microbial transformations based on compound substructure recognition. Transformation rules in the latter two systems are based on data contained in EAWAG-BBD, which is manually maintained collection of literature-reported, microbially mediated metabolic pathways and enzyme-catalyzed reactions [23]. As EAWAG-BBD PPS is freely

accessible and all rules applied are clearly assigned, it is the most common prediction tool in suspect screening.

Other *in silico* prediction tools for the prediction step in environmental analysis such as Meteor and PathPred are available. Meteor is based on mammalian biotransformation reactions of common functional groups, providing in parallel relevant literature references while PathPred is a multi-step reaction prediction server for biodegradation pathways of xenobiotic compounds and biosynthesis pathways of secondary metabolites.

Prediction of TPs is followed by the HR-MS analysis; the exact mass for each of the predicted TPs is extracted from the chromatogram and checked by comparing it with control samples. An intensity-threshold value is applied to cut off unclear spectra. The plausibility of the chromatographic t_R, isotopic pattern, and ionization efficiency are used as further filters to narrow down the number of candidate peaks. Furthermore, using MS/MS or MS^n, structures of suspected TPs are suggested based on the observed fragmentation pattern and diagnostic fragment ions.

Another data-processing method based on peak detection, time-trend filtration and structure assignment can be used for the identification of key TPs in terms of persistence over the time of the experiment. Peak peaking and processing of the chromatograms can be carried out by open-source software (e.g., MZmine, enviMass). After blank subtraction, a meaningful time trend is acquired and the remaining candidate peaks are compared with a list from EAWAG-BBD PPS or literature for tentative identification [19].

2.1.2.4 Non-target screening

Non-target screening involves masses that are detected in the samples, but where no *a priori* information on the underlying compound is available beforehand. Full identification of the non-target mass is often difficult, with no guarantee of a successful outcome. High accuracy, high resolution data from full-scan and MS/MS modes are strongly required to improve the chances of a unique molecular formula assignment to detected masses [40, 44].

Open-source and commercial software option for non-target screening, such as MZmine, XCMS, enviMass, Bruker Metabolite Tools and Profile Analysis, Waters MassLynx and MetaboLynx, Thermo Scientific MetWorks and SIEVE, and Agilent MassHunter providing rapid, accurate and efficient data mining are necessary for post-acquisition data-processing.

As described in **Figure 3**, the first step is peak peaking which is important to exclude irrelevant peaks by comparison of the sample with control or blank samples. The removal of noise peaks, mass recalibration and componentization of isotopes and adducts is usually carried out automatically as the next step. Even after filtering, strict criteria and thresholds, the number of peaks which correspond to non-targets can exceed 1000. Thus, prioritization of the most intense peaks is a common strategy [19].

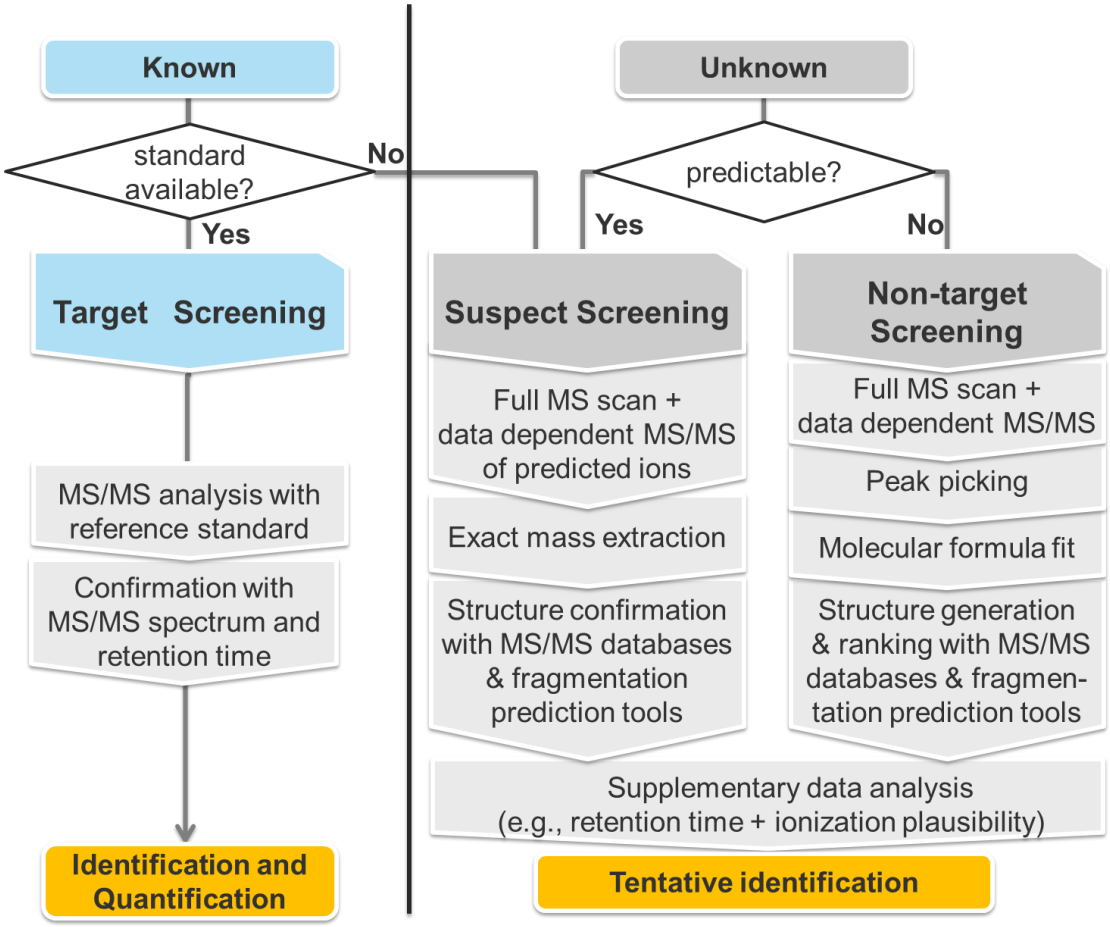

Figure 3: Flow chart of screening procedure of TPs. 'Known' TPs have been confirmed or confidently identified before, other TPs are considered 'Unknown' [19].

2.1.2.5 Structure elucidation and identification confidence levels in HR-MS

High mass accuracy together with high isotopic abundance accuracy is essential to obtain a possible molecular formula generated by the software incorporated in the HR-MS instruments. According to the instrument specifications, the acceptable deviation from the theoretical m/z values of parent ions is usually set up at 5 ppm, which guarantees the correct assignment of their molecular formula. Lightly higher errors (generally below 10 ppm) are occasionally accepted when they correspond to characteristic fragment ions. However, the accurate assignation of the elemental composition of a TP is essential but not sufficient for a reliable structure proposal. Characterization of TPs requires the application of sophisticated tools capable of providing complementary information to complete the assignment of structures [20].

Exploration of databases, such as ChemSpider, PubChem, DAIOS database or NIST, may lead to candidate structures. Thereby, information on the parent compound (e.g., molecular formula, substructures) can help to restrict the search of databases and possible structures are likely to be proposed for the compound. Additionally, the observation of the presence or the absence of common characteristic ions in the fragmentation pattern of both the parent compound and the TPs, evidencing the stability or reactivity of certain parts of the molecule, can be helpful.

For ranking the candidate structures, information from MS/MS spectra has to be explored by comparing the experimental fragmentation spectra with *in silico* mass spectral fragmentation tools (e.g., MetFrag, MetFusion, Mass Frontier, MOLGEN-MS, ACD/MS Fragmenter) or with mass spectra in libraries (e.g., MassBank, MetLin) [19]. However, the use of mass spectral libraries for the confirmation of compounds is still limited for LC/HR-MS data, as the libraries are small and the comparability of spectra is limited among different instruments [21]. Moreover, overall candidate ranking obtained by Mass Frontier and MOLGEN-MS outmatches the one from MetFrag as the former use fragmentation rules, while MetFusion, the newest development, combines MetFrag with spectral database searching [19].

A level system **(Figure 4)** to ease the communication of identification confidence of TPs was proposed by Schymanski et al. [49]. Target, suspect, and non-target compounds start by definition at Levels 1 (confirmed structure), 3 (tentative candidate(s)), and 5 (exact mass of interest), respectively. If sufficient MS (exact mass, isotope, adduct), MS/MS (i.e., fragmentation), and experimental information (e.g. retention behaviour, presence of related substances) is available, suspect and non-target components can gain in confidence through to Level 2 (library match and/or diagnostic fragments) and even Level 1 after purchase of the corresponding standard for identification. Compounds with a confirmed identity then can become target compounds in future investigations [50].

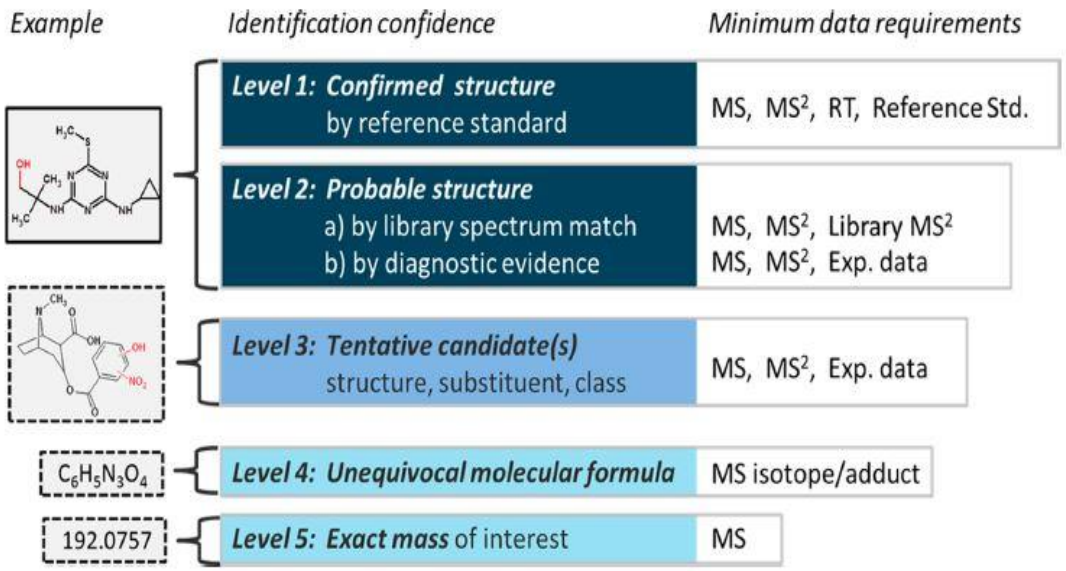

Figure 4: Proposed identification confidence levels in HR-MS analysis [49].

2.2 Profiling Citalopram in the environment

Nowadays, as a consequence of the higher prevalence of psychiatric disorders and the increasing awareness of mental health issues, the number of prescriptions for psychiatric pharmaceuticals, particularly antidepressants, promptly rose. Representative of these is citalopram (CTR), which has demonstrated incomplete removal by conventional wastewater treatment making WWTP a major source to the environment and leading to environmental exposure at low levels, but in a continuous way [51, 52].

2.2.1 Mechanism of action, metabolism and excretion of CTR

The most widespread class of second-generation antidepressant drugs comprises selective serotonin re-uptake inhibitors (SSRIs), which are becoming the drugs of first choice for the treatment of depression [12]. SSRIs have been widely marketed since the mid-1980s and are primarily prescribed to patients diagnosed with clinical depression and these are also being used to treat obsessive-compulsive disorder, panic disorder, social phobia, and attention-deficit disorder [53]. The members of this class include fluoxetine, CTR, paroxetine, sertraline and fluvoxamine. CTR is typically marketed under the trade name Cipramil which is a racemic mixture of (R)-CTR and (S)-CTR enantiomers with different potencies, but since (S)-CTR is more potent it is also marketed as the single (S)-enantiomer formulation, esCTR (Cipralex) [12].

SSRIs act by regulating the levels of neurotransmitter serotonin, which is involved in hormonal and neuronal mechanisms, and in important functions such as food intake and sexual behaviour. While a transporter enzyme directs serotonin from the synaptic space back to the presynapse, SSRIs inhibit this enzyme, thus increasing the serotonin level at the postsynaptic receptor sites [12].

SSRIs, following oral ingestion, undergo hepatic metabolism in order to form more hydrophilic excretable compounds. The first-phase metabolic reactions of CTR include N-demethylation to N-desmethylCTR, further demethylation at the secondary amine to N-didesmethylCTR, N-oxidation to CTR-N-oxide, and deamination to a CTR propionic acid derivative. N-desmethyCTR and N-didesmethylCTR retain their pharmacological activity, but they are, less potent than the parent compound. During second-phase metabolism, these compounds are conjugated, mostly by glucuronide or sulfate and, afterwards eliminated by urine or feces. The excretion of the unchanged compound ranges between 12% and 20% [12, 54, 55].

CTR is a lipophilic, basic drug (pKa 9.05), designed to produce a specific pharmacological response, and, in order to reach the specific site of action within the organism, presenting a certain chemical stability. This stability may be later manifested in their insufficient removal during wastewater treatment,

sometimes resulting in minor structural alterations (i.e., TPs) instead of complete mineralization [12].

2.2.2 Analytical methodologies for the determination of CTR and its metabolites in environmental matrices

Trace-level concentrations of SSRIs present in complex environmental samples require robust analytical methods with great sensitivity and selectivity Gas chromatography (GC) and capillary electrophoresis (CE) with MS detection have been reported, nonetheless, until now, liquid chromatography with tandem mass spectrometry detection (LC-MS/MS) has been the preferred technique for the determination of SSRIs in wastewater, surface, and drinking water Hence, the fundamental step of this type of analysis is considered to be sample preparation since the use of an appropriate cleanup technique is still required in order to handle the complexity of these samples and improve selectivity [12, 56].

The analytical methods, reported below, are multi-residue methods for the determination of pharmaceuticals or SSRIs and their metabolites (including CTR, N-desmethylCTR and N-didesmethylCTR) in environmental matrices.

2.2.2.1 Sample preparation

When dealing with aqueous environmental matrices, sample preparation usually involves SPE. Its purpose is to preconcentrate the analytes and to avoid interferences by cleaning up the sample [12]. Several SPE sorbents, including strong cation-exchange [54], strong cation mixed-mode [57, 58] and hydrophilic-lipophilic reversed-phase cartridges [53, 59-63] have been tested in order to achieve sufficient extraction of the compounds, with the latter to be the most preferred.

To reduce matrix interferences, Vasskog et al. developed a sample preparation procedure for the extraction of five SSRIs, including CTR, with an additional clean-up step using liquid-liquid extraction (LLE) after SPE [64].

An alternative to SPE is solid-phase micro-extraction (SPME), which offers a significant reduction in extraction time, lower extraction volumes and

automation of the procedure. SPME is normally used in combination with GC to improve analyte volatility. Lamas et al. introduced an in-situ acetylation step prior to SPME for the determination of four SSRIs, including CTR [65].

In another study of Vasskog et al., a relatively new extraction technique, called hollow-fiber liquid-phase micro-extraction (HF-LPME), was utilized in the extraction of five SSRIs and four metabolites, among them CTR, N-desmethylCTR and N-didesmethylCTR, from seawater, WWTP influents and effluents. Compared to traditional SPE, the advantages of this sample preparation are the high pre-concentration factor, a single-step procedure, clean extracts, shorter extraction time, lower costs and reduced consumption of organic solvents. However, because of the low-partition coefficients of the analytes, the recoveries in HF-LPME are lower than normally expected with SPE [66].

2.2.2.2 Instrumental analysis

LC-MS/MS is now considered the method of choice for determining residues of pharmaceuticals, including SSRIs, in environmental samples. Most studies employ mass detectors, which allow MS^2. QqQ analyzer, equipped with an ESI source operating in positive mode is the most widely used in order to achieve sufficient selectivity and sensitivity for the analysis of SSRIs residues [54, 57-59, 63, 64, 66-68]. Moreover, a triple quadrupole-linear ion trap mass spectrometer (QTrap), which provides more scanning modes than conventional QqQ has been reported in several studies [53, 60-62, 69-72]. In particular, multiple-scan MS^n and enhanced product-ion scans are important for further confirmation of analyte identity, particularly structure elucidation of TPs [12].

One aspect that has to be considered in environmental analysis is the chirality of SSRIs. In particular, CTR has a chiral center and thus can have different interactions with enzymes and biological receptors since biotic processes can be enantioselective in contrast to abiotic [73]. MacLeod et al. developed an LC-MS/MS method, using a vancomycin-based enantioselective column, in

order to measure enantiomer fractions and concentrations of CTR and fluoxetine in wastewater samples [69].

An alternative to HPLC is CE which has several advantages compared to HPLC, such as higher separation efficiency, smaller sample volume required, speed of analysis, and lower costs due to lower solvent consumption. Coupling to MS, typically after ESI, offers the possibility of structural information and easy separation of co-eluting peaks using mass information as a second dimension. A CE system interfaced to a TOF-MS analyzer was used to determine seven antidepressants in a series of sewage plant effluent samples in a study performed by Himmelsbach et al [74].

GC coupled to MS (GC-MS) has been also applied in SSRIs analysis by Lamas et al. directly after the SPME, which was discussed in the subchapter 2.2.2.1 [65].

2.2.3 Occurrence of CTR and its metabolites in environmental matrices

A literature review on worldwide monitoring programs clearly reveals the presence of CTR and its primary metabolite N-desmethylCTR in different aquatic environments. As shown in **Tables 1** and **2**, the presence of these residues was found in a wide range of water samples, including wastewater, surface and river water, groundwater, and drinking water, within concentrations of up to several ng L^{-1}. However, studies on the occurrence of the discussed analytes in sludge are limited. Moreover, only one study performed by Vaskoog et al. detected N-didesmethylCTR in WWTP samples with concentrations ranging between 5.6 and 20.0 ng L^{-1} in influents and between 0.9 and 10.0 ng L^{-1} in effluents [66].

Table 1: Occurrence of CTR (expressed as a concentration range or mean concentration) in various environmental samples from different countries.

Country	Sample type	Concentration reported	Reference
Austria	WWTP effluent	44-322 ng L^{-1}	[74]
Canada	WWTP influent	307 ng L^{-1}	[69]
	WWTP effluent	207 ng L^{-1}	
	WWTP influent	52.2-52.7 ng L^{-1}	[54]
	WWTP effluent	46.8-57.8 ng L^{-1}	
	River water	3.4-11.5 ng L^{-1}	
	WWTP influent	136-223 ng L^{-1}	[70]
	River water	4-206 ng L^{-1}	
	WWTP influent	144-326 ng L^{-1}	[57]
	WWTP effluent	86-223 ng L^{-1}	
	Sludge	95-1381 ng g^{-1}	
	Raw sewage	207 ng L^{-1}	[75]
	WWTP effluent	148 ng L^{-1}	
	Biosolid	172 ng g^{-1}	
China	Hospital influent	67-261 ng L^{-1}	[76]
	Hospital effluent	19-162 ng L^{-1}	
	WWTP influent	0.4-4 ng L^{-1}	
	WWTP effluent	2-5 ng L^{-1}	
Czech Republic	WWTP influent	27-180 ng L^{-1}	[77]
	WWTP effluent	30-120 ng L^{-1}	
Germany	WWTP influent	160-180 ng L^{-1}	[71]
	WWTP effluent	120-180 ng L^{-1}	
	Surface water	<0.3-96 ng L^{-1}	
Greece	WWTP influent	109.7-540.6 ng L^{-1}	[58]
	WWTP effluent	19.9-766.2 ng L^{-1}	
India	WWTP effluent	430 µg L^{-1}	[78]
	Surface water	2000-8000 ng L^{-1}	
	River water	40-7600 ng L^{-1}	
	Drinking water	76-1400 ng L^{-1}	

Country	Sample type	Concentration reported	Reference
Korea	Sludge	1.02-63.4 ng g^{-1}	[59]
Norway	WWTP influent	13.0-612 ng L^{-1}	[64]
	WWTP effluent	9.2-382 ng L^{-1}	
	WWTP influent	62.9-303.6 ng L^{-1}	[66]
	WWTP effluent	21.9-238.4 ng L^{-1}	
Poland	River water	4.3-17 ng L^{-1}	[60]
	Tap water	<1.3-1.5 ng L^{-1}	
Portugal	WWTP influent	99.20-213.60 ng L^{-1}	[61]
	WWTP effluent	82.80-95.60 ng L^{-1}	
Slovakia	WWTP influent	86 ng L^{-1}	[79]
	WWTP effluent	84 ng L^{-1}	
	Sludge water	38 ng L^{-1}	
Spain	WWTP effluent	340 ng L^{-1}	[65]
	River water	3-120 ng L^{-1}	[67]
	WWTP influent	163-319 ng L^{-1}	[72]
	WWTP effluent	21-288 ng L^{-1}	
	River water	5-11 ng L^{-1}	
	Seawater	4 ng L^{-1}	
USA	Surface water	40-90 ng L^{-1}	[53]
	Surface water	<0.5-219 ng L^{-1}	[62]
	Water sediment	0.36-14.95 ng g^{-1}	
	Surface water	85 ng L^{-1}	[80]
	WWTP effluent	160 ng L^{-1}	[68]
	WWTP influent	35.1-170 ng L^{-1}	[63]
	WWTP effluent	104-414 ng L^{-1}	
	Sludge	131-429 ng g^{-1}	

Table 2: Occurrence of N-desmethylCTR (expressed as a concentration range or mean concentration) in environmental samples from different countries.

Country	Sample type	Concentration reported	Reference
Canada	WWTP influent	104-133 ng L^{-1}	[70]
	River water	8-110 ng L^{-1}	
Germany	WWTP influent	73-100 ng L^{-1}	[71]
	WWTP effluent	58-97 ng L^{-1}	
	Surface water	<1-78 ng L^{-1}	
Korea	Sludge	27.7-131 ng g^{-1}	[59]
Norway	WWTP influent	118-425.7 ng L^{-1}	[66]
	WWTP effluent	36.3-300.5 ng L^{-1}	
USA	Surface water	74 ng L^{-1}	[80]
	WWTP effluent	80 ng L^{-1}	[68]
	WWTP influent	55.3-120 ng L^{-1}	[63]
	WWTP effluent	35.9-310 ng L^{-1}	
	Sludge	36.8-434 ng g^{-1}	

2.2.4 Removal of CTR under various treatment conditions, fate and transformation

In contrast with studies on the occurrence of CTR, fewer publications deal with the fate, the behaviour and the transformation of SSRIs in the environment or during wastewater treatment.

In 2005, Kwon and Armbrust examined primarily the photolytic and hydrolytic stability of CTR which was found to be hydrolytically stable at pH 5, 7 and 9 and photolytically stable at pH 5 and 7. Photodegradation at pH 9 was faster in synthetic humic water, resulting to the formation of two TPs. LC-MS/MS was used to tentatively identify the structures of the major, N-desmethylCTR and the minor photoproduct, CTR-N-oxide [81].

Vasskog et al. investigated the depletion of five SSRIs, including CTR and four known SSRIs' metabolites, including N-desmethylCTR and N-didesmethylCTR during sewage sludge aerobic composting. The reduction rate of CTR was the

lowest (0.88) among the compounds. In addition, N-didesmethylCTR was not found in any compost sample while N-desmethylCTR showed a significant increase in concentration during the 21-day composting period [82].

The fate of pharmaceuticals and PCPs in lab-scale bioreactors working under nitrifying (aerobic) and denitrifying (anoxic) conditions was studied by Suarez et al. CTR was moderately biotransformed under both conditions with elimination rate of 60% and 44%, respectively. Additionally, increase of SRT (>50 days) and temperature ranging between 16 and 26 °C were found to have a slight positive effect on its removal [83]. The better removal of CTR under aerobic conditions is in agreement with a latter work by Suarez et al. Their investigations confirmed that operating at different redox conditions could result in an increased microbial diversity and a broader enzyme spectrum inside the biological reactor influencing the biotransformation metabolic route of pharmaceutical compounds and in particular of CTR. Moreover, the effect of an increase in the internal recirculation ratio from 3 to 4 (from the aerobic to the anoxic compartment of the pilot reactor) increased its removal efficiency from 25% to 50% [18]. Similar elimination efficiency of CTR (67%) to the respective one obtained under the enriched nitrifying conditions of the first study by Suarez et al., was achieved also in the *"ELiminación Autótrofa de Nitrógeno"* (ELAN) pilot-plant process, where nitritation/anammox activity takes place simultaneously in a single reactor, performed by Alvarino et al. Biodegradation was considered to be the most important removal mechanism of CTR while the contribution of sorption and volatilization seemed to be negligible [84].

The first study on anaerobic degradation of five SSRIs, including CTR and four SSRIs' metabolites, including N-desmethylCTR and N-didesmethylCTR was reported in literature by Bergersen et al. Anaerobic lab-scale digesters were set up to investigate whether the compounds would be reduced or accumulated in sewage sludge. CTR was found to be almost completely reduced at day 24 at a percentage of 85%, whereas, none of the metabolites was detected in the samples [85].

CTR did not exhibit significant sorption onto secondary sewage sludge with short sludge age, approximately calculated at about 10% and presented in a study by Hörsing et al. [86]

Ozonation experiments under controlled conditions presented high removal efficiency for CTR (93%) in wastewater samples as reported by Rosal et al. [87]. The removal and transformation of CTR at neutral pH under advanced water treatment technologies (O_3, ClO_2 oxidation, UV irradiation and Fenton oxidation), was also investigated in a more recent study of Hörsing et al., in 2012. Under the prevailing test conditions for UV-irradiation and Fenton oxidation, no TPs were found. However, when O_3 and ClO_2 were used, degradation rate of CTR was similar (80% and 95% reduction, respectively), while two metabolites (N-desmethylCTR and CTR-N-oxide) and three novel TPs (3-oxo-CTR, a hydroxylated dimethylamino-side chain derivative and a defluorinated derivative of CTR) were formed and identified by HR-MS/MS [38]. On the contrary, CTR yielded lower removal efficiency, being 34% at ozonation of the primary-treated effluent performed by Lajeunesse et al. [75].

The biodegradation of several pharmaceuticals, including CTR in hospital wastewater by staged MBBRs has been also reported by Casas et al. The removal was studied in two experiments; a batch experiment and a continuous flow experiment presenting elimination of 80% and 20%, respectively [88].

2.2.5 Bioaccumulation, ecotoxicity and risk assessment of CTR

As well as evaluating the presence and the fate of CTR, a starting point to assess its importance as EC is also to examine its bioaccumulation and toxicity by determining possible effects that can be expected at relevant concentrations [12, 89]. SSRIs act by modulating and mimicking the effects of the neurotransmitter serotonin, which regulates a wide range of physiological systems in fish, molluscs, and protozoans. The amphoteric feature of these drugs and their ionization state during exposure seem to contribute to the alteration of the biological activity of aquatic organisms and, they may lead to reproduction reduction, abnormalities in embryo development, delay in physiological development and sexual maturation [51].

Despite this, few studies have investigated the uptake and bioaccumulation of CTR in aquatic organisms, such as white suckers (*Catostomus commersoni*) [62], fathead minnows (*Pimephales promelas*) [70], bull sharks (*Carcharhinus leucas*) [90] and bivalves [91]. Moreover, most CTR ecotoxicity data is available from studies describing endpoints that do not include direct measurements of survival, development or reproduction but rather describe behavioural effects, which are uncertain for an environmental risk assessment [92]. CTR showed to be the SSRI with lower acute and chronic toxicity [93] while it does not affect the aggressive or reproductive behaviour in fish at water concentrations regularly found in the environment. Nonetheless, in the environment, fish may be exposed for longer times to several SSRIs acting additively and in concert with other contaminants and other abiotic or biotic factors [92].

CHAPTER 3
Scope and objectives

Continuous contamination of the environment with pharmaceuticals and their adverse effects on both ecosystem and human health is one of the most relevant environmental issues of today. After excretion, metabolites and some percentage of unmetabolized compounds are discharged into the municipal sewage system where further biotic and abiotic transformation processes may also take place, giving rise to TPs. Despite the wide distribution of pharmaceuticals in the environment, research in the field of degradation mechanisms, the identity of TPs, and their origin, fate and transformation is still limited.

Among pharmaceuticals, SSRIs and specifically the selected compound, CTR, has demonstrated incomplete removal by conventional wastewater treatment making WWTP a point source to the environment. Therefore, it is of paramount environmental importance to characterize its fate during WWT and investigate the potential formation of TPs. However, it is challenging to assess the pollution of formed TPs, since it is difficult to identify the signal of TPs in environmental samples with a lot of interfering environmental matrix. Laboratory batch experiments allow the estimation of kinetic parameters and identification of TPs, which can be screened in environmental matrices. Additionally, HR-MS is strongly required in order to have mass accuracy for confirmation of the molecular formula and reliable interpretation of the MS/MS spectra.

The present study aims to contribute to the existing knowledge on fate and transformation of CTR during the biological breakdown process, when exposed to microorganisms. As far as we know, there is no reported literature about biotransformation of CTR in activated sludge and identification of its TPs. In particular, the objectives of this master thesis were:

(a) to carry out biodegradation batch experiments on CTR under aerobic conditions with activated sludge from a WWTP and study its degradation kinetics;

(b) to investigate the occurrence and formation of CTR TPs during activated sludge treatment and to identify the potential TPs by an integrated workflow for suspect and non-target screening;

(c) to study the use of HILIC as a complementary and orthogonal approach to RPLC-QTOF-MS for the identified TPs, and;

(d) to determine environmental concentrations of both the parent compound and its TPs in influent and effluent WWTP samples through retrospective analysis.

CHAPTER 4
Materials and methods

4.1 Chemicals and reagents

All pharmaceutical standards were of high-purity grade. CTR was purchased from LGC Promochem (Molsheim, France) and 3-oxo-CTR (CTR Related Compound C) was provided by US Pharmacopoeia (Twinbrook Parkway, Rockville, MD, USA). N-DesmethylCTR, CTR amide and CTR carboxylic acid were obtained by Jubilant Life Sciences Ltd (Shanghai, China).

Methanol (MeOH) and acetonitrile (ACN) of LC-MS grade were purchased from Merck (Darmstadt, Germany), whereas 2-propanol and ethyl acetate of LC-MS grade was from Fisher Scientific (Geel, Belgium). Sodium hydroxide monohydrate for trace analysis ≥99.9995%, ammonium formate ≥99.0%, ammonium acetate and formic acid 99% were purchased from Fluka (Buchs, Switzerland). Distilled water was provided by a Milli-Q purification apparatus (Millipore Direct-Q UV, Bedford, MA, USA).

The biotransformation batch experiments were performed in amber Schott glass bottles from Isolab (Wertheim, Germany). Regarding the consumables for the sample preparation of influent and effluent WWTP samples, the empty solid phase extraction polypropylene tubes (6 mL), as well as the cartridge sorbent materials Sepra ZT (Strata-X), Sepra ZT-WCX (Strata-X-CW) and ZT-WAX (Strata-X-AW) were obtained from Phenomenex (Torrance, USA). The Isolute ENV+ sorbent material and the frits (20 μm, 6 mL) were from Biotage (Ystrad Mynach, UK). Glass fiber filters (GFFs) (pore size 0.7 μm, diameter 47 mm) used in wastewater filtration and disposable GFF syringe filters (pore size 1.0 μm, diameter 25 mm) were obtained from Whatman (Maidstone, UK). Regenerated cellulose syringe filters (RC) (pore size 0.2 μm, diameter 15 mm) were purchased from Phenomenex (Torrance, CA, USA).

Stock standard solutions of individual compounds (1000 μg mL^{-1}) were prepared in MeOH and stored at −20 °C in amber glass bottles to prevent photodegradation.

4.2 Sampling and storage

Activated sludge and effluent wastewater for biotransformation batch experiments were collected on the 28th of October 2014 (Tuesday) while influent and effluent wastewater samples (24-hour composite flow proportional samples) for detection of the TPs in real samples on the 8th of March 2015 (Sunday) from the WWTP of Athens, Greece.

The WWTP of Athens is designed with primary sedimentation, activated sludge process with biological nitrogen and phosphorus removal and secondary sedimentation. The estimated sewage flow for the collected samples is 750,000 m^3 day^{-1}. The closest connected household is 0.5 km and the most remote 30 km from the WWTP. The residential population connected to the WWTP based on official census, excluding commuters, is 3,700,000 and the number of people estimated based on the number of house connections is 4,562,500. The WWTP is designed to serve a population equivalent of 5,200,000 and thus is by far the largest in Greece and one of the largest in the world.

Activated sludge and sewage treatment plant influents and effluents were sampled in pre-cleaned high-density polyethylene (HDPE) bottles. Untreated and treated samples were filtered with 0.7 μm GFFs immediately after arrival at the laboratory and stored in the dark at 4 °C until analysis. Biotransformation experiments commenced within 24 hours after sampling.

4.3 Biotransformation batch experiments

Biotransformation of CTR was investigated within a 6-day batch experiment. The biodegradation test system was prepared in 500mL amber glass bottles with 200 mL of appropriate content.

Activated sludge was sampled in order to seed the biotic reactor. Total suspended solids (TSS) concentration was measured using Standard Method 2540B [94]. A defined amount of sludge was filtered through a 0.7 μm previously weighed GFF and dried for at least 2 hours before it was weighed again. Additionally, two different control experiments were carried out. A batch reactor with WW effluent was run as hydrolysis and volatilization control

(abiotic reactor) and another batch reactor with sterilized sludge (autoclaved at 121 °C for 24 hours) diluted with WW effluent was set up to examine the sorption losses (sorption reactor) [95]. All bioreactors were spiked with 400 µL of CTR standard stock solution to obtain a final concentration of 2 mg L^{-1}. Non-spiked blank reactor seeded with activated sludge was always run in parallel to check for potential cross-contamination between sampling and subtract the background in post-acquisition data treatment caused by the natural sludge matrices.

Each bioreactor was loosely covered with a perforated cap to allow oxygen diffusion but avoid contamination and evaporation, and placed on a magnetic stirrer to further simulate the CAS system. Initial pH was in the range 7.4-8.4 and the bottles were at controlled temperature (20 °C) under dark conditions.

Samples were taken immediately after spiking, 1, 2, 4, 6, 8 and 10 hours later and after 1, 2, 3, 4, 5 and 6 days. 1 mL was taken from each reactor and filtered through a 1.0 µm disposable GF syringe filter.

Finally, the extracts were filtered through a 0.2 µm RC syringe filter and divided in two aliquots. In RP mode the extracts were diluted with MeOH to achieve an in-vial composition of 50:50 MeOH:H_2O. For HILIC analysis the extracts were dried and reconstituted in ACN:H_2O (95:5) prior to analysis.

4.4 Determination of environmental concentrations of TPs in real wastewater samples

Sample extraction was carried out using a slight variation of the protocol developed by Kern et al. [24]. Sample aliquots of 100 mL were adjusted to pH 6.5. SPE was conducted using four different SPE materials simultaneously in an in-house cartridge to achieve sufficient enrichment for a very broad range of compounds (200 mg Oasis HLB, 150 mg Isolute ENV+, 100 mg Strata-X-AW and 100 mg Strata-X-CW). The cartridges were preconditioned with MeOH and H_2O and the water samples were loaded, then there was a drying step under vacuum. The elution was conducted with 4 mL of MeOH:ethyl acetate (50:50) containing 2% ammonia, followed by 2 mL of MeOH:ethyl acetate (50:50) containing 1.7% formic acid. Extracts were evaporated under a gentle

nitrogen stream to a volume of 100 µL and then reconstituted to 0.5 mL with a final proportion of MeOH:H_2O (50:50). Finally, the extracts were filtered through a 0.2 µm RC syringe filter and were ready for injection in the RP chromatographic system.

4.5 LC–HR-MS/MS analysis

An ultrahigh-performance liquid chromatography (UHPLC) (Dionex UltiMate 3000 RSLC, Thermo Fisher Scientific, Germany) interfaced to a Quadrupole-Time of Flight mass spectrometer (QTOF Maxis Impact, Bruker Daltonics, Bremen, Germany) was used to identify potential TPs during biotransformation experiments and semi-quantify the identified TPs in influent and effluent wastewater samples. The QTOF-MS system was equipped with an ESI source, operating in positive and negative ionization mode. The chromatographic separation was performed on both an RP and a HILIC chromatographic system for the complementarity of the results.

In RP mode, an Acclaim RSLC C18 column (2.1 × 100 mm, 2.2 µm) from Thermo Fisher Scientific (Dreieich, Germany), preceded by an ACQUITY UPLC BEH C18 1.7 µm, VanGuard Pre-Column from Waters (Dublin, Ireland), and thermostated at 30 °C, was used. For positive ionization mode, the aqueous phase consisted of H_2O:MeOH 90:10 with 5 mM ammonium formate and 0.01% formic acid and the organic phase was MeOH with 5 mM ammonium formate and 0.01% formic acid. For negative ionization mode, the aqueous phase consisted of H_2O:MeOH 90:10 with 5 mM ammonium acetate and the organic phase was MeOH with 5 mM ammonium acetate. The adopted elution gradient for both ionization modes started with 1% of organic phase (flow rate 0.2 mL min^{-1}) for one minute, increasing to 39 % by 3 min (flow rate 0.2 mL min^{-1}), and then to 99.9 % (flow rate 0.4 mL min^{-1}) in the following 11 min. These almost pure organic conditions were kept constant for 2 min (flow rate 0.48 mL min^{-1}) and then initial conditions were restored within 0.1 min, kept for 3 min and then the flow rate decreased to 0.2 mL min^{-1} for the last minute. The injection volume was set to 5 µL.

An ACQUITY UHPLC BEH Amide column (2.1 × 100 mm, 1.7 µm) from Waters (Dublin, Ireland), preceded by a guard column of the same packaging material, ACQUITY UPLC BEH Amide 1.7 µm, VanGuard Pre-Column from Waters (Dublin, Ireland), and thermostated at 40 °C was used in HILIC analysis. For positive ionization, the aqueous phase consisted of H_2O with 1 mM ammonium formate and 0.01% formic acid and the organic phase was ACN/H_2O 95:5 with 1 mM ammonium formate and 0.01% formic acid. For negative ionization, the aqueous phase consisted of H_2O with 10 mM ammonium formate and the organic phase was ACN:H_2O 95:5 with 10 mM ammonium formate. The adopted elution gradient, for both ionization modes, started with 100% of organic phase and kept stable for 2 minute, decreasing to 5 % in 10 min, and kept constant for the following 5 min. The initial conditions were restored within 0.1 min and let to re-equilibrate for 8 min. The flow rate was 0.2 mL min^{-1} and the injection volume was set to 5 µL.

When RP chromatographic system was used, the operation parameters of ESI were the following: capillary voltage, 2500 V for positive and 3000 V for negative mode; end plate offset, 500 V; nebulizer pressure, 2 bar (N_2); drying gas, 8 L min^{-1} (N_2); and drying temperature, 200 °C while with HILIC chromatographic separation, the corresponding MS parameters were: capillary voltage, 3500 V for positive and 2500 V for negative mode; end plate offset, 500 V; nebulizer pressure, 2 bar (N_2); drying gas, 10 L min^{-1} (N_2); and drying temperature, 200 °C.

All the samples were first analyzed in full scan mode. The QTOF-MS system was operating in broadband collision-induced dissociation (bbCID) acquisition mode and recorded spectra over the range m/z 50−1000 with a scan rate of 2 Hz. The Bruker bbCID mode provides MS and MS/MS spectra at the same time working at two different collision energies; at low collision energy (4 eV), MS spectra were acquired, where all of the ions from the preselected mass range are heading towards the flight tube without isolation at the quadrupole and there is no collision-induced dissociation at the collision cell. At high collision energy (25 eV), no isolation is taking place at the quadrupole, and the ions from the preselected mass range are fragmented at the collision cell.

A second analysis was performed in AutoMS acquisition mode. Data-dependent MS/MS acquisition was conducted using an inclusion (preselected) mass list containing the exact masses of the precursor ion of the parent compound and plausible TPs with an intensity threshold of 1,000 counts. Spectra time was shortened to 0.25 seconds. The collision energy applied was set to predefined values, according to the mass and the charge state of every ion.

A QTOF-MS external calibration was daily performed with a sodium formate solution, and a segment (0.1−0.25 min) in every chromatogram was used for internal calibration, using a calibrant injection at the beginning of each run. The sodium formate calibration mixture consists of 10 mM sodium formate in a mixture of water/isopropanol (1:1). The theoretical exact masses of calibration ions with formulas $Na(NaCOOH)_{1\text{-}14}$ in the range of 50−1000 Da were used for calibration. The instrument provided a typical resolving power of 36000−40000 during calibration (39274 at m/z 226.1593, 36923 at m/z 430.9137, and 36274 at m/z 702.8636).

Data treatment and evaluation were processed with DataAnalysis 4.1 and TargetAnalysis 1.3 (Bruker Daltonics, Bremen, Germany).

4.6 Suspect and non-target screening for the identification of TPs

A two-step post-acquisition data processing approach was employed to identify candidate TPs of CTR.

First, a suspect database of plausible TPs was compiled by scientific literature and *in silico* prediction tools. Two different *in silico* predictions of possible TPs were performed. The EAWAG-BBD PPS, an artificial intelligence system, predicted microbial metabolic reactions, without the “relative reasoning mode”, based on biotransformation rules set in the EAWAG-BBD and scientific literature [96], while Metabolite Predict (Metabolite Tools 2.0, Bruker Daltonics, Bremen, Germany), using a rule-based expert system, predicted metabolites from Phase I, II and Cytochrome P450 reactions. The prediction results from both programs, including the molecular formula, exact mass and structures of

TPs, generated from two subsequent reactions in the metabolic pathway. Already known and reported metabolites from the pharmacokinetic literature were also added to the suspect database.

All the time interval samples were screened in full scan, in both chromatographic systems and in both ionization modes, for the detection of suspect TPs from the database. The suspect peak list was obtained by using an automatic database search function Find Compounds-Chromatogram in TargetAnalysis, which extracts the exact mass for each of the plausible TPs from the chromatograms by applying thresholds of intensity and peak area to cut-off unclear spectra, excluding the isotopic peaks. This reverse database search reported hits from the LC-QTOF-MS bbCID acquisition data within the selected identification criteria: peak area counts of 2,000 for ESI (+) and of 800 for ESI (-), intensity threshold counts of 500 for ESI (+) and 200 for ESI (-), a mass tolerance of ±5 ppm, and an isotopic pattern match, mSigma, threshold of 100 (a lower mSigma value indicates a better fit). The characterization of an exact mass as possible TP was based on the additional following criteria: presence in biotic sample and occurrence of a meaningful time trend, and absence (or presence in low percentage) from the zero-time samples, the blank samples and the control samples.

Second, a non-target screening was performed. Background subtraction and peak picking were carried out using Metabolite Detect (Metabolite Tools 2.0, Bruker Daltonics, Bremen, Germany). The parameters that were used to calculate the differences between the biotic sample and the reference sample (blank sample) were the following: eXpose mode algorithm, delta time ≤0.1 min, delta mass ≤0.05 m/z while a ratio from 3 to 5 was tested, so as a mass peak compared to a peak detected in the reference to be accepted as a different peak. As for the peak detection parameters, delta time of ≤0.1 min, trace width of ≤0.05 m/z, intensity threshold of 30% (the intensity of a peak should be at least 30% of the intensity of the most intense peak so as to be included in the peak list) with a maximum number of 20 peaks for the mass spectrum were set. The outcome was the generation of a peak list of unknown. Relevant peaks that were not present either in the blank samples or in the existing suspect database were selected, based on the intensity and the

presence of distinctive isotopic pattern and meaningful time trend and were treated further as “suspect peaks”.

The data-dependent MS/MS acquisition by QTOF-MS allowed the determination of the accurate mass of the parent compound, the suspect and the non-target TPs and their product ions in order to unambiguously annotate their elemental composition. The possible ion formulas were evaluated by the SmartFormula Manually function, a DataAnalysis built-in tool, based on the accurate mass and isotopic pattern. In addition to C, H, O, and N, the element F was also taken into account. The nitrogen rule, ring structures, double bonds and the number of carbon atoms were automatically checked by the program. The maximum mass deviation was set at ±10 ppm and the threshold of the mSigma value was set at 200.

Structure elucidation of TPs was based on the use of characteristic fragmentation (i.e., fragmentation pattern) undergone by TPs during MS/MS fragmentation events, since it can be assumed that many TPs maintain a structure similar to the parent compound and therefore have common fragment ions. The interpretation of the mass spectral data in order to propose a structure for the TPs was supported by literature data [38, 97, 98] and Mass Frontier (Thermo Fisher Scientific, Germany), a predictive mass spectral fragmentation software.

4.7 Communication of the achieved levels of confidence

The system presented by Schymanski et al. (Figure 4) to communicate the level of confidence achieved in the identification of the detected compounds was used. Level 1 corresponds to confirmed structures where a reference standard is available, level 2 to probable structures, level 3 for tentative candidate(s), level 4 to unequivocal molecular formulas and level 5 to exact mass(es) of interest [49].

4.8 Retrospective suspect screening of the identified TPs

Retrospective suspect screening of the identified TPs in real wastewater samples was performed by applying the identification criteria of suspect

screening mentioned in subchapter 4.6. Confirmation of the identity of the compounds detected was based on the accurate m/z of the protonated molecule together with the agreement in retention time and MS/MS spectra. Retention time, which was used as reference, was derived from the biotransformation experiments.

CHAPTER 5

Results and discussion

5.1 Degradation of CTR in batch experiments with activated sludge

Incomplete aerobic degradation of CTR was observed in the activated sludge system (biotic reactor) after 6 days. CTR (spiked at 2 mg L^{-1} with an initial TSS concentration of 3 g L^{-1}) was dissipated by approximately 70% until 3 days and then remained stable for the last 3 days. An exponential decrease **(Figure 5a)** during the first 24 hours of the experiment was observed, indicating pseudo-first order degradation kinetics **(Figure 5b)**. Outliers were removed in order to obtain good linearity.

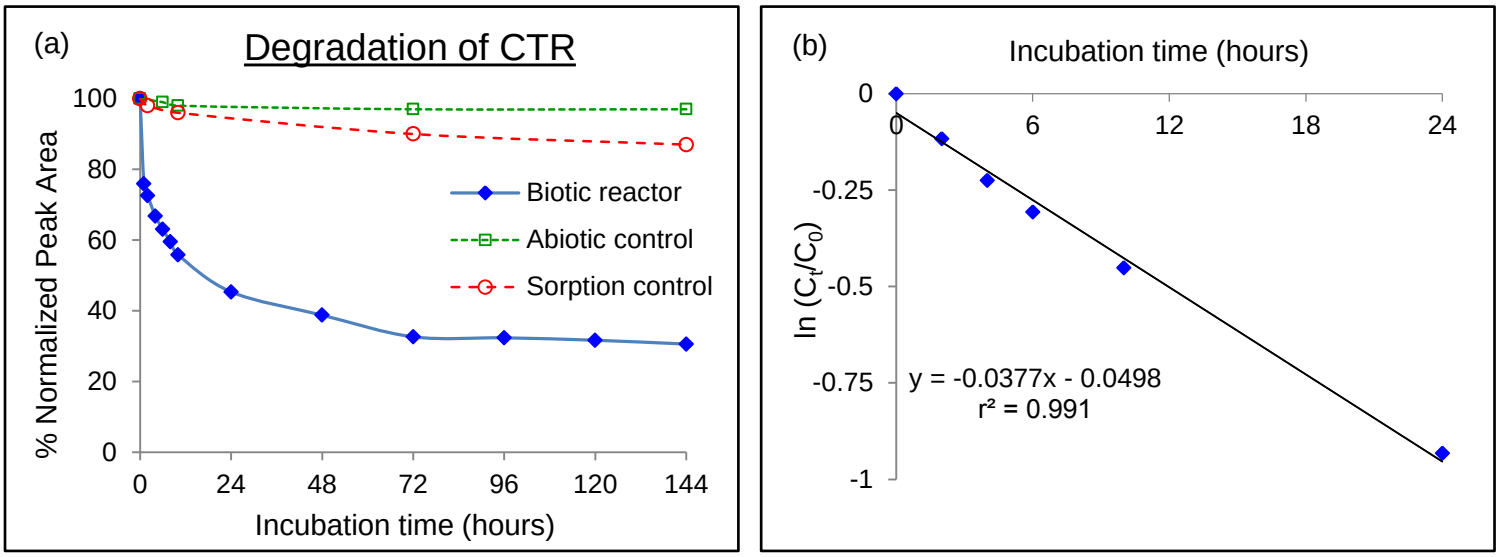

Figure 5: (a) Degradation of CTR in aerobic batch experiments in the course of the time; (b) line: fit of the pseudo-first order kinetic of CTR.

The 'first order' refers to the direct proportionality of the transformation rate to the soluble substance concentration. Therefore, the biotransformation rate constant k_{biol} (Equation 1) and the degradation half-life $t_{1/2}$ (Equation 2) were calculated as follows:

$$k_{biol} = -\frac{ln\left(\frac{C_t}{C_0}\right)}{t} \quad (1)$$

$$t_{1/2} = \frac{ln(2)}{k_{biol}} \quad (2)$$

where $\ln(C_t/t_0)/t$ is the slope of the equation in **Figure 5b**. A biological transformation rate constant of 0.04 h^{-1} and a half-life of 18.4 h were attained for CTR.

The control experiments with diluted autoclaved sludge (sorption reactor) showed that only small fractions (13%) were lost due to sorption to or reaction with sludge particles. The losses could also be explained by a partial reactivation of the autoclaved sludge as the sludge can be contaminated by active bacteria each time it is sampled. The control reactor with WWTP effluent (abiotic reactor) showed negligible losses (3%) of CTR as it was still present at the initial concentration after 6 days. Thus, decreasing CTR concentration in the active bioreactor can be clearly associated with biotransformation.

The pH was measured in the active bioreactor of the CTR degradation experiment and increased slightly from 7.35 to 8.15 within the first 48 hours, and subsequently decreased continuously to pH 6.56 until CTR was removed at 70%. This shift in pH is presumably due to nitrification processes that occurred independent of CTR transformation.

5.2 Identification of biotransformation products of CTR

Candidate TPs of CTR were detected and identified using suspect and non-target screening and post-acquisition data processing methods, as described in the subchapter 4.6. During the biotransformation batch experiments, fourteen compounds were formed in the biotic reactor. All TPs were detected in the positive-ion mode. Analysis under negative mode did not reveal additional TPs to those observed in positive mode. Thirteen out of them were detected in the RP chromatographic system, while one additional TP was detected with HILIC chromatographic separation. **Figures 6** and **8** represent the time profile of the plausible TPs in RP and HILIC analysis, respectively, whereas **Figures 7** and **9** present a better picture of the time profile of minor TPs detected in both chromatographic systems. The candidate TPs characterized by retention time in RP and HILIC, and distinct peak area patterns over time (either increasing peak areas over time or increasing and decreasing peak areas) are listed in **Table 3**.

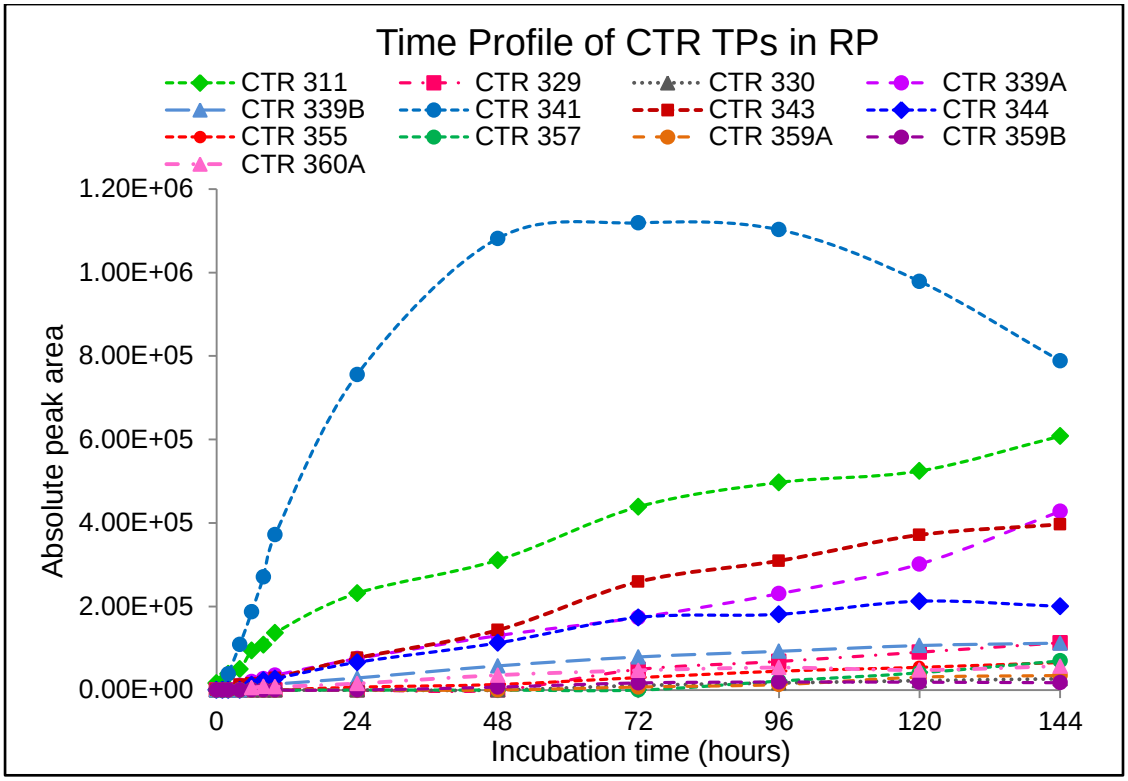

Figure 6: Time profile of TPs of CTR in RP chromatographic system.

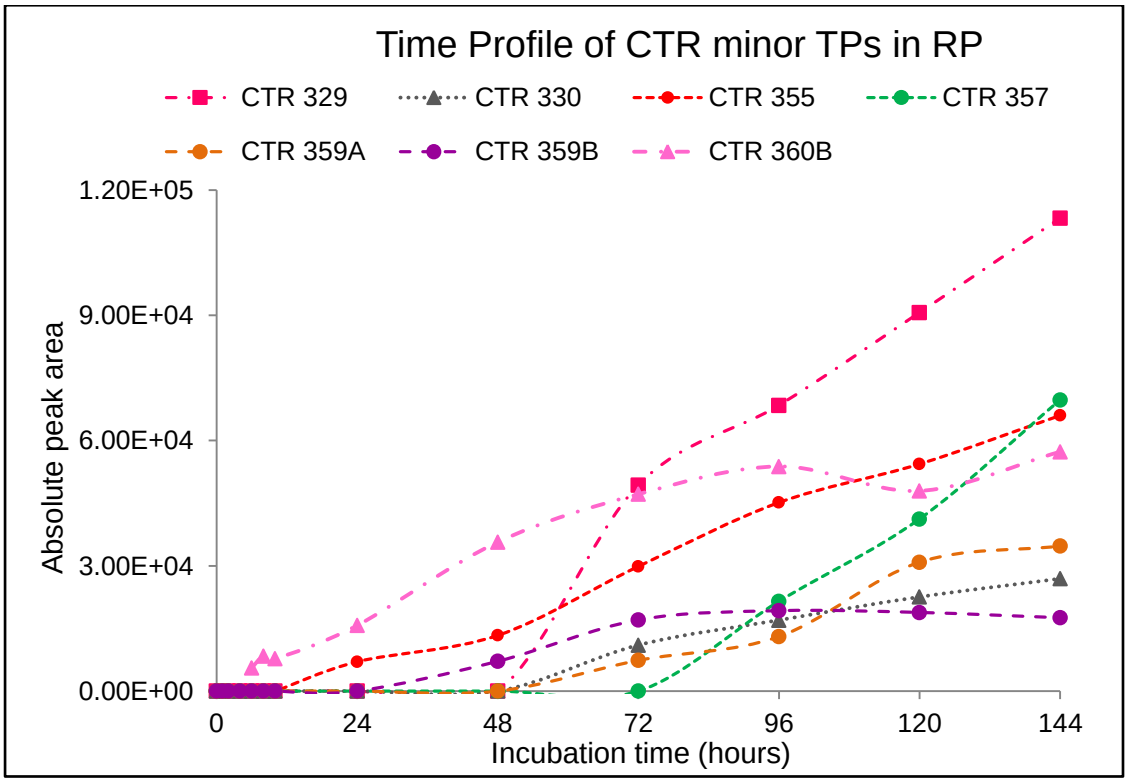

Figure 7: Time profile of minor TPs of CTR in RP chromatographic system.

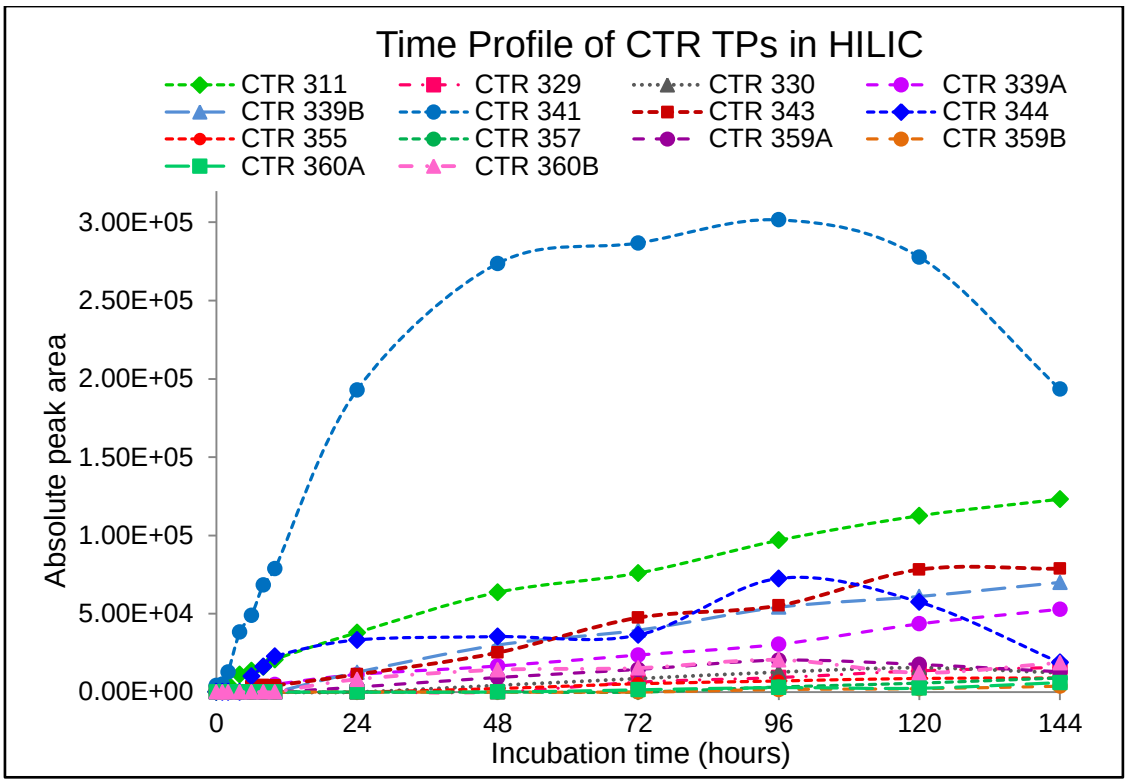

Figure 8: Time profile of TPs of CTR in HILIC chromatographic system.

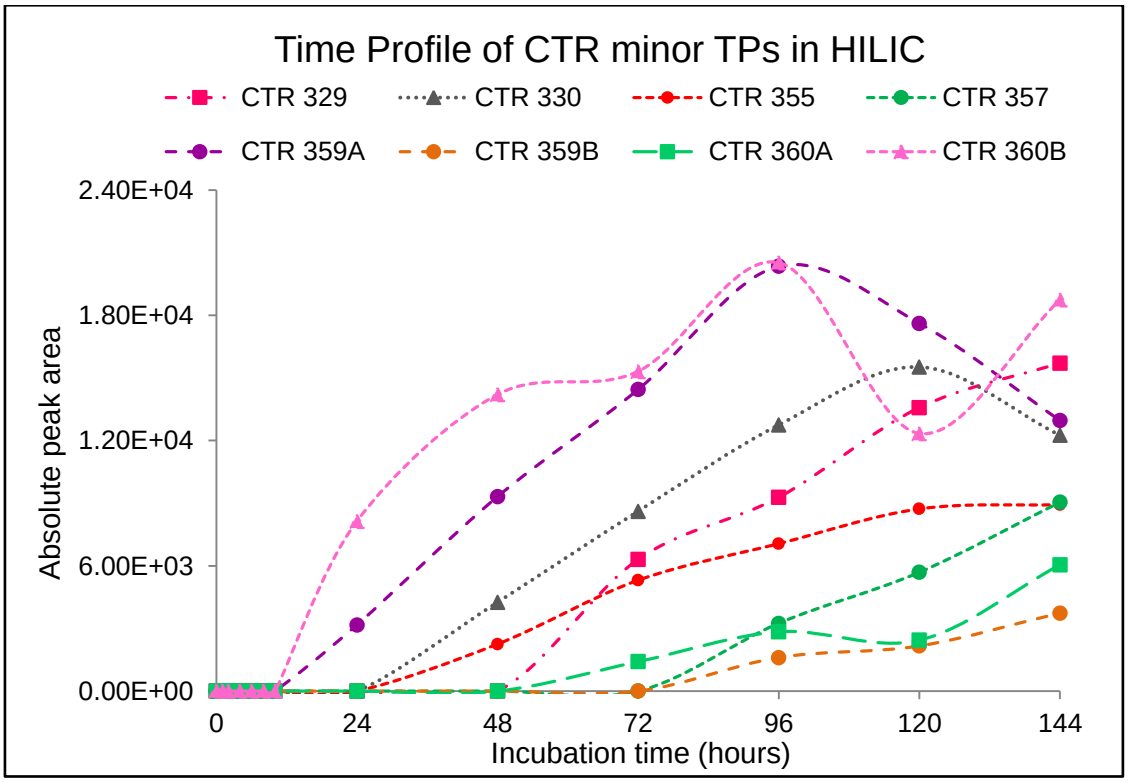

Figure 9: Time profile of minor TPs of CTR in HILIC chromatographic system.

Table 3: Candidate TPs characterized by retention time in RP and HILIC, and distinct peak area patterns over time.

					RP			HILIC		
TP	Theoretical Mass of $[M+H]^+$	Time Trend	First appea-rance (h)	Appea-rance of maximum intensity (h)	t_R (min)	Maximum peak area	Maximum intensity	t_R (min)	Maximum peak area	Maximum intensity
CTR 311	311.1554	↗	0	144	6.8	608,028	101,860	5.9	123,180	39,527
CTR 329	329.1660	↗	72	144	5.3	113,269	20,565	6.1	15,713	5,203
CTR 330	330.1500	↗	72	144	6.0	26,919	4,448	6.4	15,526	4,568
CTR 339A	339.1503	↗	4	144	6.4	427,950	72,326	5.9	52,884	16,704
CTR 339B	339.1867	↗	6	144	6.6	112,450	21,536	5.8	70,026	22,824
CTR 341	341.1660	↗↘	2	72	7.1	1,111,808	184,820	5.9	301,551	98,639
CTR 343	343.1816	↗	4	144	5.2	396,743	74,405	6.0	78,745	25,372
CTR 344	344.1656	↗↘	6	120	5.9	212,803	36,297	6.4	72,553	18,723
CTR 355	355.1452	↗	24	144	6.8	66,002	12,208	5.9	8,930	2,900
CTR 357	357.1609	↗	96	144	5.2	69,739	12,245	6.0	9,046	2,541
CTR 359A	359.1765	↗	72	144	4.7	34,724	2,903	6.4	20,346	5,264
CTR 359B		↗↘	48	96	5.6	19,252	3,303	6.1	3,735	1,454
CTR 360A	360.1606	↗	-	144	6.3	57,310	10,484	6.7	18,744	3,872
CTR 360B		↗	6	144	-	-	-	6.5	6,049	2,000

Four TPs (CTR 311, CTR 339A, CTR 341 and CTR 343) were also formed in control reactors, probably catalyzed by matrix components **(Figure 10)**. It can be assumed that their appearance in the control samples indicate that these TPs are present in the effluent wastewater, being sorbed to TSS and moreover that their formation is also a result of abiotic processes but in a negligible rate (the peak area of the former TPs in control samples corresponds approximately to 5-10% of their peak area in biotic sample of 6 days).

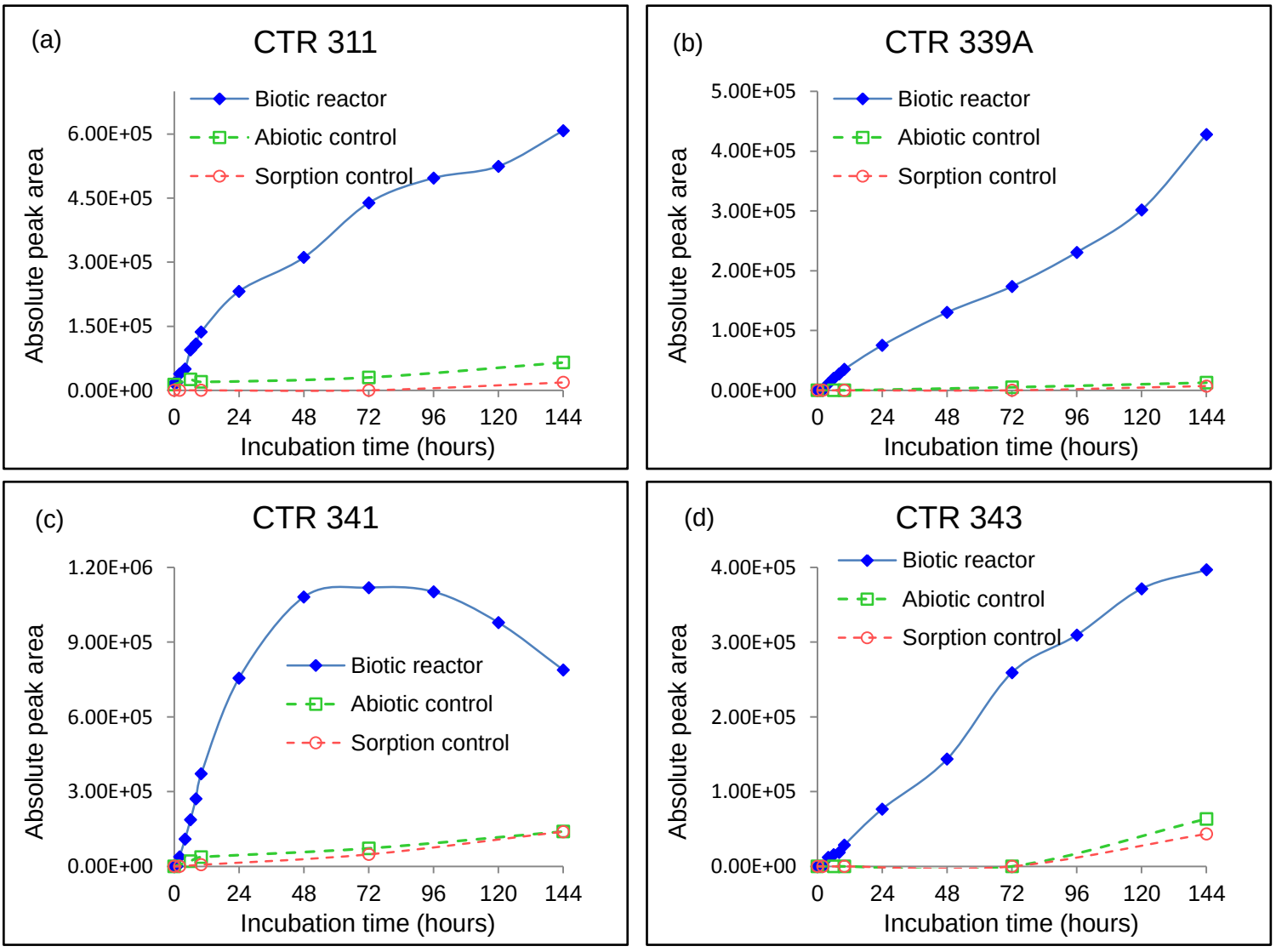

Figure 10: Absolute peak area versus time course plots of TPs formed in both biotic reactor and control reactors (a) CTR 311; (b) CTR 339A; (c) CTR 341; (d) CTR 343.

The fragmentation pattern of the most of TPs was quite clear and was in a good agreement with the fragmentation pattern of their parent compound. As can be seen, CTR **(Figure 11)** has a retention time of 6.7 min and 5.9 min in RP and HILIC, respectively and its molecular formula is $C_{20}H_{21}FN_2O$. **Figure 12** shows the eXtracted Ion Chromatogram (XIC) and MS/MS spectra in RP and HILIC chromatographic systems of the parent compound, CTR, in zero-time biotic sample. In the MS/MS spectrum, the ions 307 ($C_{20}H_{20}FN_2^+$) and 280 ($C_{18}H_{15}FNO^+$) were formed by cleaving off a water molecule H_2O and a dimethyl amino group $NH(CH_3)_2$, and belong to the diagnostic neutral losses of CTR. The major characteristic fragment with nominal mass 262 ($C_{18}H_{13}FN^+$) can be explained by the cleavage of either a $NH(CH_3)_2$ unit from 307 or H_2O from 280. Further on, 262 is subjected to losses of a methyl ($-CH_3$) and an ethyl group ($-CH_2CH_2$), exhibiting ions at 247 ($C_{17}H_{10}FN^+$) and 234 ($C_{16}H_9FN^+$), respectively. Additional characteristic fragments of CTR are 109 ($C_7H_6F^+$) and 58 ($C_3H_8N^+$).

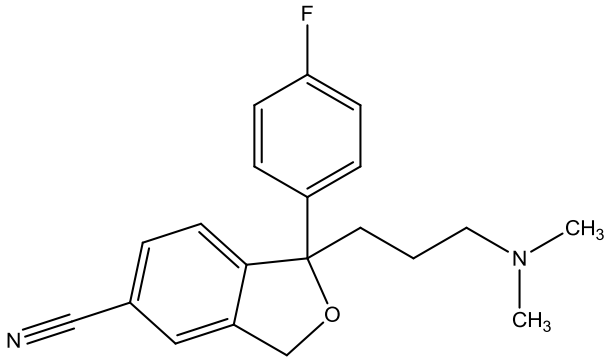

Figure 11: CTR.

The XICs at incubation time points and the MS/MS spectra of the TPs, which are presented below, are derived from the analysis of biotic samples at the time point of their highest intensity. The elemental composition of CTR and its TPs along with their main product ions, used for their identification, the measured m/z, the theoretical m/z and the mass error in ppm in both chromatographic systems are summarized in **Table 4**.

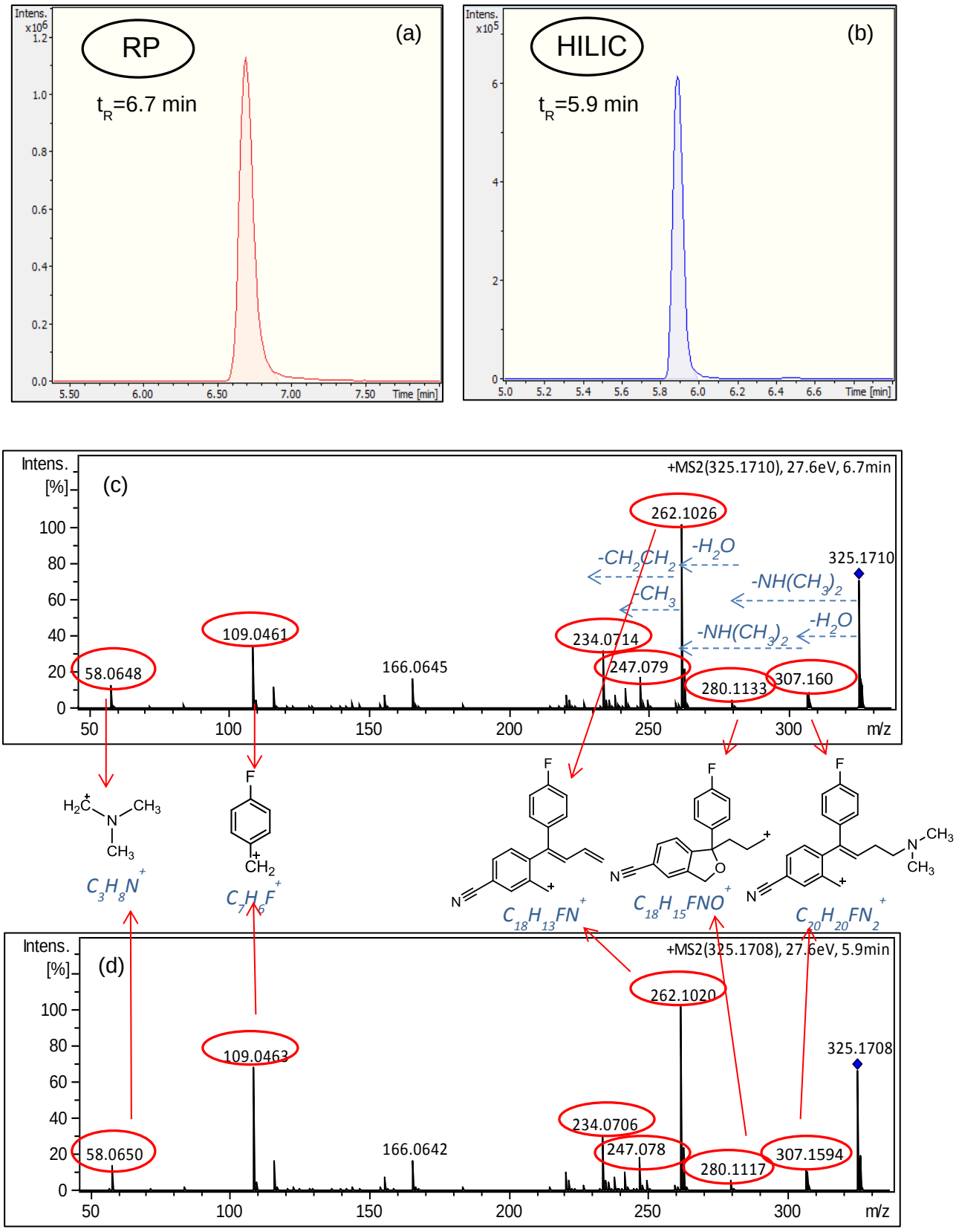

Figure 12: Analytical data for CTR; XICs of CTR at zero-time biotic samples in (a) RP and (b) HILIC; MS/MS spectra at t=0 h in (c) RP and (d) HILIC showing the fragmentation and proposed fragments of CTR.

Table 4: Elemental composition of CTR, TPs and their fragment ions along with the measured m/z, the theoretical m/z and the mass error in ppm in RP and HILIC chromatographic systems.

			RP		HILIC		
Compound	Nominal ion mass of $[M+H]^+$	Theoretical ion mass of $[M+H]^+$	Measured ion mass of $[M+H]^+$	Mass error (ppm)	Measured ion mass of $[M+H]^+$	Mass error (ppm)	Elemental Composition
CTR	325	325.1711	325.1710	0.4	325.1708	0.9	$C_{20}H_{22}FN_2O^+$
	307	307.1605	307.1605	0	307.1594	-3.5	$C_{20}H_{20}FN_2^+$
	280	280.1132	280.1133	0.1	280.1117	5.4	$C_{18}H_{15}FNO^+$
	262	262.1027	262.1026	-0.1	262.1020	-2.4	$C_{18}H_{13}FN^+$
	247	247.0792	247.0793	-0.4	247.0784	3.2	$C_{17}H_{10}FN^+$
	234	234.0714	234.0714	-0.4	234.0706	3.2	$C_{16}H_9FN^+$
	109	109.0448	109.0461	-11.8	109.0463	-14	$C_7H_6F^+$
	58	58.0651	58.0648	6.1	58.0650	1.7	$C_3H_8N^+$
CTR 311	311	311.1554	311.1551	0.9	311.1555	-0.2	$C_{19}H_{20}FN_2O^+$
	293	293.1449	293.1444	1.5	293.1442	-2.3	$C_{19}H_{18}FN_2^+$
	280	280.1132	280.1136	-1.2	280.1152	-7	$C_{18}H_{15}FNO^+$
	262	262.1027	262.1022	-1.9	262.1027	0.1	$C_{18}H_{13}FN^+$
	234	234.0714	234.0705	3.6	234.0711	1.1	$C_{16}H_9FN^+$
	109	109.0448	109.0455	6.4	109.0454	-5.2	$C_7H_6F^+$
CTR 329	329	329.1660	329.1656	1.0	329.1663	1.0	$C_{19}H_{22}FN_2O_2^+$
	311	311.1554	311.1551	1.0	311.1560	-1.9	$C_{19}H_{20}FN_2O^+$
	298	298.1238	298.1245	-3.3	298.1236	0.3	$C_{18}H_{17}FNO_2^+$
	280	280.1132	280.1140	-2.7	280.1131	-0.6	$C_{18}H_{15}FNO^+$
	237	237.1074	237.1076	-0.6	237.1071	1.3	$C_{17}H_{14}F^+$
	109	109.0448	109.0451	-2.5	109.0445	-3.1	$C_7H_6F^+$
CTR 330	330	330.1500	330.1480	6.1	330.1500	0	$C_{19}H_{21}FNO_3^+$
	312	312.1394	312.1383	3.7	312.1393	0.6	$C_{19}H_{19}FNO_2^+$
	299	299.1078	299.1100	-7.4	299.1054	8.0	$C_{18}H_{16}FO_3^+$
	281	281.0972	281.0951	7.5	281.0981	-3.0	$C_{18}H_{15}FNO^+$
	237	237.1074	237.1067	2.9	237.1066	-3.2	$C_{17}H_{14}F^+$
	109	109.0448	109.0441	6.6	109.0446	-2.2	$C_7H_6F^+$
CTR 339 A	339	339.1503	339.1504	0.3	339.1505	-0.5	$C_{20}H_{20}FN_2O_2^+$
	321	321.1398	321.1395	-0.8	321.1391	1.9	$C_{20}H_{18}FN_2O^+$

			RP		HILIC		
Compound	Nominal ion mass of $[M+H]^+$	Theoretical ion mass of $[M+H]^+$	Measured ion mass of $[M+H]^+$	Mass error (ppm)	Measured ion mass of $[M+H]^+$	Mass error (ppm)	Elemental Composition
	294	294.0925	294.0932	2.4	294.0919	-1.9	$C_{18}H_{13}FNO_2^+$
	276	276.0819	276.0821	-0.6	276.082	-0.5	$C_{18}H_{11}FNO^+$
	258	258.0714	258.0716	1.1	258.0709	1.8	$C_{18}H_9FN^+$
	248	248.0870	248.0875	2.1	248.0866	-1.7	$C_{17}H_{11}FN^+$
	58	58.0651	58.0651	0.7	58.0644	13.1	$C_3H_8N^+$
CTR 341	341	341.1660	341.1664	1.1	341.1660	0.1	$C_{20}H_{22}FN_2O_2^+$
	280	280.1132	280.1128	1.3	280.1129	-1.1	$C_{18}H_{15}FNO^+$
	262	262.1027	262.1028	0.5	262.1030	-1.4	$C_{18}H_{13}FN^+$
	234	234.0714	234.0709	1.9	234.0717	-1.3	$C_{16}H_9FN^+$
	109	109.0448	109.0448	0.1	109.0453	4.9	$C_7H_6F^+$
CTR 343	343	343.1816	343.1815	-0.4	343.1819	0.6	$C_{20}H_{24}FN_2O_2^+$
	325	325.1711	325.1701	-2.8	325.1710	-0.2	$C_{20}H_{22}FN_2O^+$
	298	298.1238	298.1241	1.1	298.1232	1.8	$C_{18}H_{17}FNO_2^+$
	280	280.1132	280.1130	-0.9	280.1134	-0.5	$C_{18}H_{15}FNO^+$
	237	237.1074	237.1072	-1.0	237.1075	-0.3	$C_{17}H_{14}F^+$
	109	109.0448	109.0448	0.4	109.0453	4.5	$C_7H_6F^+$
	58	58.0651	58.0646	8.2	58.0648	-5.4	$C_3H_8N^+$
CTR 344	344	344.1656	344.1661	1.3	344.1654	-0.7	$C_{20}H_{23}FNO_3^+$
	326	326.1551	326.1546	-1.6	326.1553	-0.6	$C_{20}H_{21}FNO_2^+$
	299	299.1078	299.1080	-0.6	299.1063	5.0	$C_{18}H_{16}FO_3^+$
	281	281.0972	281.0970	-0.8	281.0976	1.4	$C_{18}H_{14}FO_2^+$
	237	237.1074	237.1069	1.9	237.1075	-0.3	$C_{17}H_{14}F^+$
	109	109.0448	109.0456	-7.5	109.0460	-10.7	$C_7H_6F^+$
	58	58.0651	58.0653	-2.6	58.0653	3.4	$C_3H_8N^+$
CTR 357	357	357.1609	357.1615	1.7	357.1613	1.2	$C_{20}H_{22}FN_2O_3^+$
	339	339.1503	339.1496	2.2	339.1509	-1.6	$C_{20}H_{20}FN_2O_2^+$
	312	312.1030	312.1017	4.3	312.1032	0.4	$C_{18}H_{15}FNO_3^+$
	294	294.0925	294.0924	-0.2	294.0927	0.7	$C_{18}H_{13}FNO_2^+$
	276	276.0819	276.0815	1.4	276.0826	2.4	$C_{18}H_{11}FNO^+$
	251	251.0867	251.0872	-2.0	251.0860	2.6	$C_{17}H_{12}FO^+$
	58	58.0651	58.0634	9.7	58.0621	-12	$C_3H_8N^+$
CTR 359A	359	359.1765	359.1770	-1.3	359.1759	1.8	$C_{20}H_{24}FN_2O_3^+$

			RP		HILIC		
Compound	Nominal ion mass of $[M+H]^+$	Theoretical ion mass of $[M+H]^+$	Measured ion mass of $[M+H]^+$	Mass error (ppm)	Measured ion mass of $[M+H]^+$	Mass error (ppm)	Elemental Composition
	341	341.1660	341.1648	3.4	341.1646	4.0	$C_{20}H_{22}FN_2O_2^+$
	323	323.1554	323.1546	-2.5	323.1546	2.7	$C_{20}H_{20}FN_2O^+$
	280	280.1081	280.1122	3.6	280.1117	5.5	$C_{18}H_{15}FNO^+$
	237	237.1074	237.1087	-5.6	237.1069	2.0	$C_{17}H_{14}F^+$
	109	109.0448	109.0446	1.9	109.0448	0.1	$C_7H_6F^+$
	58	58.0651	58.0649	3.9	58.0646	9.4	$C_3H_8N^+$
CTR 359B	359	359.1765	359.1771	-1.5	359.1755	2.9	$C_{20}H_{24}FN_2O_3^+$
	298	298.1238	298.1216	7.4	298.1218	-6.6	$C_{18}H_{17}FNO_2^+$
	280	280.1132	280.1109	8.4	280.1136	-1.4	$C_{18}H_{15}FNO^+$
	237	237.1074	237.1060	5.9	237.1075	-0.3	$C_{17}H_{14}F^+$
	109	109.0448	109.0441	6.3	109.0446	2.1	$C_7H_6F^+$
CTR 360A	360	360.1606	360.1593	3.5	360.1613	-2.0	$C_{20}H_{23}FNO_4^+$
	299	299.1078	299.1076	0.7	299.1099	-7.2	$C_{18}H_{16}FO_3^+$
	281	281.0972	281.0970	0.9	281.0977	1.6	$C_{18}H_{14}FNO_2^+$
	237	237.1074	237.1072	1.0	237.1063	4.6	$C_{17}H_{14}F^+$
	109	109.0448	109.0448	0.1	109.0446	1.9	$C_7H_6F^+$
CTR 360B	360	360.1606	-	-	360.1600	1.6	$C_{20}H_{23}FNO_4^+$
	342	342.1500	-	-	342.1501	-0.3	$C_{20}H_{21}FNO_3^+$
	324	324.1394	-	-	324.1395	-0.3	$C_{20}H_{19}FNO_2^+$
	281	281.0972	-	-	281.0986	-4.8	$C_{18}H_{14}FNO_2^+$
	237	237.1074	-	-	237.1084	-4.1	$C_{17}H_{14}F^+$
	109	109.0448	-	-	109.0453	-4.5	$C_7H_6F^+$
	58	58.0651	-	-	58.656	-8.2	$C_3H_8N^+$
CTR 339B	339	339.1867	339.1877	2.9	339.1841	-7.7	$C_{21}H_{24}FN_2O^+$
	280	280.1132	280.1119	4.9	280.1108	8.7	$C_{18}H_{15}FNO^+$
	262	262.1027	262.1027	0.1	262.1013	5.3	$C_{18}H_{13}FN^+$
	247	247.0792	247.0797	-2.0	247.0772	-8.2	$C_{17}H_{10}FN^+$
	234	234.0714	234.0717	-1.4	234.0696	-7.5	$C_{16}H_9FN^+$
	109	109.0448	109.0435	12	109.0455	-6.4	$C_7H_6F^+$
CTR 355	355	355.1452	355.1455	0.6	355.1445	-2.2	$C_{20}H_{20}FN_2O_3^+$
	294	294.0925	294.0926	-0.5	294.0926	-0.2	$C_{18}H_{13}FNO_2^+$
	276	276.0819	276.0806	4.8	276.0820	-0.5	$C_{18}H_{11}FNO^+$

			RP		HILIC		
Compound	Nominal ion mass of $[M+H]^+$	Theoretical ion mass of $[M+H]^+$	Measured ion mass of $[M+H]^+$	Mass error (ppm)	Measured ion mass of $[M+H]^+$	Mass error (ppm)	Elemental Composition
	258	258.0714	258.0713	0.3	258.0739	-9.8	$C_{18}H_9FN^+$
	252	252.0455	252.0476	-12.9	252.0468	5.0	$C_{15}H_7FNO_2^+$

5.2.1 CTR 343

CTR 343 corresponds to an elemental composition of $C_{20}H_{24}FN_2O_2^+$, a compound with an additional atom of oxygen and two atoms of hydrogen in comparison to the parent compound.

With diagnostic neutral losses of H_2O and $NH(CH_3)_2$, the ion fragments at m/z 325 ($C_{20}H_{22}FN_2O^+$) and 298 ($C_{18}H_{17}FNO_2^+$) appear, whereas, the subsequent cleavage of either $NH(CH_3)_2$ from 325 or H_2O from 298, produce the fragment 280 ($C_{18}H_{15}FNO^+$). A further loss of NHCO, indicating the presence of an amide moiety, forms the most abundant ion 237 ($C_{17}H_{14}F^+$). The characteristic fragments 109 ($C_7H_6F^+$) and 58 ($C_3H_8N^+$) are also present here. Thus, the obtained MS/MS spectrum **(Figure 13)** confirms the proposed structure from the suspect list, which corresponds to CTR amide **(Figure 14)**.

The compound was fully identified reaching the first level of identification of TPs according to **Figure 4**, considering t_R and MS/MS spectra.

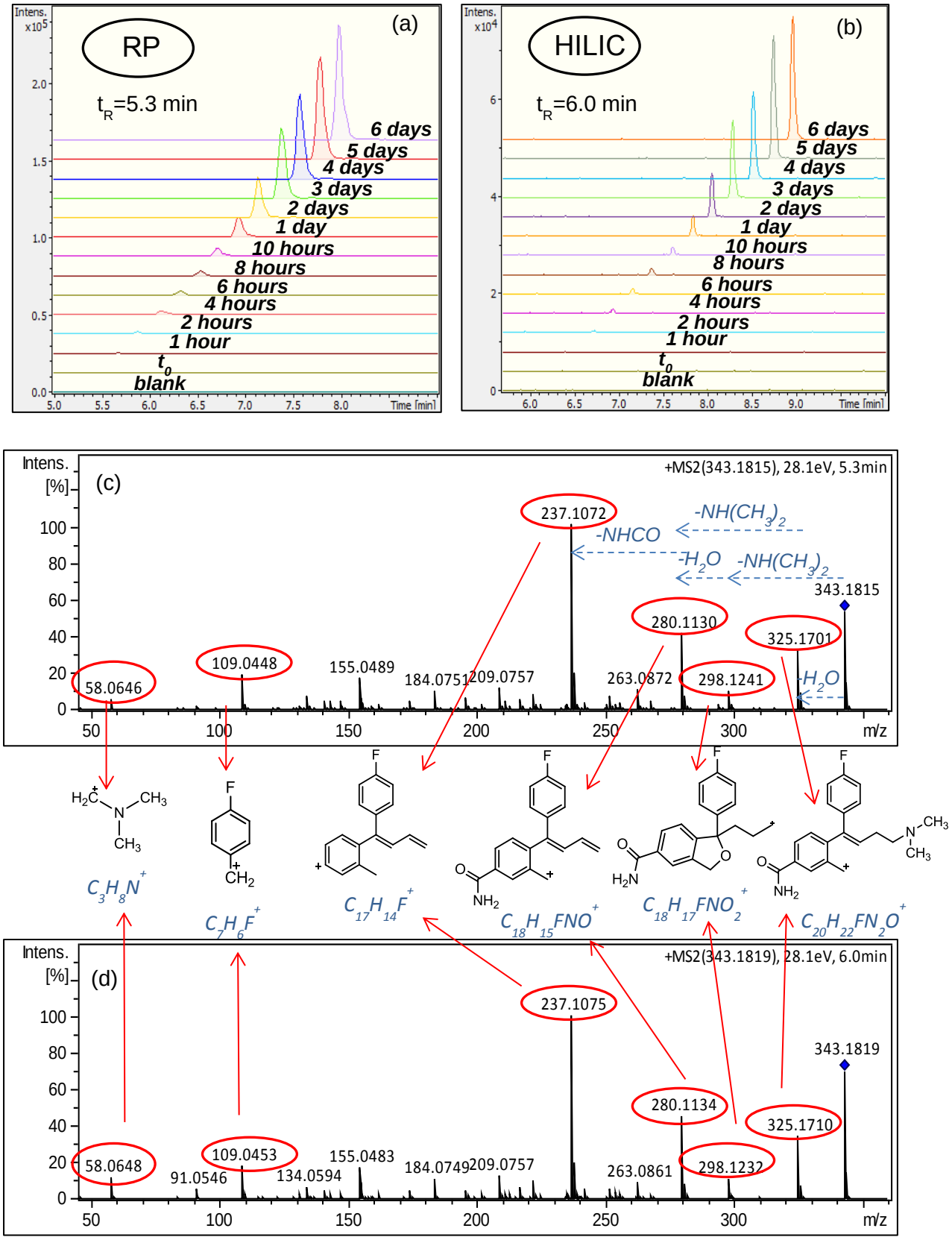

Figure 13: Analytical data for CTR 343; XICs of CTR 343 at incubation time points (time trend) in (a) RP and (b) HILIC; MS/MS spectra at t=144 h in (c) RP and (d) HILIC showing the fragmentation and proposed fragments of CTR 343.

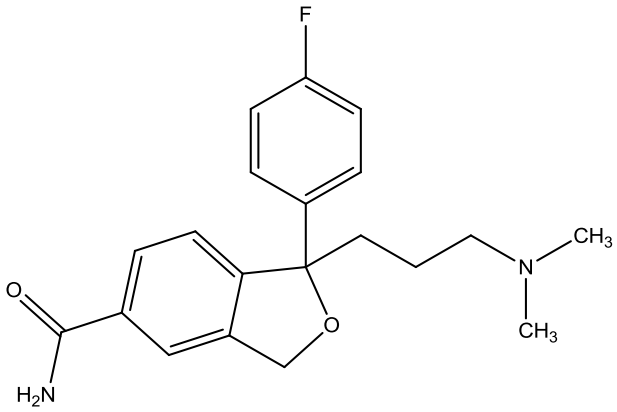

Figure 14: CTR amide.

5.2.2 CTR 344

The protonated form of CTR 344 has an elemental composition of $C_{20}H_{23}FNO_3^+$, and thus one nitrogen atom less as well two oxygen atoms and one hydrogen more, as compared to CTR, indicating the presence of a carboxylic acid group. One structure from the suspect database corresponds to the previous ion formula which is CTR carboxylic acid **(Figure 15)**.

Likewise **(Figure 16)**, initial fragmentation involves neutral losses of H_2O and $NH(CH_3)_2$ to the ions 326 ($C_{20}H_{21}FNO_2^+$) and 299 ($C_{18}H_{16}FO_3^+$), respectively. Stepwise, fragmentation of either m/z 326 or m/z 299, leads to the fragment ion at 281 ($C_{18}H_{14}FO_2^+$). Subsequent loss of CO_2 results in the formation of the major fragment 237 ($C_{17}H_{14}F^+$) confirming the carboxylic acid functional group.

The standard of CTR carboxylic acid was purchased and the identification was confirmed to achieve Level 1.

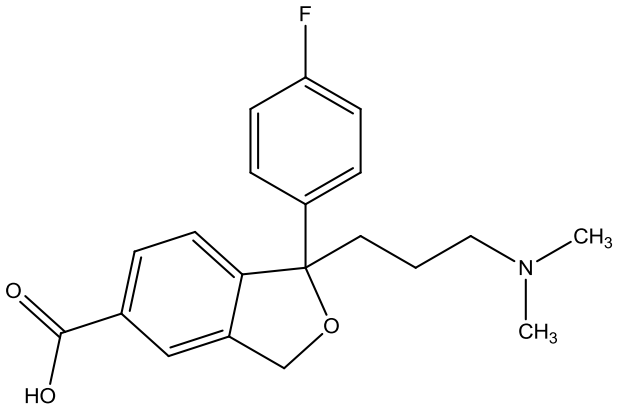

Figure 15: CTR carboxylic acid.

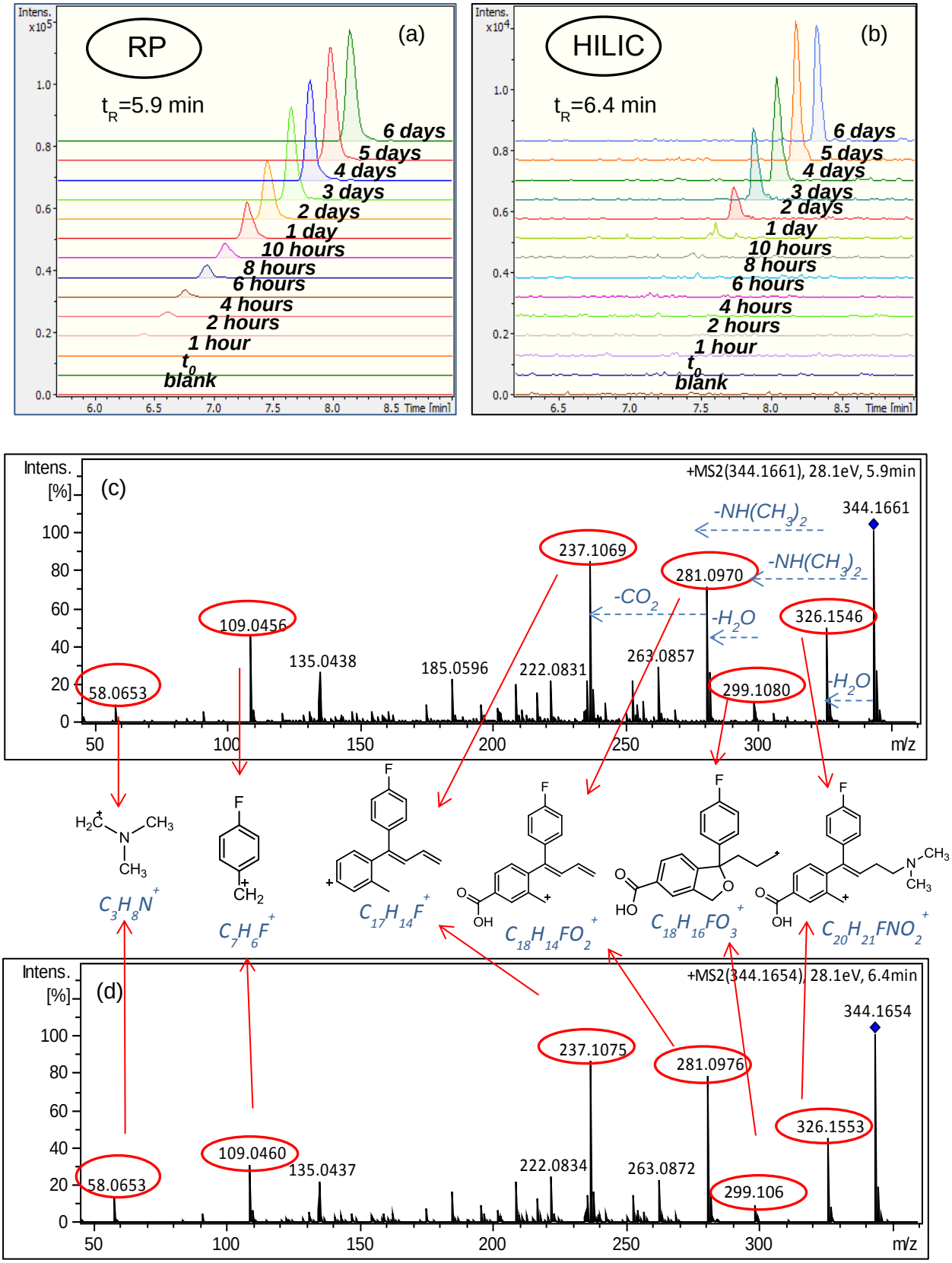

Figure 16: Analytical data for CTR 344; XICs of CTR 344 at incubation time points (time trend) in (a) RP and (b) HILIC; MS/MS spectra at t=120 h in (c) RP and (d) HILIC showing the fragmentation and proposed fragments of CTR 344.

5.2.3 CTR 311

The protonated molecule of CTR 311 indicates an elemental composition of $C_{19}H_{20}FN_2O^+$. This compound lacks one carbon atom and two hydrogens in comparison to CTR, suggesting the loss of a methyl group.

MS/MS fragmentation **(Figure 18)** revealed different neutral losses: $[M+H-18]^+$ attributable to the typical cleavage of H_2O and $[M+H-31]^+$ attributable to the loss of a methyl amino group ($-NH_2CH_3$), producing the fragments 293 ($C_{19}H_{18}FN_2^+$) and 280 ($C_{18}H_{15}FN_2O^+$). The formation of the ion m/z 262 ($C_{18}H_{13}FN_2^+$) can be explained by the elimination of either NH_2CH_3 from 293 or H_2O from 280. The ions from m/z 262 and below correspond to those found in the MS/MS spectrum of the parent compound. The only difference is the absence of characteristic fragment 58 which implies the cleavage of C-N bond with N-demethylation that transforms the tertiary amino group into a secondary one.

The identity of N-desmethylCTR **(Figure 17)** was confirmed through the purchase and analysis of the standard for this compound, reaching level 1.

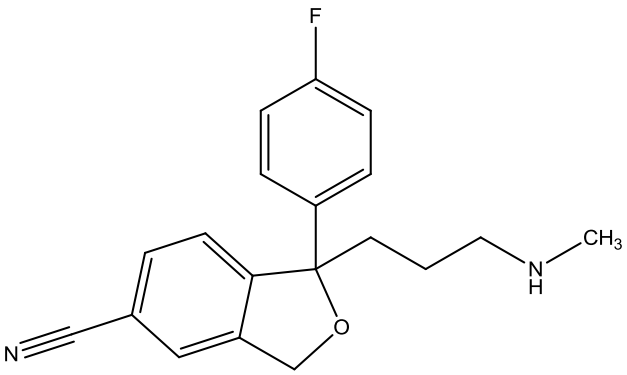

Figure 17: N-desmethyl CTR.

N-desmethylCTR is not only a TP that is formed during biodegradation experiments but also a product of human metabolism which is further metabolized in the liver into N-didesmethylCTR. However, the latter was not detected as a TP in the investigated treatment process, indicating that N-desmethylCTR is subjected to a transformation pathway that differs from human metabolism as it is described below.

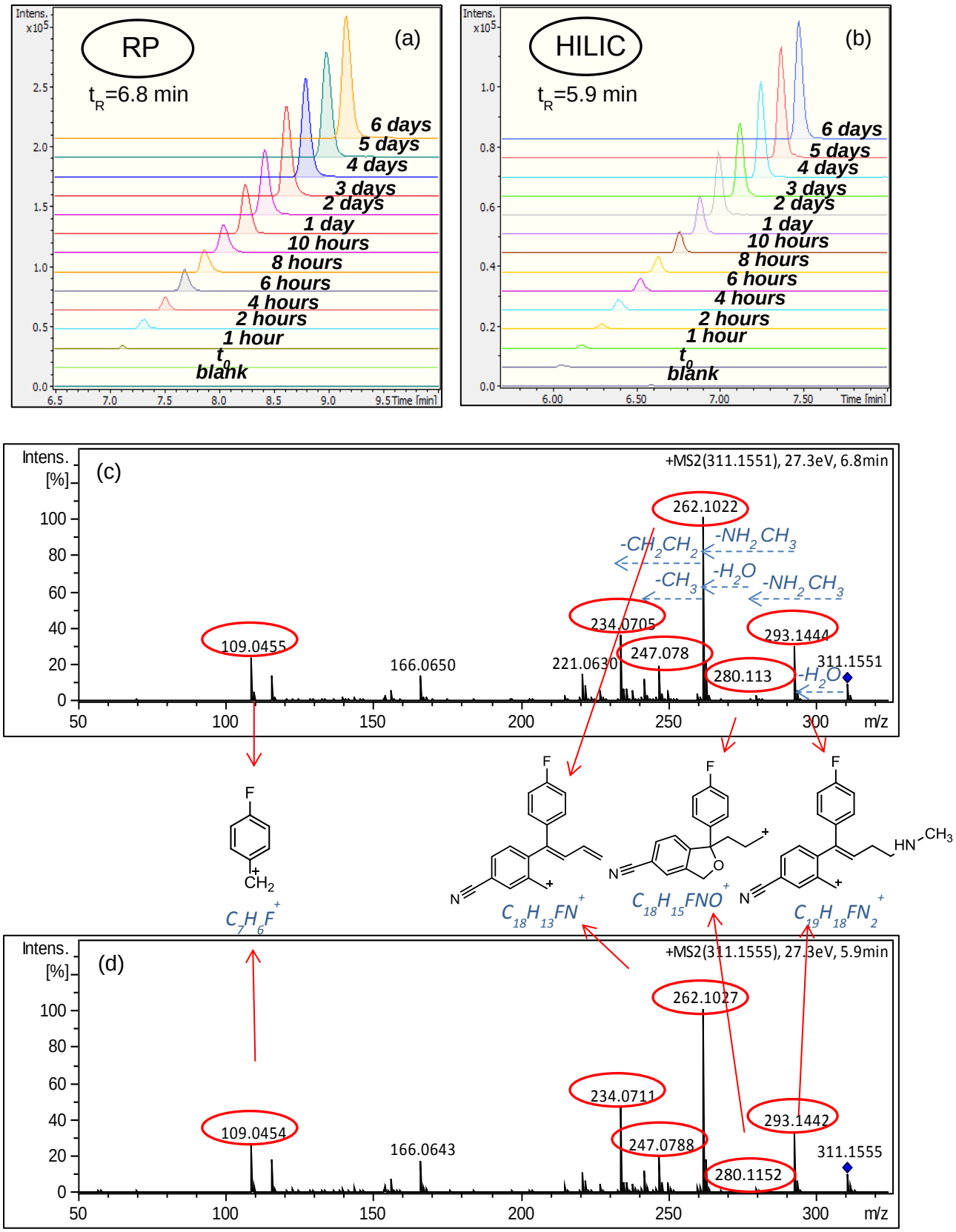

Figure 18: Analytical data for CTR 311; XICs of CTR 311 at incubation time points (time trend) in (a) RP and (b) HILIC; MS/MS spectra at t=144 h in (c) RP and (d) HILIC showing the fragmentation and proposed fragments of CTR 311.

5.2.4 CTR 329

With respect to the protonated formula of CTR 329 ($C_{19}H_{22}FN_2O_2^+$) and the observed fragment ions being similar to those of CTR 343, the cyano group of CTR substituted with an amide moiety.

The additional close analogy between the MS/MS spectra of CTR 311 and 329 clearly indicates that the modification took place at the side chain of the molecule and specifically at the tertiary amino group. Similar to CTR 311, MS/MS spectrum of CTR 329 **(Figure 20)** represents the same characteristic cleavages of H_2O and NH_2CH_3 producing 311 ($C_{19}H_{20}FN_2O^+$) and 298 ($C_{18}H_{17}FNO_2^+$), respectively. The subsequent loss of NHCO forming the fragment 237 ($C_{17}H_{14}F^+$) can be attributed to the presence of the amide group. Moreover, the absence of 58 confirms the N-demethylated amide derivative.

Thus, CTR 329 is proposed to be N-desmethylCTR amide **(Figure 19)** achieving a confidence level of 2b.

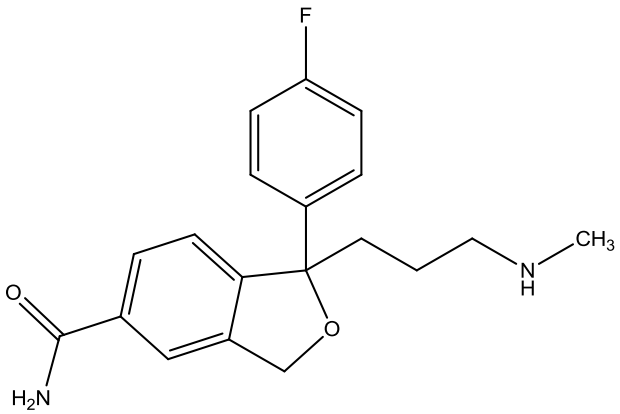

Figure 19: N-desmethylCTR amide.

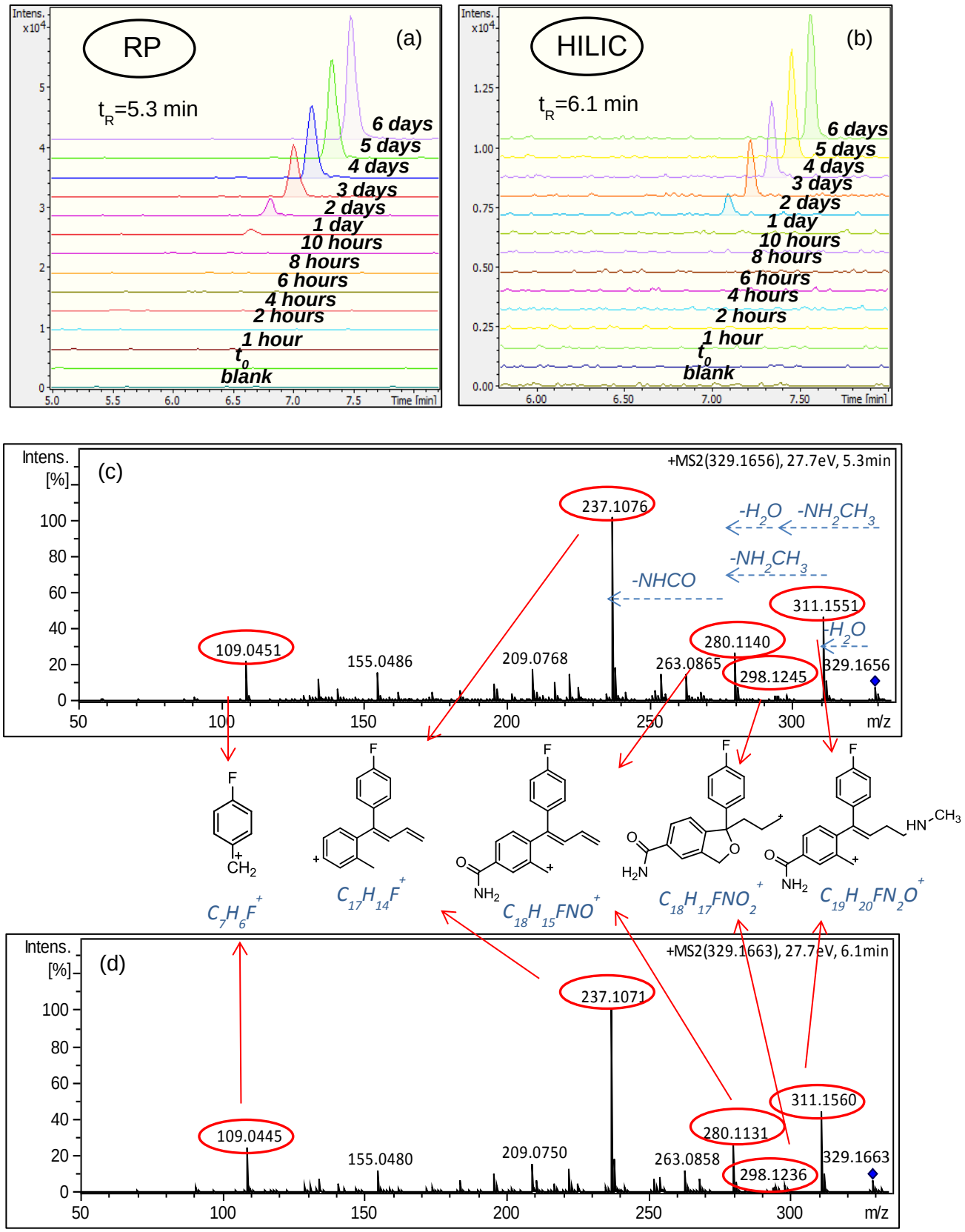

Figure 20: Analytical data for CTR 329; XICs of CTR 329 at incubation time points (time trend) in (a) RP and (b) HILIC; MS/MS spectra at t=144 h in (c) RP and (d) HILIC showing the fragmentation and proposed fragments of CTR 329.

5.2.5 CTR 330

The elemental composition of $C_{19}H_{21}FNO_3^+$ was assigned to CTR 330. On the basis of the fragmentation pathway of CTR 344, the abundant product ion formation of 237 ($C_{17}H_{14}F^+$) by decarboxylation was attributed to the presence of a carboxylic acid group. Moreover, similar to CTR 311, MS/MS spectrum of CTR 330 **(Figure 22)** represent the same initial cleavages of H_2O and NH_2CH_3 forming the ions 312 ($C_{19}H_{19}FNO_2^+$) and 299 ($C_{18}H_{16}FO_3^+$), respectively. The additional lack of fragment 58 leads to the suggestion of N-desmethylCTR carboxylic acid **(Figure 21)** and a confidence level of 2b for CTR 330.

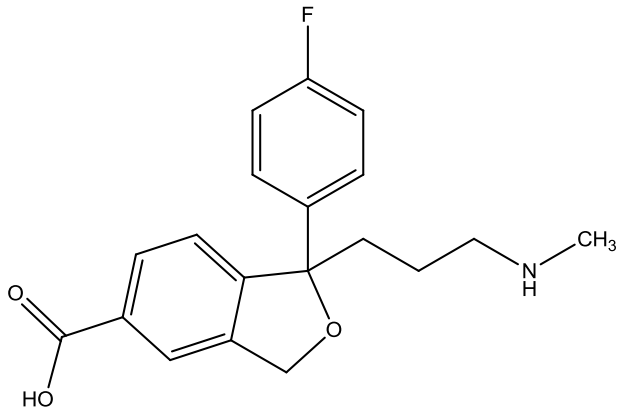

Figure 21: N-desmethylCTR carboxylic acid.

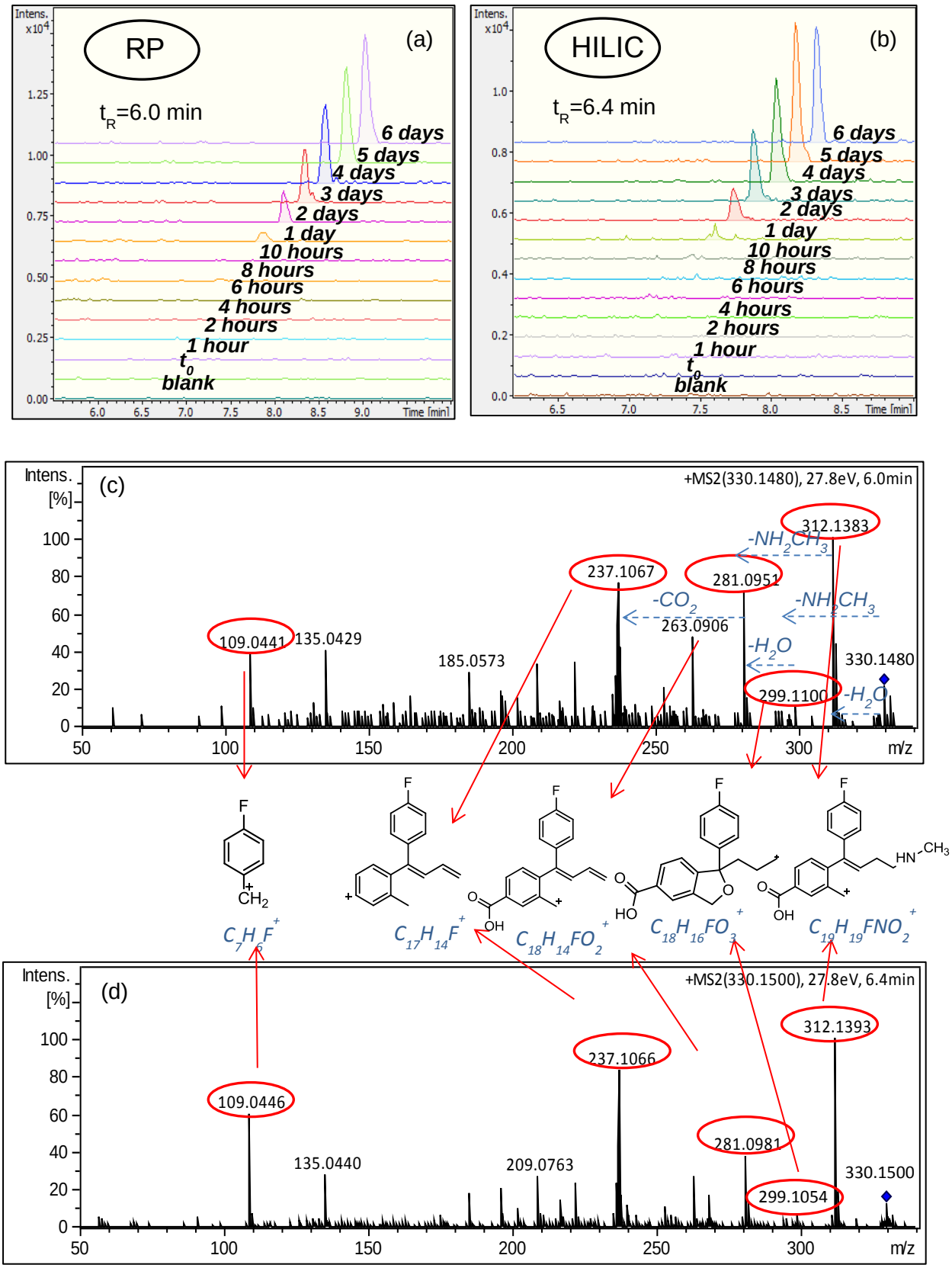

Figure 22: Analytical data for CTR 330; XICs of CTR 330 at incubation time points (time trend) in (a) RP and (b) HILIC; MS/MS spectra at t=144 h in (c) RP and (d) HILIC showing the fragmentation and proposed fragments of CTR 330.

5.2.6 CTR 341

The elemental composition of CTR 341 ($C_{20}H_{22}FN_2O_2^+$) indicates that one additional oxygen is being introduced into CTR and suggests a compound, which could, in principle, correspond to either an N-oxygenated or a hydroxylated TP. The fragmentation pattern **(Figure 24)** shows the direct cleavage of -$NH(CH_3)_2O$ group forming the fragment ion at m/z 280 ($C_{18}H_{15}FNO^+$). This is subjected to a further loss of H_2O at m/z 262, characteristic for CTR and N-desmethylCTR. As they share the fragment ions at m/z 280 and 262, it is revealed that this part of the molecule remained intact and that the structural change occurred at the tertiary amino group. Moreover, the absence of characteristic fragment 58 indicates the position of the additional oxygen. Consequently, CTR 341 is proposed to be CTR-N-oxide **(Figure 23)** reaching the 2a level of confidence matching literature data [38].

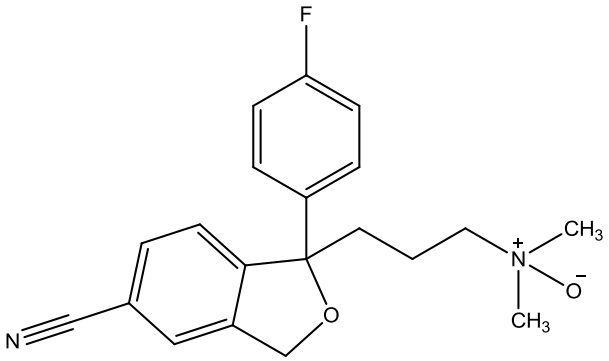

Figure 23: CTR-N-oxide.

CTR 341 (CTR N-oxide) was the most dominant TP in this experiment and peaked at 72 hours after its appearance, indicating further transformation. Apart from a TP, it is also a human metabolite formed from CTR *via* N-oxidation.

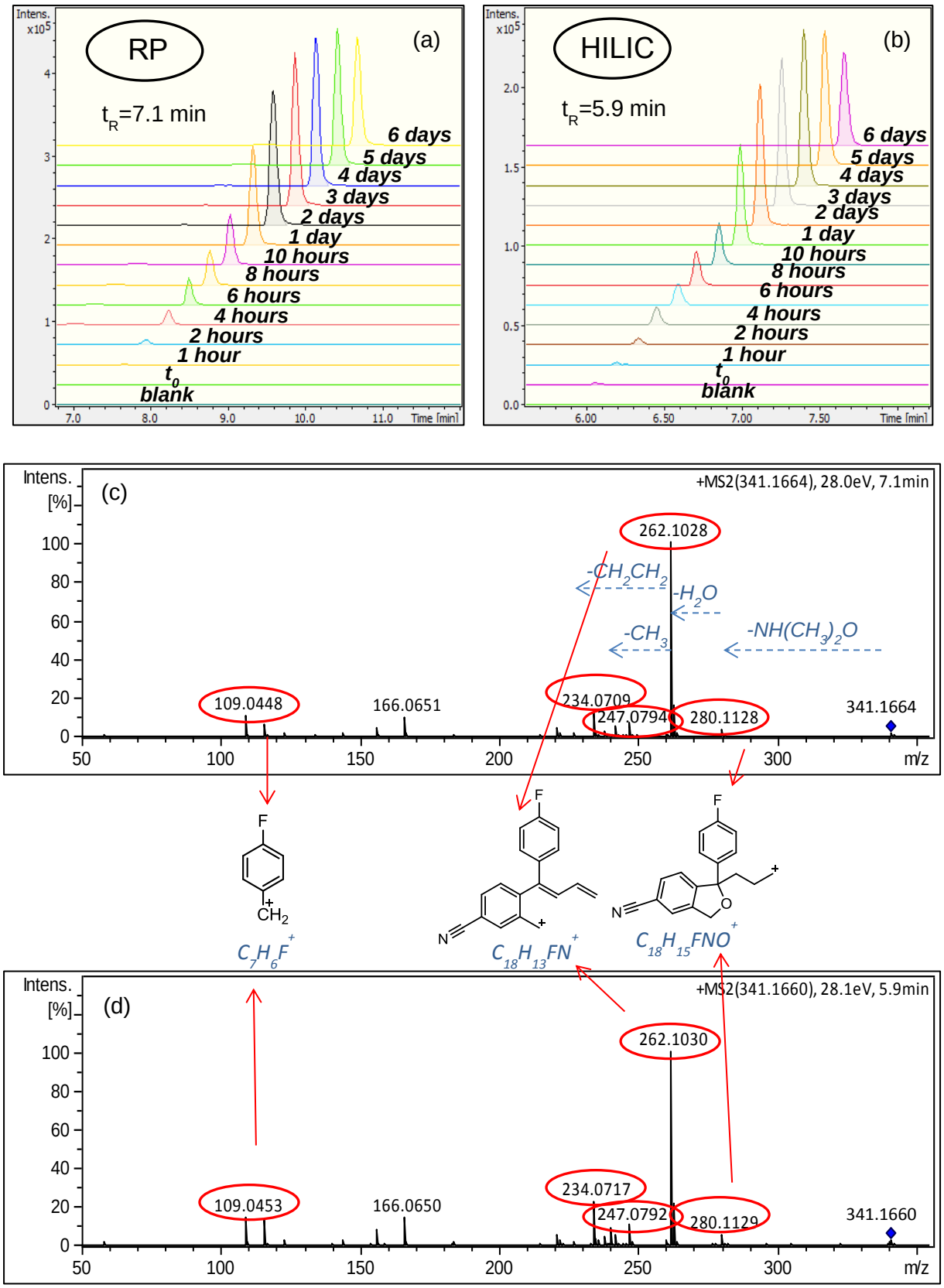

Figure 24: Analytical data for CTR 341; XICs of CTR 341 at incubation time points (time trend) in (a) RP and (b) HILIC; MS/MS spectra at t=72 h in (c) RP and (d) HILIC showing the fragmentation and proposed fragments of CTR 341.

5.2.7 CTR 359A and CTR 359B

Two more TPs **(Figure 25)**, detected by post-acquisition data processing, eluted at t_R 4.7 and 5.4 min in RP chromatographic system showing their protonated molecules at $[M+H]^+$ 359.1770 (CTR 359A) and 359.1771 (CTR 359B), respectively. The TPs could be separated both chromatographically and by HR-MS. The same elemental composition, $C_{20}H_{24}FN_2O_3^+$, was assigned to both of them. Despite the unique elemental composition, their t_R and their MS/MS spectra prove their different identity. Both MS/MS spectra of the TPs show similarities with the MS/MS spectra of CTR 343 which is a sign of the presence of an amide moiety.

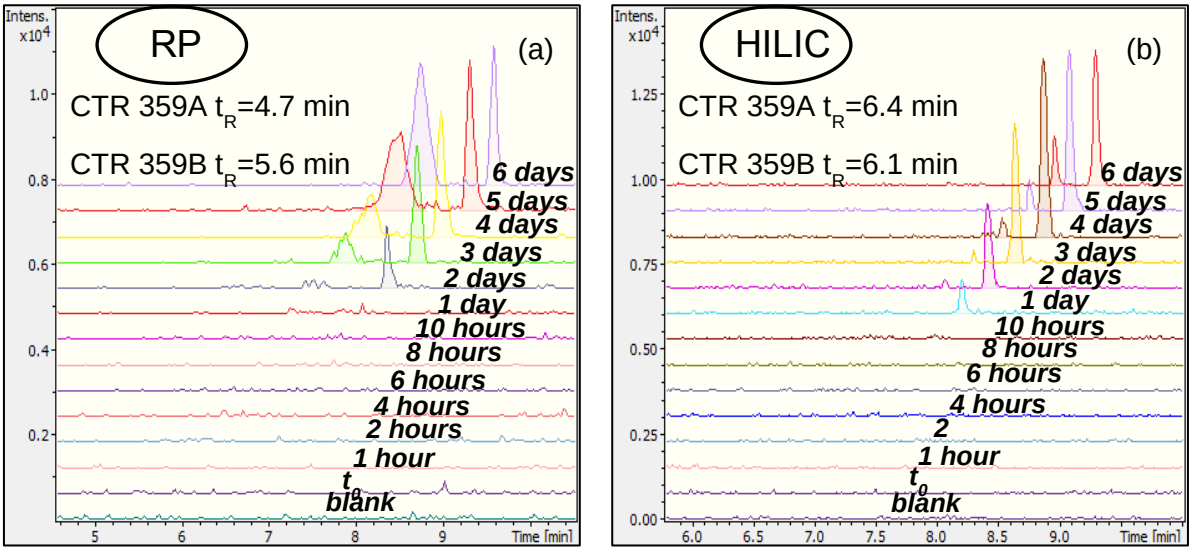

Figure 25: XICs of CTR 359A and CTR 359B at incubation time points (time trend) in (a) RP and (b) HILIC.

More specifically, the MS/MS spectrum of CTR 359A **(Figure 26)** exhibited fragment ions at m/z 341 ($C_{20}H_{22}FN_2O_2^+$) and m/z 323 ($C_{20}H_{20}FN_2O^+$), both generated by one or two cleavages of H_2O. The cleavage of $NH(CH_3)_2O$ from 341 produces the fragment 280 ($C_{18}H_{15}FNO^+$), which along with the presence of m/z 58, indicates one possible position of hydroxylation in tertiary amine aliphatic chain. As a result, CTR 359A can be identified as a hydroxylated derivative of CTR amide **(Figure 27)**, reaching level 2b.

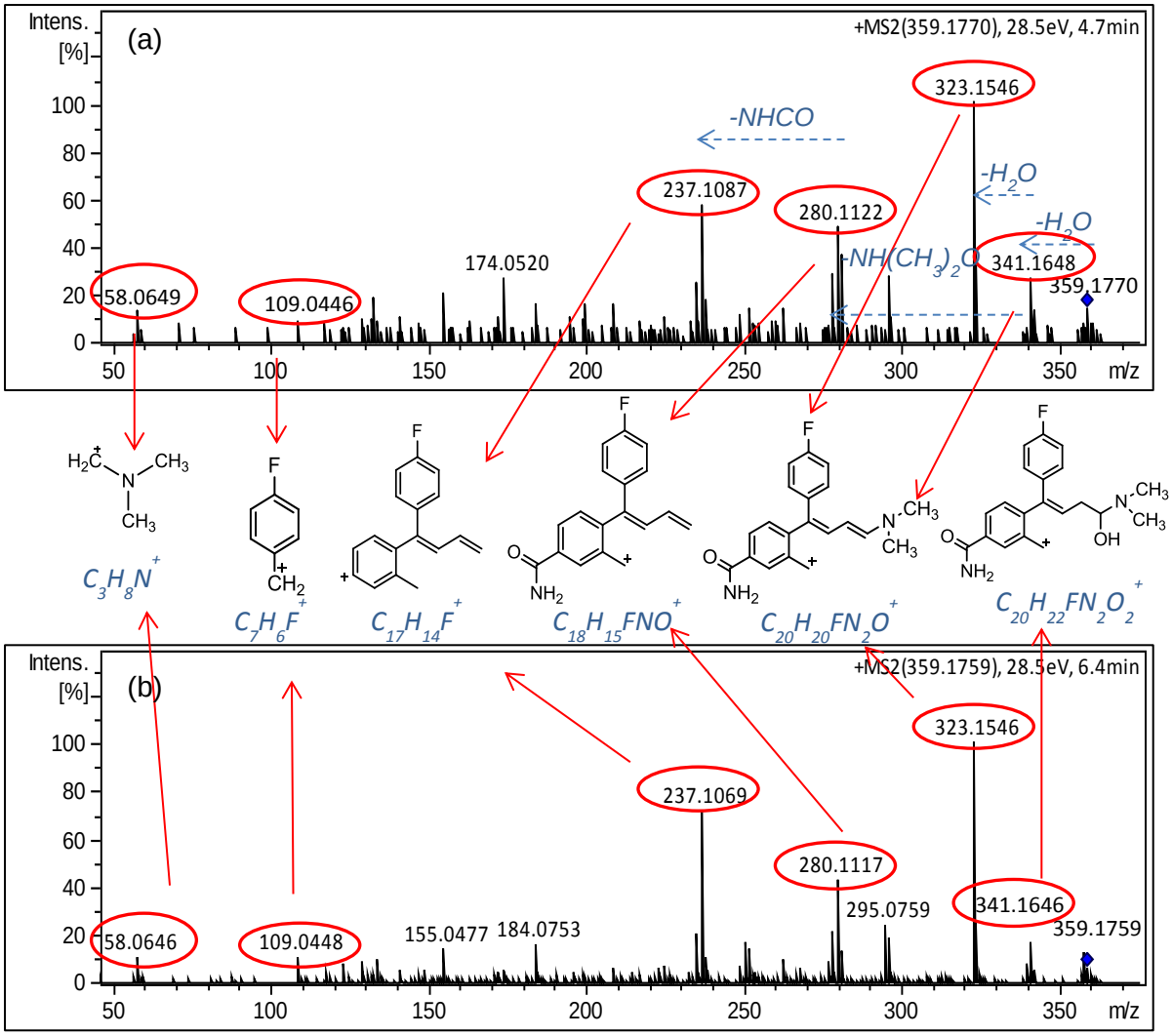

Figure 26: MS/MS spectra of CTR 359A at t=144 h in (a) RP and (b) HILIC showing the fragmentation and proposed fragments.

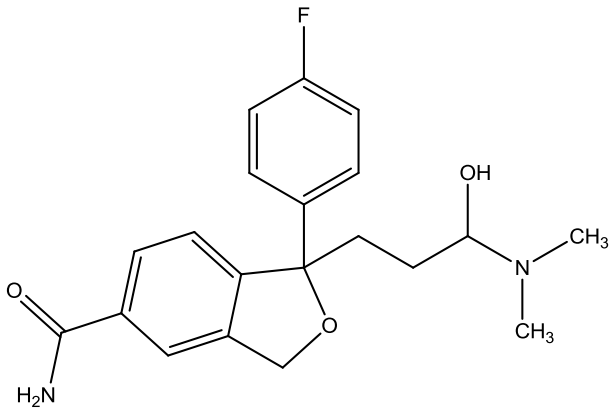

Figure 27: Hydroxylated derivated of CTR amide.

The second-eluted TP shows an MS/MS fragmentation pattern **(Figure 28)** that also corresponds to that of CTR 341 showing a direct loss of -$NH(CH_3)_2O$ at m/z 298 ($C_{18}H_{17}FNO_2^+$). Further on, the absence of m/z 58 suggests the formation of an N-oxygenated amide derivative. With this evidence, an identification level of 2b was assigned to CTR 359B which is proposed to be the amide of CTR-N-oxide **(Figure 29)**.

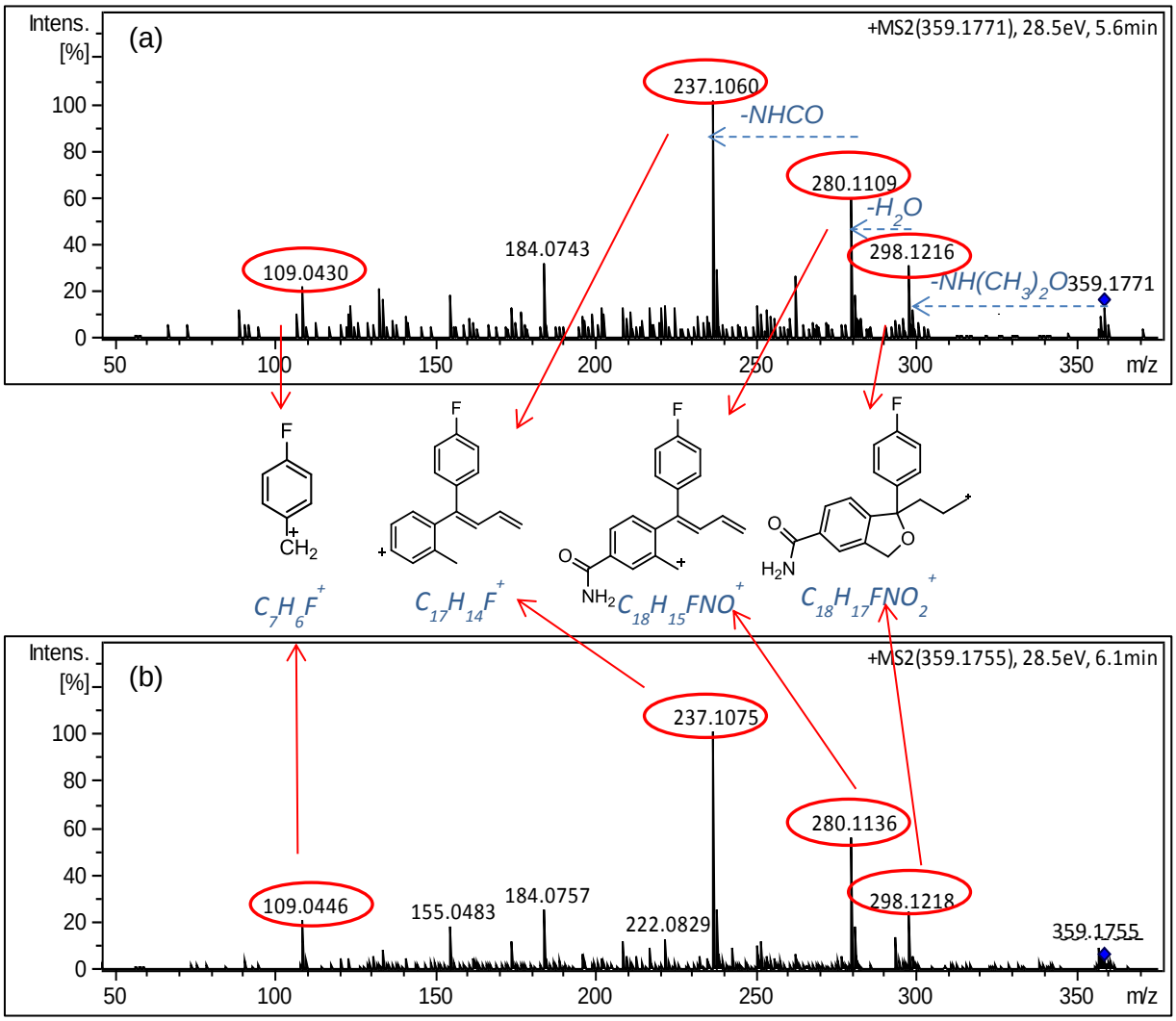

Figure 28: MS/MS spectra of CTR 359B at t=96 h in (a) RP and (b) HILIC showing the fragmentation and proposed fragments.

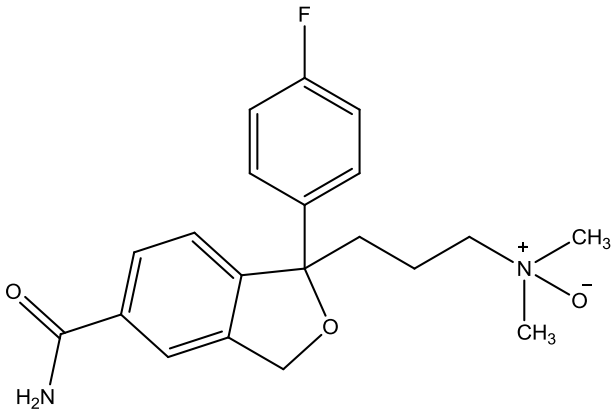

Figure 29: Amide of CTR-N-oxide.

5.2.8 CTR 360A and CTR 360B

CTR 360A has a retention time of 6.3 min and 6.7 min in RP and HILIC chromatographic systems **(Figure 30)**, respectively and an elemental composition of $C_{20}H_{23}FNO_4^+$. Its MS/MS spectrum **(Figure 31)** represents a direct elimination of $NH(CH_3)_2O$ at m/z 299 ($C_{18}H_{16}FO_3^+$) implying the presence of an N-oxide group. The ions from 299 and below correspond to those found in the MS/MS spectrum of CTR 344, apart from fragment m/z 58. Consequently, CTR 360A is proposed to be the carboxylic acid of CTR-N-oxide **(Figure 32)**, increasing the confidence to reach level 2b.

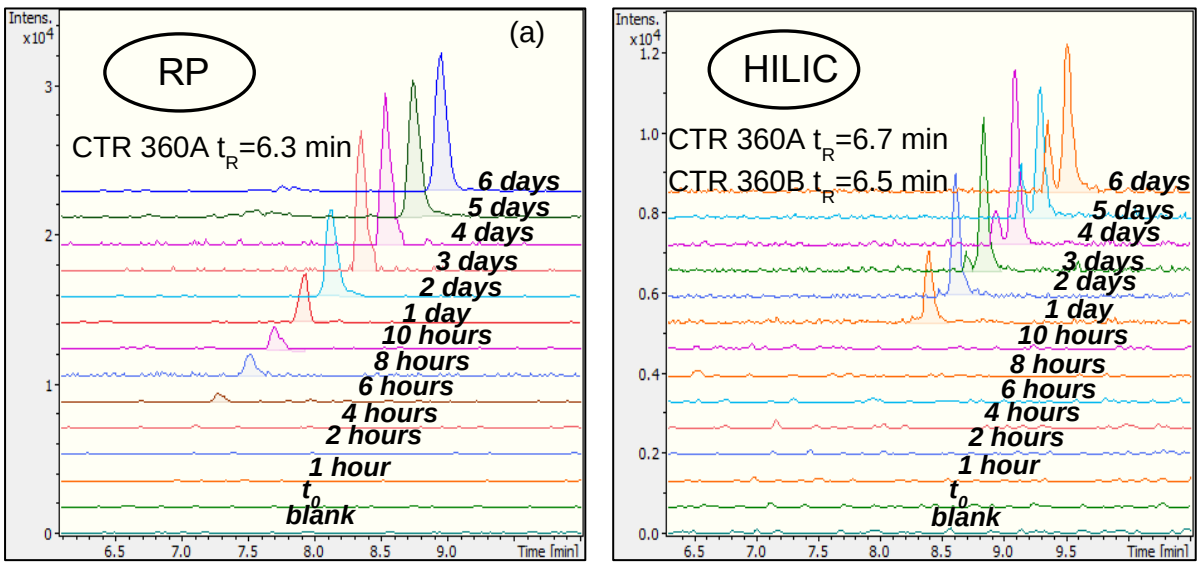

Figure 30: XICs of CTR 360A and CTR 360B at incubation time points (time trend) in (a) RP and (b) HILIC.

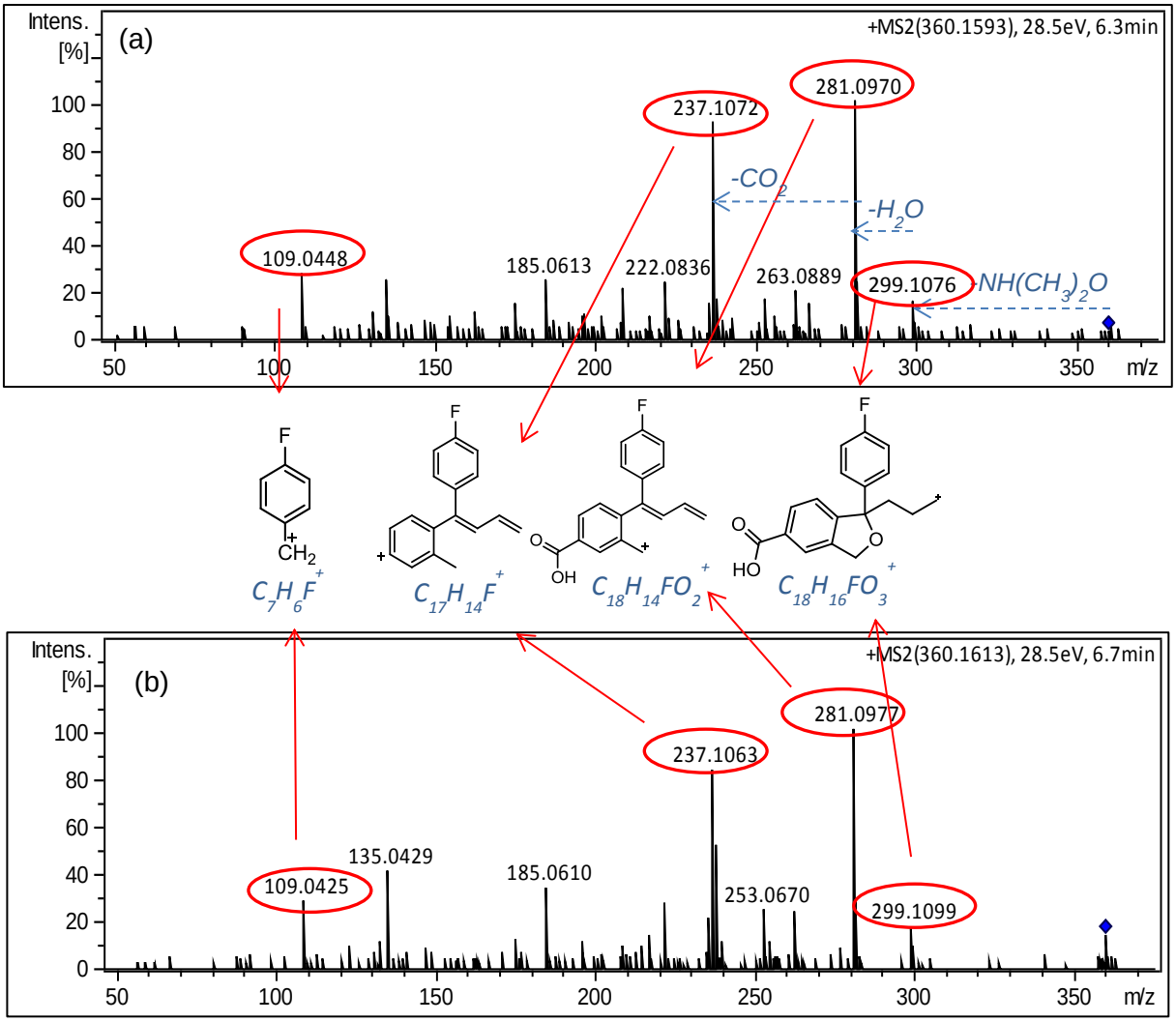

Figure 31: MS/MS spectra of CTR 360A at t=144 h in (a) RP and (b) HILIC showing the fragmentation and proposed fragments.

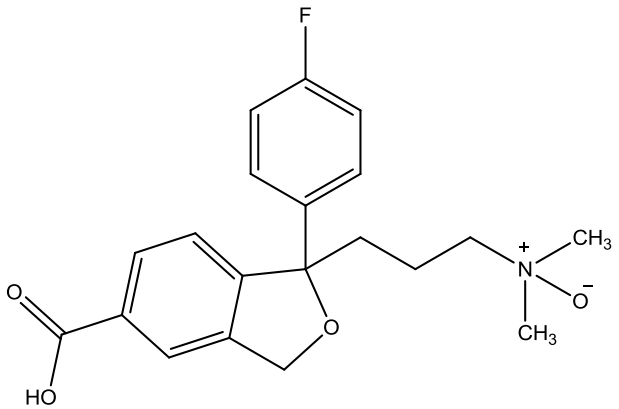

Figure 32: Carboxylic acid of CTR-N-oxide.

However, when HILIC chromatographic separation was performed, another TP of CTR (CTR 360B) emerged at 6.5 min with the same nominal mass and elemental composition as CTR 360A. It can be assumed that when RP analysis was conducted, the isomers could not be separated chromatographically.

CTR 360B shows a MS/MS fragmentation pattern **(Figure 33)** that is also analogous to that of CTR 344, but differing in that two H_2O molecules are cleaved, forming ions 342 ($C_{20}H_{21}FNO_3^+$) and 324 ($C_{20}H_{19}FNO_2^+$). Further fragmentation of 342 produces the fragment 281 ($C_{18}H_{14}FO_2^+$), succeeded by the loss of $NH(CH_3)_2O$.

Thus, CTR 360B is suggested to be a hydroxylated derivative of CTR carboxylic acid with an achieved confidence level of 2b **(Figure 34)**.

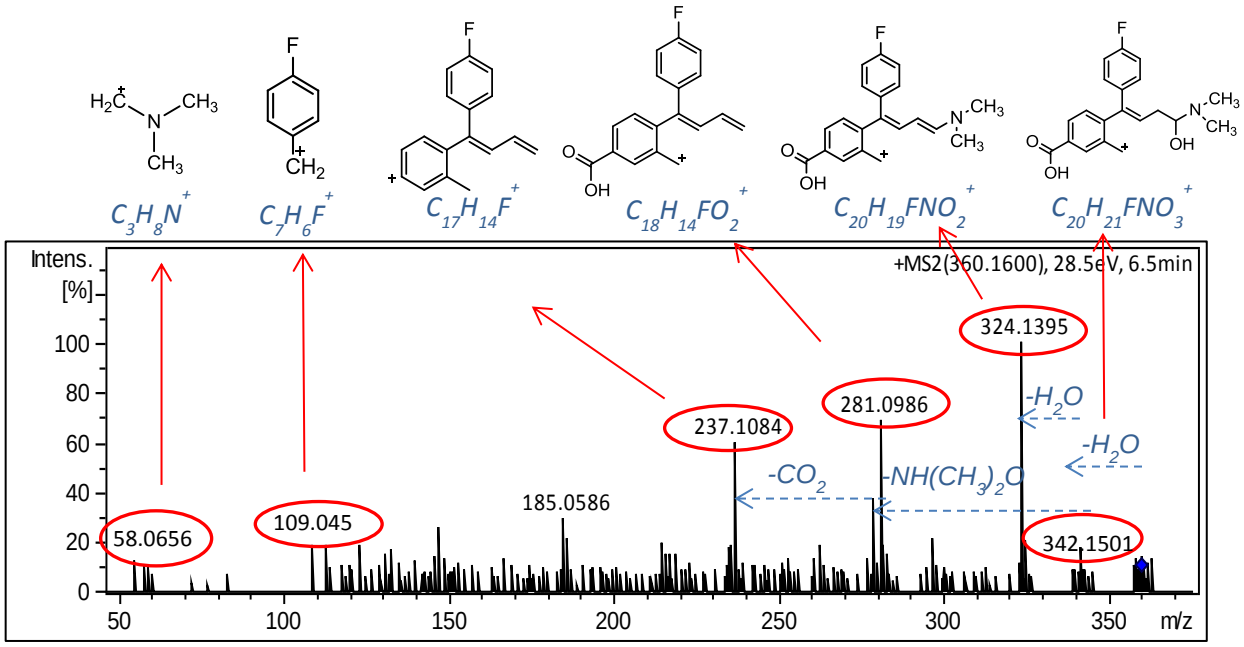

Figure 33: MS/MS spectrum at t=144 h in HILIC showing the fragmentation and proposed fragments of CTR 360B.

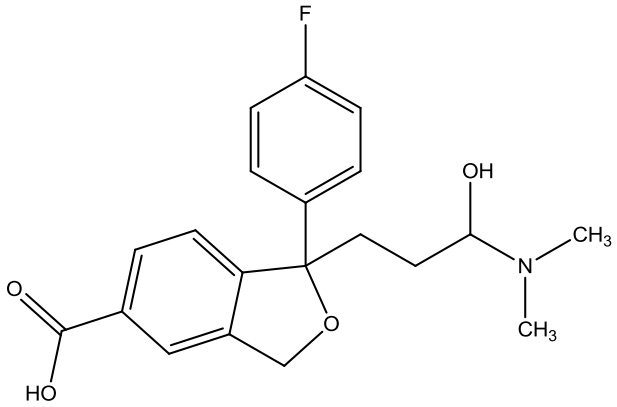

Figure 34: Hydroxylated derivative of CTR carboxylic acid.

5.2.9 CTR 339A

CTR 339A has an elemental composition of $C_{20}H_{20}FN_2O_2^+$ and contains one oxygen more and two protons less as compared to CTR. It can be observed **(Figure 35)** that the same characteristic losses of H_2O and $NH(CH_3)_2$ occur, yielding the fragment ions 321 ($C_{20}H_{18}FN_2O^+$) and 294 ($C_{18}H_{13}FNO_2^+$). The subsequent cleavage of either $NH(CH_3)_2$ or H_2O from 321 and 294 respectively, leads to the most abundant fragment at m/z 276 ($C_{18}H_{11}FNO^+$). However, the crucial fragment ions at m/z 258 ($C_{18}H_9FN^+$) and m/z 248 ($C_{17}H_{11}FN^+$), which represent the elimination of H_2O and CO moieties, denote the proposed structure of 3-oxo-CTR **(Figure 36)**. It should be noticed that the fluorinated analogue with nominal mass 109 ($C_7H_6F^+$), which is diagnostic of CTR and its TPs, is absent here.

A commercial standard of 3-oxo-CTR was purchased and the identity of the compound was confirmed *via* appropriate MS/MS and t_R matching, reaching finally Level 1.

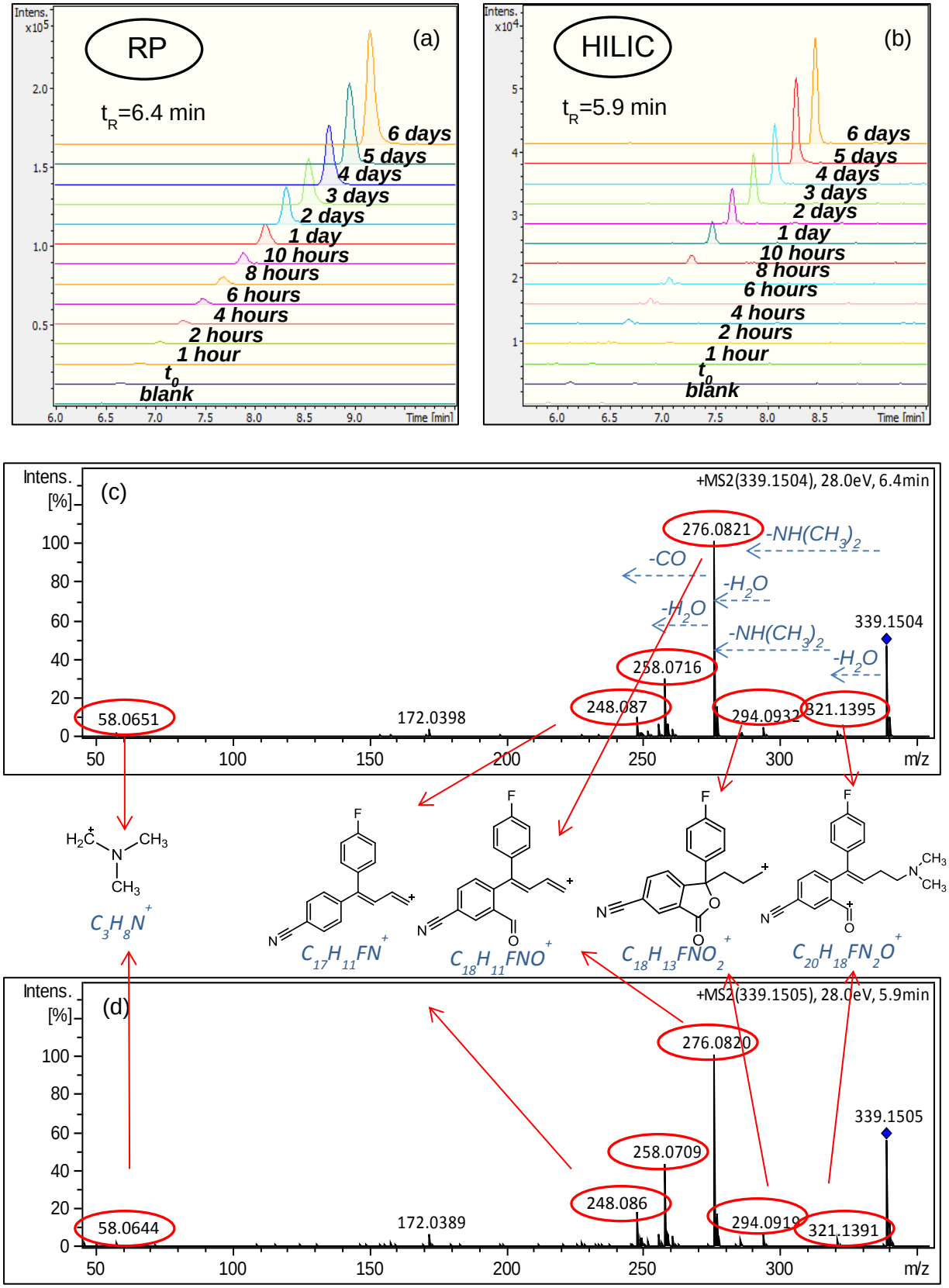

Figure 35: Analytical data for CTR 339A; XICs of CTR 339A at incubation time points (time trend) in (a) RP and (b) HILIC; MS/MS spectra at t=144 h in (c) RP and (d) HILIC showing the fragmentation and proposed fragments of CTR 339A.

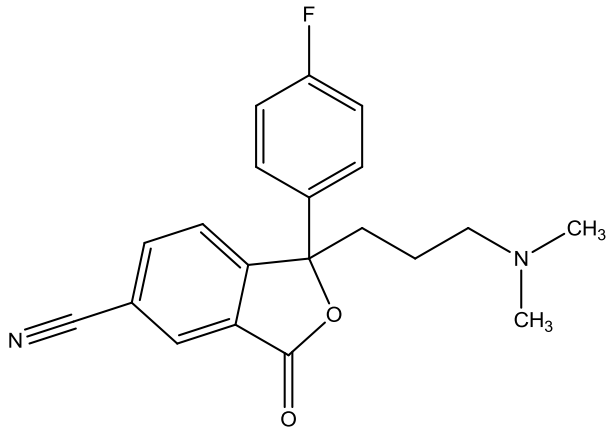

Figure 36: 3-oxo-CTR.

5.2.10 CTR 357

The protonated molecule of CTR 357 indicates a corresponding elemental composition of $C_{20}H_{22}FN_2O_3^+$.

Although the suspect database indicates several double-hydroxylated substituted compounds, the fragmentation pattern **(Figure 38)** of the TP did not correspond to any of them. The absence of characteristic fragment 109 indicates a 3-oxo-CTR derivative while the diagnostic cleavages of H_2O and $NH(CH_3)_2$ are also observed here. Further fragmentation produces the dominant ion 294 ($C_{18}H_{13}FNO_2^+$), whereas the subsequent loss of NHCO suggests the presence of an amide group.

As a result, CTR 357 is proposed to be an oxidized derivative of CTR amide **(Figure 37)**, allowing the assignment of a confidence level of 2b.

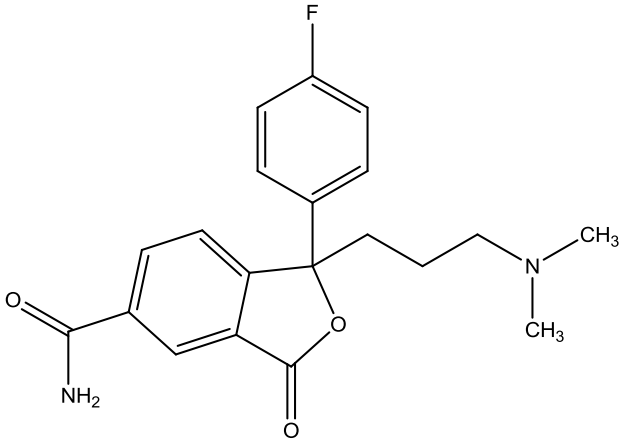

Figure 37: CTR 357.

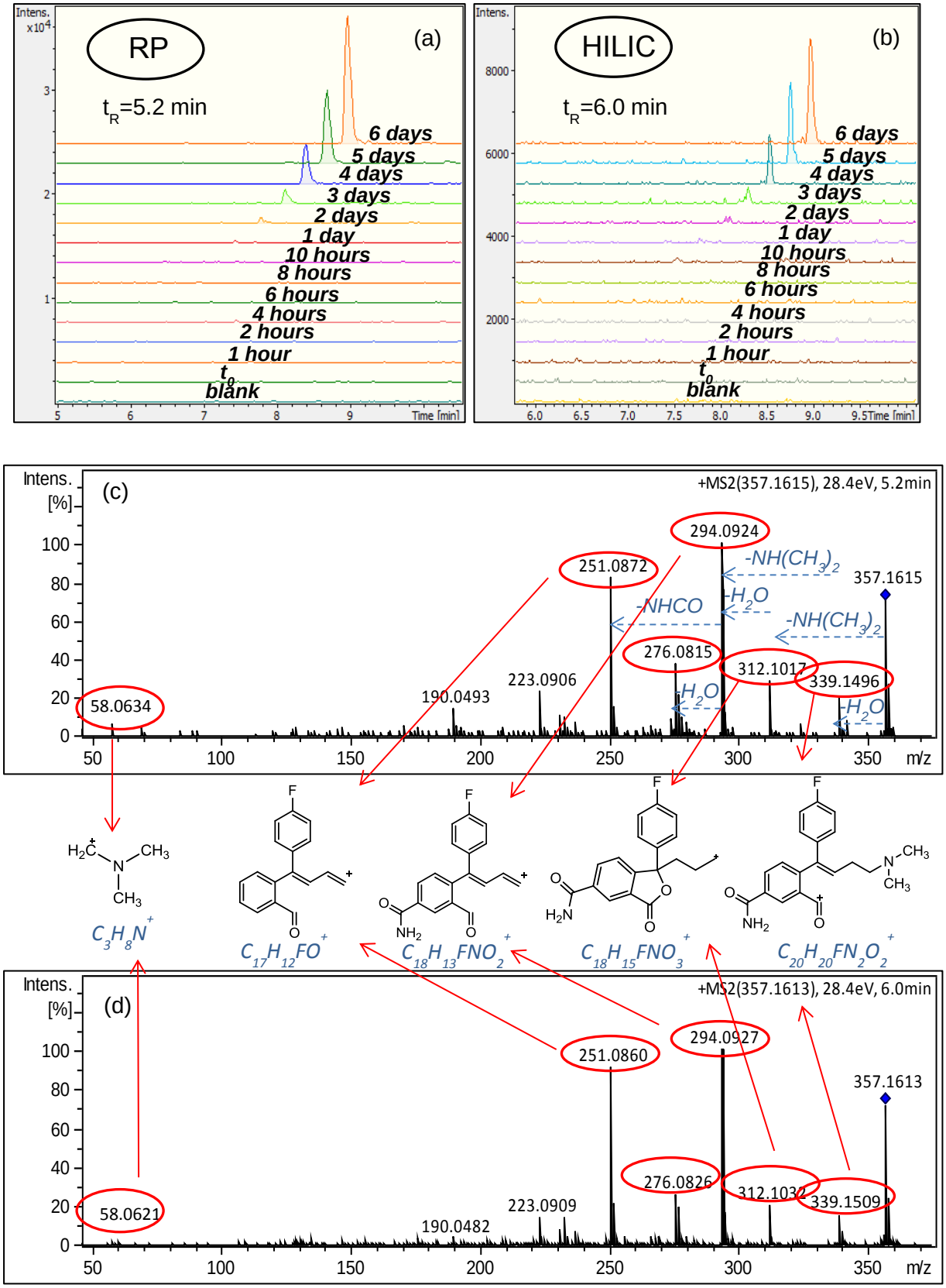

Figure 38: Analytical data for CTR 357; XICs of CTR 357 at incubation time points (time trend) in (a) RP and (b) HILIC; MS/MS spectra at t=144 h in (c) RP and (d) HILIC showing the fragmentation and proposed fragments of CTR 357.

5.2.11 CTR 355

An elemental composition of $C_{20}H_{20}FN_2O_3^+$, involving two additional oxygens and two hydrogens less in comparison to CTR, was assigned to CTR 355, which detected through non-target screening.

Although, MS/MS fragmentation **(Figure 40)** seems to be insufficient for the structure elucidation, the mass spectrum of CTR 355 displays two distinct features: on one hand, the direct cleavage of $NH(CH_3)_2O$ along with the absence of 58 provided strong evidence for the location of the one oxygen; on the other hand, the complete lack of the fragment 109 implies the formation of a 3-oxo-CTR derivative. Moreover, the conserved fragment ions at 294 and 276 clearly indicated the second oxidation to have occurred at the furan ring.

Thus, CTR 355 can gain in confidence through to level 2b, pointing out a double-oxidized TP of CTR **(Figure 39)**.

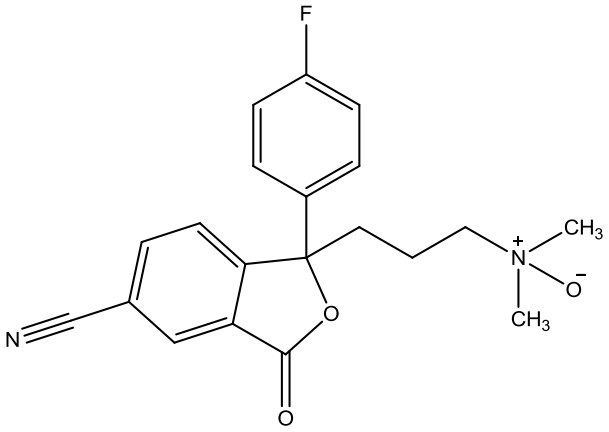

Figure 39: CTR 355.

5.2.12 CTR 339B

CTR 339B was detected also *via* the non-target screening approach with an elemental composition of $C_{21}H_{24}FN_2O^+$, suggesting the introduction of a methyl group to the parent compound **(Figure 41)**. However, it was not possible to go beyond the determination of the unequivocal molecular formula (level 4).

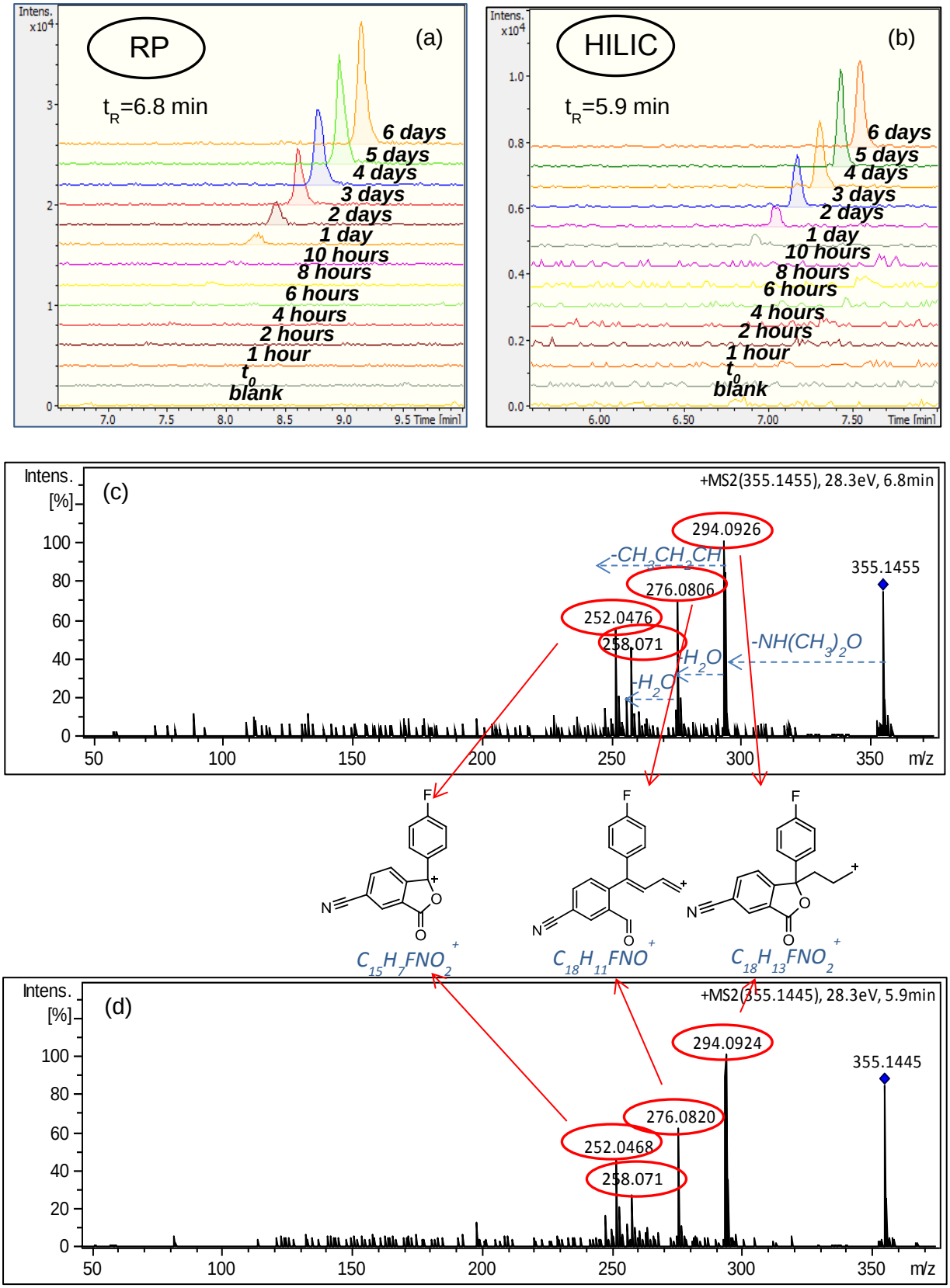

Figure 40: Analytical data for CTR 355; XICs of CTR 355 at incubation time points (time trend) in (a) RP and (b) HILIC; MS/MS spectra at t=144 h in (c) RP and (d) HILIC showing the fragmentation and proposed fragments of CTR 355.

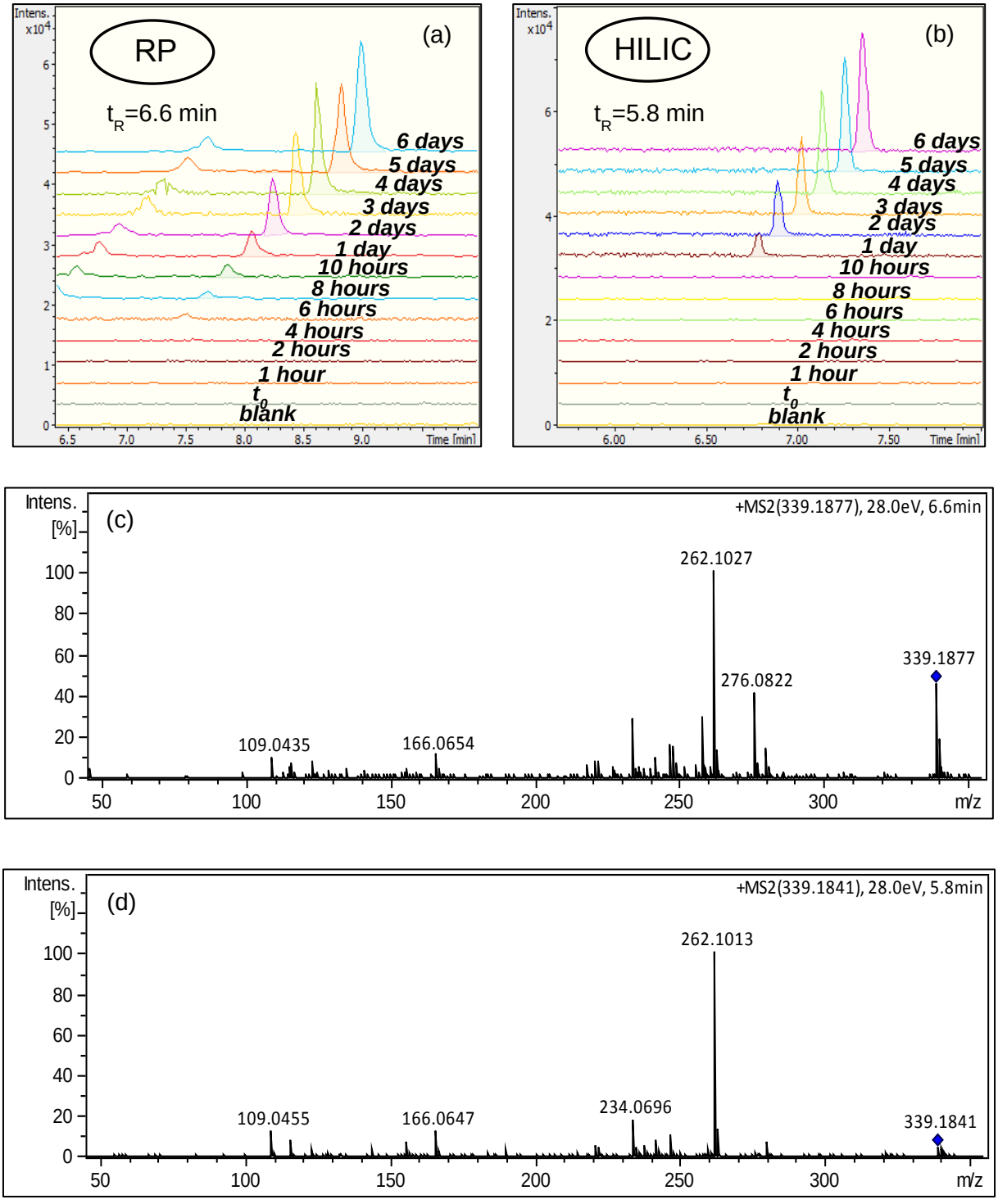

Figure 41: Analytical data for CTR 339B; XICs of CTR 339B at incubation time points (time trend) in (a) RP and (b) HILIC; MS/MS spectra at t=144 h in (c) RP and (d) HILIC of CTR 339B.

5.2.13 Proposed biotransformation pathway of CTR

A pathway for the biotic transformation of CTR was proposed **(Figure 42)** based on both the chemical structures of the identified TPs and the sequence of TP formation in the batch system.

Oxidative reactions, such as hydroxylation, oxidation, N-oxidation and N-demethylation, were observed as the primary biotransformation mechanisms as well nitrile hydrolysis and amide hydrolysis.

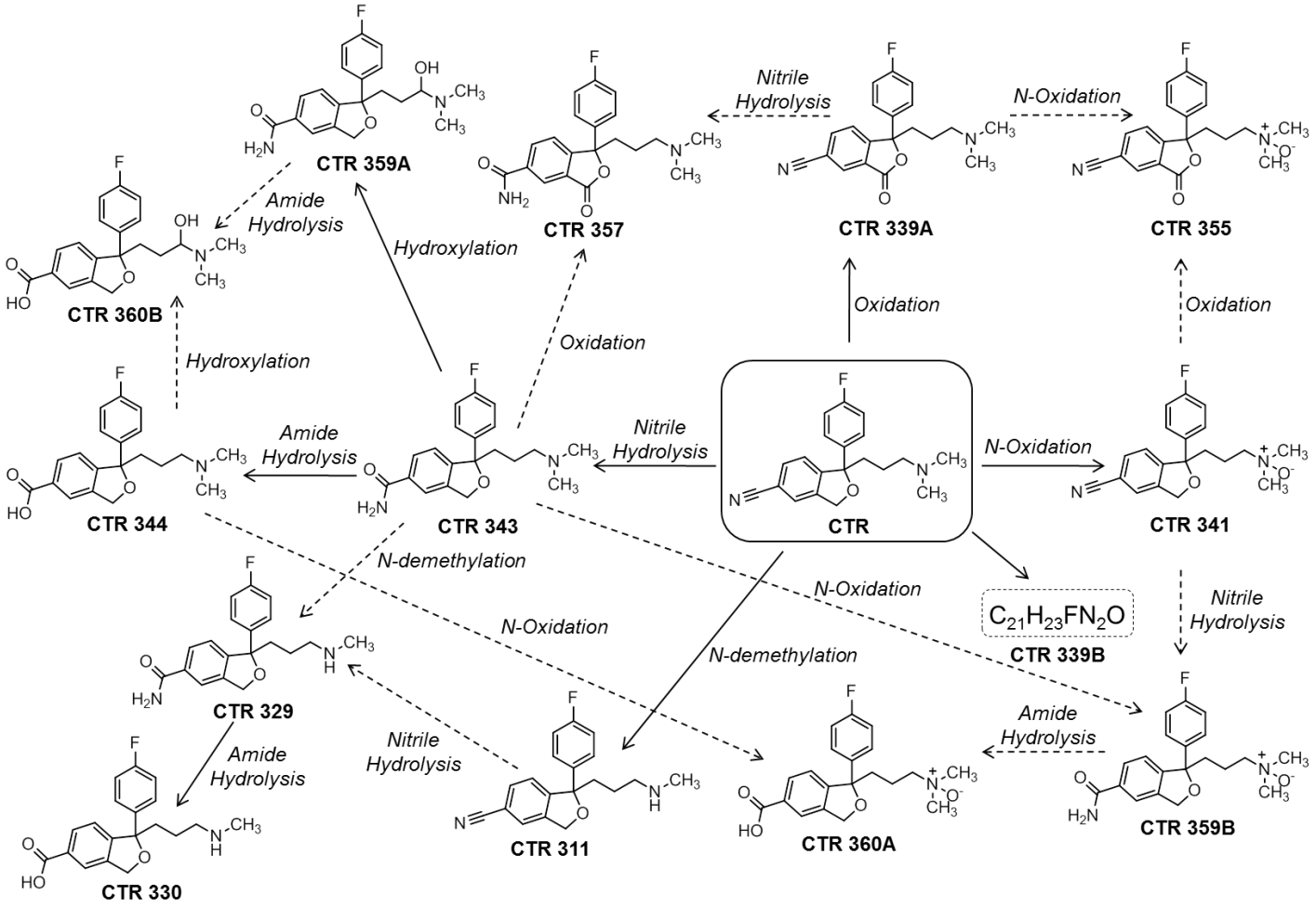

Figure 42: Proposed biotransformation pathway of CTR. Dotted arrows indicate that a single TP can be formed from different reactions of different precursor TPs.

5.3 TPs of CTR in WWTP influent and effluent samples

Once the TPs are identified, their detection in environmental samples along with the parent compound can help to assess the degradation of CTR. To this aim, 1 influent wastewater and 1 effluent wastewater sample, previously analyzed by RPLC-QTOF-MS and used in different studies performed at our laboratory, were retrospectively re-examined without the need of additional injections of sample extracts.

Only N-desmethylCTR was found in influent wastewater, which might be explained by the fact that it is a human metabolite. No other TP was detected since still no treatment has been applied for contaminants' removal. However, several TPs were detected in effluent wastewater. The presence of TPs of CTR in WWTP samples can be attributed to a double contribution: the input from human excreted metabolites and the input of microorganism metabolism in WW, which are transforming CTR in known and unknown TPs.

Semi-quantitation of the identified TPs in wastewater samples collected on March 8, 2015 is presented in **Table 5**. Concentrations of the TPs are very rough estimates, based on the assumption that the parent compound and the TPs have the same ratio between peak area and concentration.

Table 5: Environmental concentrations (ng L^{-1}) of CTR and TPs in influent and effluent wastewater samples.

Compound	Influent Concentration	Effluent Concentration
CTR	1050	1010
CTR 311	223	328
CTR 339A	-	22.9
CTR 341	-	47.6
CTR 343	-	7.78
CTR 344	-	9.91

CHAPTER 6
Conclusions

The degradation of CTR in biotransformation batch experiments followed pseudo-first order kinetics with observed reaction constant of 0.04 h^{-1} and half-life, deduced from reaction constant, of 18.4 h. Control reactors with WWTP effluent or autoclaved sludge showed insignificant losses of the parent compound. Thus, decreasing concentration of CTR in active bioreactors, with elimination rate of 70% within 6 days, can be clearly associated with biotransformation.

Parallel to the biodegradation of CTR in activated sludge, fourteen TPs were formed. Thirteen out of them were detected with RP chromatographic system in positive ionization mode. One additional TP was detected with the use of the HILIC column, enabling the separation from its isomer, which could not be detected by RP analysis. Thus, HILIC proved to be an essential tool as a complementary approach to the established RP for the identification of TPs and, in particular, for separation of isomers. MS/MS spectra of the other TPs, acquired in both chromatographic systems, were identical.

Moreover, QTOF-MS served as a very powerful tool in the structure elucidation the TPs. The identification consisted of extracting the exact mass from the chromatogram, selecting peaks of sufficient intensity, checking the plausibility of the retention time, and interpreting mass spectra by the observed fragmentation pattern and literature data. Four TPs were confirmed by corresponding reference standards (N-desmethylCTR, CTR amide, CTR carboxylic acid and 3-oxo-CTR). A probable structure based on diagnostic evidence was proposed for the additional nine TPs, whereas only an unequivocal molecular formula was assigned to the last one.

Suspect screening with *in silico* prediction tools established not a limited prediction space of plausible TPs based on metabolic logic while the non-target screening method was used to extract all compound masses that formed during the biodegradation experiment under defined constraints. These independent and complementary screening approaches provided a more

comprehensive identification of TPs formed within specific biotransformation systems and allowed structure-based interpretation of the results for identification of preferences in biotransformation pathways.

The presence of five TPs in the WWTP effluent, detected through retrospective suspect screening, denotes that monitoring of CTR is not enough to investigate the impact of this widely consumed pharmaceutical in the aquatic ecosystem. Up to our knowledge, there is no reported literature about biotransformation of CTR and identification of its TPs and as a result most of them have never been investigated in water samples.

To conclude, the results obtained in the present work illustrate the importance of investigating TPs in order to have a realistic overview of CTR effect on the aquatic environment. Reference standards would be required to unequivocally confirm the identity of these compounds, and to develop analytical methodologies able to accurately quantify their concentration levels in waters.

ABBREVIATIONS AND ACRONYMS

Table 6: Abbreviations and acronyms

ACN	Acetonitrile
AOPs	Advanced Oxidation Processes
bbCID	broadband Collision-Induced Dissociation
CAS	Conventional Activated Sludge
CE	Capillary Electrophoresis
CTR	Citalopram
Eawag-BBD PPS	Eawag Biocatalysis/Biodegradation Database Pathway Prediction System
EDCs	Endocrine Disrupting Compounds
ELAN	ELiminación Autótrofa de Nitrógeno
EP	Emerging Pollutant
EC	Emerging Contaminant
ESI	ElectroSpray Ionization
FT-ICR	Fourier Transform-Ion Cyclotron Resonance
GC	Gas Chromatography
GC-MS	Gas Chromatography coupled to Mass Spectrometry
GFF(s)	Glass Fiber Filter(s)
HDPE	High-Density PolyEthylene
HF-LPME	Hollow-Fiber Liquid-Phase Micro-Extraction
HILIC	Hydrophilic Interaction LIquid Chromatography
HPLC	High-Performance Liquid Chromatography
HR-MS	High Resolution Mass Spectrometry
HRT	Hydraulic Retention Time

LC	Liquid Chromatography
LC-HRMS	Liquid Chromatography coupled to High Resolution Mass Spectrometry
LC-QqQ MS/MS	Liquid Chromatography coupled with triple-Quadrupole Mass Spectrometry
LC-MS/MS	Liquid Chromatography tandem Mass Spectrometry
LC-QTOF-MS	Liquid Chromatography–Quadrupole-Time-Of-Flight-Mass Spectrometry
LLE	Liquid-Liquid Extraction
MBRs	Membrane BioReactors
MBBRs	Moving Bed Biological Reactors
MeOH	Methanol
NKUA	National and Kapodistrian University of Athens
PCPs	Personal-Care Products
PFCs	PerFluorinated Compounds
QTrap	triple Quadrupole-linear ion Trap mass spectrometer
RC	Regenerated Cellulose
RP	Reversed Phase
RPLC-QTOF-MS	Reversed Phase Liquid Chromatography-Quadrupole-Time-Of-Flight Mass Spectrometry
SPE	Solid-Phase Extraction
SPME	Solid-Phase Micro-Extraction
SRM	Selected Reaction Monitoring
SRT	Sludge Retention Time
SSRI(s)	Selective Serotonin Re-uptake Inhibitor(s)
TOF	Time-Of-Flight
TP	Transformation Product

TSS	Total Suspended Solids
UHPLC	UltraHigh-Performance Liquid Chromatography
UM-BBD PPS	University of Minnesota Biocatalysis/Biodegradation Database Pathway Prediction System
WWTP	WasteWater Treatment Plant
XIC	eXtracted Ion Chromatogram

REFERENCES

[1] N. Mastroianni, M. López de Alda, and D. Barceló, Emerging organic contaminants in aquatic environments: state-of-the-art and recent scientific contributions, *Contributions to Science,* vol. 6, 2010, pp. 193-97.

[2] A. J. M. Horvat, M. Petrović, S. Babić, D. M. Pavlović, D. Ašperger, S. Pelko, A. D. Mance, and M. Kaštelan-Macan*,* Analysis, occurrence and fate of anthelmintics and their transformation products in the environment, *Trends in Analytical Chemistry,* vol. 31, 2012, pp. 61-84.

[3] M. l. Farré, S. Pérez, L. Kantiani, and D. Barceló, Fate and toxicity of emerging pollutants, their metabolites and transformation products in the aquatic environment, *Trends in Analytical Chemistry,* vol. 27, 2008, pp. 991-1007.

[4] M. l. Farré, L. Kantiani, M. Petrović, S. Pérez, and D. Barceló, Achievements and future trends in the analysis of emerging organic contaminants in environmental samples by mass spectrometry and bioanalytical techniques, *Journal of Chromatography A,* vol. 1259, 2012, pp. 86-99.

[5] T. Kosjek, E. Heath, M. Petrović, and D. Barceló, Mass spectrometry for identifying pharmaceutical biotransformation products in the environment, *Trends in Analytical Chemistry,* vol. 26, 2007, pp. 1076-1085.

[6] D. Barceló, Pharmaceutical-residue analysis, *Trends in Analytical Chemistry,* vol. 26, 2007, pp. 454-455.

[7] K. Kümmerer, *Pharmaceuticals in the Environment: Sources, Fate, Effects and Risks*, 3rd ed. Heidelberg, Berlin, Germany: Springer Verlag, 2008.

[8] S. Pérez and D. Barceló, Application of advanced MS techniques to analysis and identification of human and microbial metabolites of

pharmaceuticals in the aquatic environment, *Trends in Analytical Chemistry,* vol. 26, 2007, pp. 494-514.

[9] A. Barra Caracciolo, E. Topp, and P. Grenni, Pharmaceuticals in the environment: biodegradation and effects on natural microbial communities. A review, *Journal of Pharmaceutical and Biomedical Analysis,* vol. 106, 2015, pp. 25-36.

[10] D. Fatta-Kassinos, M. I. Vasquez, and K. Kümmerer, Transformation products of pharmaceuticals in surface waters and wastewater formed during photolysis and advanced oxidation processes-degradation, elucidation of byproducts and assessment of their biological potency, *Chemosphere,* vol. 85, 2011, pp. 693-709.

[11] L. Tong, P. Eichhorn, S. Pérez, Y. Wang, and D. Barceló, Photodegradation of azithromycin in various aqueous systems under simulated and natural solar radiation: kinetics and identification of photoproducts, *Chemosphere,* vol. 83, 2011, pp. 340-8.

[12] T. Kosjek and E. Heath, Tools for evaluating selective serotonin re-uptake inhibitor residues as environmental contaminants, *Trends in Analytical Chemistry,* vol. 29, 2010, pp. 832-847.

[13] B. I. Escher and K. Fenner, Recent advances in environmental risk assessment of transformation products, *Environmental Science & Technology,* vol. 45, 2011, pp. 3835-47.

[14] D. Löffler, J. Römbke, M. Meller, and T. A. Ternes, Environmental Fate of Pharmaceuticals in Water/Sediment Systems, *Environmental Science & Technology,* vol. 39, 2005, pp. 5209-5218.

[15] X. S. Miao, J. J. Yang, and C. D. Metcalfe, Carbamazepine and its metabolites in wastewaster and in biosolids in a municipal wastewater treatment plant, *Environmental Science & Technology,* vol. 39, 2005, pp. 7469-7475.

[16] M. Petrović, S. Pérez, and D. Barceló, *Analysis, Removal, Effects and Risk of Pharmaceuticals in the Water Cycle Occurrence and Transformation in the Environment* vol. 62: Elsevier, 2013.

[17] R. Gulde, D. E. Helbling, A. Scheidegger, and K. Fenner, pH-dependent biotransformation of ionizable organic micropollutants in activated sludge, *Environmental Science & Technology,* vol. 48, 2014, pp. 13760-8.

[18] S. Suarez, R. Reif, J. M. Lema, and F. Omil, Mass balance of pharmaceutical and personal care products in a pilot-scale single-sludge system: influence of T, SRT and recirculation ratio, *Chemosphere,* vol. 89, 2012, pp. 164-71.

[19] A. A. Bletsou, J. Jeon, J. Hollender, E. Archontaki, and N. S. Thomaidis, Targeted and non-targeted liquid chromatography-mass spectrometric workflows for identification of transformation products of emerging pollutants in the aquatic environment, *Trends in Analytical Chemistry,* vol. 66, 2015, pp. 32-44.

[20] *TOF-MS within Food and Environmental Analysis* vol. 58: Elsevier, 2012.

[21] Y. Picó and D. Barceló, Transformation products of emerging contaminants in the environment and high-resolution mass spectrometry: a new horizon, *Analytical and Bioanalytical Chemistry,* vol. 407, 2015, pp. 6257-73.

[22] C. Prasse, M. Wagner, R. Schulz, and T. A. Ternes, Biotransformation of the antiviral drugs acyclovir and penciclovir in activated sludge treatment, *Environmental Science & Technology,* vol. 45, 2011, pp. 2761-69.

[23] D. E. Helbling, J. Hollender, H.-P. E. Kohler, and K. Fenner, Structure-based interpretation of biotransformation pathways of amide-containing compounds in sludge-seeded bioreactors, *Environmental Science & Technology,* vol. 44, 2010, pp. 6628-35.

[24] S. Kern, K. Fenner, H. Singer, R. P. Schwarzenbach, and J. Hollender, Identification of transformation products of organic contaminants in natural waters by computer-aided prediction and high-resolution mass spectrometry, *Environmental Science & Technology,* vol. 43, 2009, pp. 7039-46.

[25] A. Wick, M. Wagner, and T. A. Ternes, Elucidation of the transformation pathway of the opium alkaloid codeine in biological wastewater treatment, *Environmental Science & Technology,* vol. 45, 2011, pp. 3374-85.

[26] R. Beel, C. Lutke Eversloh, and T. A. Ternes, Biotransformation of the UV-filter sulisobenzone: challenges for the identification of transformation products, *Environmental Science & Technology,* vol. 47, 2013, pp. 6819-28.

[27] A. Rubirola, M. Llorca, S. Rodriguez-Mozaz, N. Casas, I. Rodriguez-Roda, D. Barceló, and G. Buttiglieri*,* Characterization of metoprolol biodegradation and its transformation products generated in activated sludge batch experiments and in full scale WWTPs, *Water Research,* vol. 63, 2014, pp. 21-32.

[28] S. Huntscha, T. B. Hofstetter, E. L. Schymanski, S. Spahr, and J. Hollender, Biotransformation of benzotriazoles: insights from transformation product identification and compound-specific isotope analysis, *Environmental Science & Technology,* vol. 48, 2014, pp. 4435-43.

[29] T. Kosjek, N. Negreira, M. L. de Alda, and D. Barceló, Aerobic activated sludge transformation of methotrexate: identification of biotransformation products, *Chemosphere,* vol. 119, 2015, pp. S42-50.

[30] M. Mardal and M. R. Meyer, Studies on the microbial biotransformation of the novel psychoactive substance methylenedioxypyrovalerone (MDPV) in wastewater by means of liquid chromatography-high resolution mass spectrometry/mass spectrometry, *Science of the Total Environment,* vol. 493, 2014, pp. 588-95.

[31] S. Terzic, I. Senta, M. Matosic, and M. Ahel, Identification of biotransformation products of macrolide and fluoroquinolone antimicrobials in membrane bioreactor treatment by ultrahigh-performance liquid chromatography/quadrupole time-of-flight mass spectrometry, *Analytical and Bioanalytical Chemistry,* vol. 401, 2011, pp. 353-63.

[32] S. Mejia Avendano and J. Liu, Production of PFOS from aerobic soil biotransformation of two perfluoroalkyl sulfonamide derivatives, *Chemosphere,* vol. 119, 2015, pp. 1084-90.

[33] Z. Li, M. P. Maier, and M. Radke, Screening for pharmaceutical transformation products formed in river sediment by combining ultrahigh performance liquid chromatography/high resolution mass spectrometry with a rapid data-processing method, *Analytica Chimica Acta,* vol. 810, 2014, pp. 61-70.

[34] M. Radke and M. P. Maier, Lessons learned from water/sediment-testing of pharmaceuticals, *Water Research,* vol. 55, 2014, pp. 63-73.

[35] C. Boix, M. Ibanez, L. Bijlsma, J. V. Sancho, and F. Hernandez, Investigation of cannabis biomarkers and transformation products in waters by liquid chromatography coupled to time of flight and triple quadrupole mass spectrometry, *Chemosphere,* vol. 99, 2014, pp. 64-71.

[36] L. Bijlsma, C. Boix, W. M. Niessen, M. Ibanez, J. V. Sancho, and F. Hernandez, Investigation of degradation products of cocaine and benzoylecgonine in the aquatic environment, *Science of the Total Environment,* vol. 443, 2013, pp. 200-8.

[37] A. Muller, S. C. Weiss, J. Beisswenger, H. G. Leukhardt, W. Schulz, and W. Seitz, Identification of ozonation by-products of 4- and 5-methyl-1H-benzotriazole during the treatment of surface water to drinking water, *Water Res,* vol. 46, 2012, pp. 679-90.

[38] M. Hörsing, T. Kosjek, H. R. Andersen, E. Heath, and A. Ledin, Fate of citalopram during water treatment with O3, ClO2, UV and Fenton oxidation, *Chemosphere,* vol. 89, 2012, pp. 129-35.

[39] F. Hernandez, M. Ibanez, E. Gracia-Lor, and J. V. Sancho, Retrospective LC-QTOF-MS analysis searching for pharmaceutical metabolites in urban wastewater, *Journal of Separation Science,* vol. 34, 2011, pp. 3517-26.

[40] E. L. Schymanski, H. P. Singer, P. Longree, M. Loos, M. Ruff, M. A. Stravs, C. R. Vidal, and J. Hollender, Strategies to characterize polar

organic contamination in wastewater: exploring the capability of high resolution mass spectrometry, *Environmental Science & Technology,* vol. 48, 2014, pp. 1811-8.

[41] M. Gomez-Ramos Mdel, A. Perez-Parada, J. F. Garcia-Reyes, A. R. Fernandez-Alba, and A. Aguera, Use of an accurate-mass database for the systematic identification of transformation products of organic contaminants in wastewater effluents, *Journal of Chromatography A,* vol. 1218, 2011, pp. 8002-12.

[42] C. Moschet, A. Piazzoli, H. Singer, and J. Hollender, Alleviating the reference standard dilemma using a systematic exact mass suspect screening approach with liquid chromatography-high resolution mass spectrometry, *Analytical Chemistry,* vol. 85, 2013, pp. 10312-20.

[43] A. C. Chiaia-Hernandez, M. Krauss, and J. Hollender, Screening of lake sediments for emerging contaminants by liquid chromatography atmospheric pressure photoionization and electrospray ionization coupled to high resolution mass spectrometry, *Environmental Science & Technology,* vol. 47, 2013, pp. 976-86.

[44] M. Krauss, H. Singer, and J. Hollender, LC-high resolution MS in environmental analysis: from target screening to the identification of unknowns, *Analytical and Bioanalytical Chemistry,* vol. 397, 2010, pp. 943-51.

[45] H. P. Nguyen and K. A. Schug, The advantages of ESI-MS detection in conjunction with HILIC mode separations: Fundamentals and applications, *Journal of Separation Science,* vol. 31, 2008, pp. 1465-80.

[46] M. J. Gomez, M. M. Gomez-Ramos, O. Malato, M. Mezcua, and A. R. Fernandez-Alba, Rapid automated screening, identification and quantification of organic micro-contaminants and their main transformation products in wastewater and river waters using liquid chromatography-quadrupole-time-of-flight mass spectrometry with an accurate-mass database, *Journal of Chromatography A,* vol. 1217, 2010, pp. 7038-54.

[47] A. C. Hogenboom, J. A. van Leerdam, and P. de Voogt, Accurate mass screening and identification of emerging contaminants in environmental samples by liquid chromatography-hybrid linear ion trap Orbitrap mass spectrometry, *Journal of Chromatogr A,* vol. 1216, 2009, pp. 510-19.

[48] A. Aguera, M. J. Martinez Bueno, and A. R. Fernandez-Alba, New trends in the analytical determination of emerging contaminants and their transformation products in environmental waters, *Environmental Science and Pollution Research,* vol. 20, 2013, pp. 3496-515.

[49] E. L. Schymanski, J. Jeon, R. Gulde, K. Fenner, M. Ruff, H. P. Singer, and J. Hollender, Identifying small molecules via high resolution mass spectrometry: communicating confidence, *Environmental Science & Technology,* vol. 48, 2014, pp. 2097-8.

[50] E. L. Schymanski, H. P. Singer, J. Slobodnik, I. M. Ipolyi, P. Oswald, M. Krauss, T. Schulze, P. Haglund, T. Letzel, S. Grosse, N. S. Thomaidis, A. Bletsou, C. Zwiener, M. Ibáñez, T. Portolés, R. Boer, M. J. Reid, M. Onghena, U. Kunkel, W. Schulz, A. Guillon, N. Noyon, G. Leroy, P. Bados, S. Bogialli, P. Rostkowski, and J. Hollender, Non-target screening with high-resolution mass spectrometry: critical review using a collaborative trial on water analysis, *Analytical and Bioanalytical Chemistry,* vol. 407, 2015, pp. 6237-55.

[51] L. J. Silva, C. M. Lino, L. M. Meisel, and A. Pena, Selective serotonin re-uptake inhibitors (SSRIs) in the aquatic environment: an ecopharmacovigilance approach, *Science of the Total Environment,* vol. 437, 2012, pp. 185-95.

[52] E. N. Evgenidou, I. K. Konstantinou, and D. A. Lambropoulou, Occurrence and removal of transformation products of PPCPs and illicit drugs in wastewaters: a review, *Science of the Total Environment,* vol. 505, 2015, pp. 905-26.

[53] M. M. Schulz and E. T. Furlong, Trace analysis of antidepressant pharmaceuticals and their selected degrdates in aquatic matrixes by LC/ESI/MS/MS, *Analytical Chemistry,* vol. 80, 2008, pp. 1756-62.

[54] A. Lajeunesse, C. Gagnon, and S. Sauve, Determination of basic antidepressants and their N -desmethyl metabolites in raw sewage and wastewater using solid-phase extraction and liquid chromatography-tandem mass spectrometry, *Analytical Chemistry,* vol. 80, 2008, pp. 5325-33.

[55] V. Calisto and V. I. Esteves, Psychiatric pharmaceuticals in the environment, *Chemosphere,* vol. 77, 2009, pp. 1257-74.

[56] L. J. Silva, L. M. Meisel, C. M. Lino, and A. Pena, "Profiling serotonin reuptake inhibitors (SSRIs) in the environment: trends in analytical methodologies," *Critical Reviews in Analytical Cheistrym,* vol. 44, 2014, pp. 41-67.

[57] A. Lajeunesse, S. A. Smyth, K. Barclay, S. Sauve, and C. Gagnon, Distribution of antidepressant residues in wastewater and biosolids following different treatment processes by municipal wastewater treatment plants in Canada, *Water Research,* vol. 46, 2012, pp. 5600-12.

[58] V. L. Borova, N. C. Maragou, P. Gago-Ferrero, C. Pistos, and N. S. Thomaidis, Highly sensitive determination of 68 psychoactive pharmaceuticals, illicit drugs, and related human metabolites in wastewater by liquid chromatography-tandem mass spectrometry, *Analytical and Bioanalytical Chemistry,* vol. 406, 2014, pp. 4273-85.

[59] B. Subedi, S. Lee, H. B. Moon, and K. Kannan, Psychoactive pharmaceuticals in sludge and their emission from wastewater treatment facilities in Korea, *Environmental Science & Technology,* vol. 47, 2013, pp. 13321-29.

[60] J. Giebultowicz and G. Nalecz-Jawecki, "Occurrence of antidepressant residues in the sewage-impacted Vistula and Utrata rivers and in tap water in Warsaw (Poland)," *Ecotoxicology and Environmental Safety,* vol. 104, 2014, pp. 103-9.

[61] L. J. Silva, A. M. Pereira, L. M. Meisel, C. M. Lino, and A. Pena, A one-year follow-up analysis of antidepressants in Portuguese wastewaters:

occurrence and fate, seasonal influence, and risk assessment, *Science of the Total Environment,* vol. 490, 2014, pp. 279-87.

[62] M. M. Schulz, E. T. Furlong, D. W. Kolpin, H. L. Schoenfuss, L. B. Barber, V. S. Blazer, D. O. Norris, and A. M. Vajda, Antidepressant pharmaceuticals in two U.S. effluent-impacted streams: occurrence and fate in water and sediment, and selective uptake in fish neural tissue, *Environmental Science & Technology,* vol. 44, 2010, pp. 1918-25.

[63] B. Subedi and K. Kannan, Occurrence and fate of select psychoactive pharmaceuticals and antihypertensives in two wastewater treatment plants in New York State, USA, *Science of the Total Environment,* vol. 514, 2015, pp. 273-80.

[64] T. Vasskog, U. Berger, P. J. Samuelsen, R. Kallenborn, and E. Jensen, Selective serotonin reuptake inhibitors in sewage influents and effluents from Tromso, Norway, *Journal of Chromatography A,* vol. 1115, 2006, pp. 187-95.

[65] J. Pablo Lamas, C. Salgado-Petinal, C. García-Jares, M. Llompart, R. Cela, and M. Gómez, Solid-phase microextraction–gas chromatography–mass spectrometry for the analysis of selective serotonin reuptake inhibitors in environmental water, *Journal of Chromatography A,* vol. 1046, 2004, pp. 241-247.

[66] T. Vasskog, T. Anderssen, S. Pedersen-Bjergaard, R. Kallenborn, and E. Jensen, "Occurrence of selective serotonin reuptake inhibitors in sewage and receiving waters at Spitsbergen and in Norway, *Journal of Chromatography A,* vol. 1185, 2008, pp. 194-205.

[67] S. González Alonso, M. Catalá, R. R. Maroto, J. L. R. Gil, Á. G. de Miguel, and Y. Valcárcel, Pollution by psychoactive pharmaceuticals in the Rivers of Madrid metropolitan area (Spain), *Environment International,* vol. 36, 2010, pp. 195-201.

[68] J. H. Writer, I. Ferrer, L. B. Barber, and E. M. Thurman, Widespread occurrence of neuro-active pharmaceuticals and metabolites in 24 Minnesota rivers and wastewaters, *Science of the Total Environment,* vol. 461-462, 2013, pp. 519-27.

[69] S. L. MacLeod, P. Sudhir, and C. S. Wong, Stereoisomer analysis of wastewater-derived beta-blockers, selective serotonin re-uptake inhibitors, and salbutamol by high-performance liquid chromatography-tandem mass spectrometry, *Journal of Chromatography A,* vol. 1170, 2007, pp. 23-33.

[70] C. D. Metcalfe, S. Chu, C. Judt, H. Li, K. D. Oakes, M. R. Servos, and D. M. Andrews, Antidepressants and their metabolites in municipal wastewater, and downstream exposure in an urban watershed, *Environmental Toxicology and Chemistry,* vol. 29, 2010, pp. 79-89.

[71] M. P. Schlusener, P. Hardenbicker, E. Nilson, M. Schulz, C. Viergutz, and T. A. Ternes, Occurrence of venlafaxine, other antidepressants and selected metabolites in the Rhine catchment in the face of climate change, *Environmental Pollution,* vol. 196, 2015, pp. 247-56.

[72] M. Gros, S. Rodriguez-Mozaz, and D. Barceló, Fast and comprehensive multi-residue analysis of a broad range of human and veterinary pharmaceuticals and some of their metabolites in surface and treated waters by ultra-high-performance liquid chromatography coupled to quadrupole-linear ion trap tandem mass spectrometry, *Journal of Chromatography A,* vol. 1248, 2012, pp. 104-21.

[73] S. E. Evans and B. Kasprzyk-Hordern, Applications of chiral chromatography coupled with mass spectrometry in the analysis of chiral pharmaceuticals in the environment, *Trends in Environmental Analytical Chemistry,* vol. 1, 2014, pp. e34-e51.

[74] M. Himmelsbach, W. Buchberger, and C. W. Klampfl, Determination of antidepressants in surface and waste water samples by capillary electrophoresis with electrospray ionization mass spectrometric detection after preconcentration using off-line solid-phase extraction, *Electrophoresis,* vol. 27, 2006, pp. 1220-26.

[75] A. Lajeunesse, M. Blais, B. Barbeau, S. Sauvé, and C. Gagnon, Ozone oxidation of antidepressants in wastewater–Treatment evaluation and characterization of new by-products by LC-QToFMS, *Chemistry Central Journal,* vol. 7, 2013, pp. 1-11.

[76] S. Yuan, X. Jiang, X. Xia, H. Zhang, and S. Zheng, Detection, occurrence and fate of 22 psychiatric pharmaceuticals in psychiatric hospital and municipal wastewater treatment plants in Beijing, China, *Chemosphere,* vol. 90, 2013, pp. 2520-5.

[77] O. Golovko, V. Kumar, G. Fedorova, T. Randak, and R. Grabic, Seasonal changes in antibiotics, antidepressants/psychiatric drugs, antihistamines and lipid regulators in a wastewater treatment plant, *Chemosphere,* vol. 111, 2014, pp. 418-26.

[78] J. Fick, H. Soderstrom, R. Lindberg, C. Phan, M. Tysklind, and D. G. Joakim Larsson, Contamination of surface, ground, and drinking water from pharmaceutical production, *Environmental Toxicology and Chemistry,* vol. 28, 2009, pp. 2522-27.

[79] T. Mackulak, M. Mosny, J. Skubak, R. Grabic, and L. Birosova, Fate of psychoactive compounds in wastewater treatment plant and the possibility of their degradation using aquatic plants, *Environmental Toxicology and Pharmacology,* vol. 39, 2015, pp. 969-73.

[80] I. Ferrer and E. M. Thurman, Analysis of 100 pharmaceuticals and their degradates in water samples by liquid chromatography/quadrupole time-of-flight mass spectrometry, *Journal of Chromatography A,* vol. 1259, 2012, pp. 148-57.

[81] J.-W. Kwon and K. L. Armbrust, Degradation of citalopram by simulated sunlight, *Environmental Toxicology and Chemistry,* vol. 24, 2005, pp. 1618-23.

[82] T. Vasskog, O. Bergersen, T. Anderssen, E. Jensen, and T. Eggen, "Depletion of selective serotonin reuptake inhibitors during sewage sludge composting," *Waste Management,* vol. 29, 2009, pp. 2808-15.

[83] S. Suarez, J. M. Lema, and F. Omil, Removal of pharmaceutical and personal care products (PPCPs) under nitrifying and denitrifying conditions, *Water Research,* vol. 44, 2010, pp. 3214-24.

[84] T. Alvarino, S. Suarez, E. Katsou, J. Vazquez-Padin, J. M. Lema, and F. Omil, Removal of PPCPs from the sludge supernatant in a one stage

nitritation/anammox process, *Water Research,* vol. 68, 2015, pp. 701-09.

[85] O. Bergersen, K. O. Hanssen, and T. Vasskog, Anaerobic treatment of sewage sludge containing selective serotonin reuptake inhibitors, *Bioresource Technology,* vol. 117, 2012, pp. 325-32.

[86] M. Hörsing, A. Ledin, R. Grabic, J. Fick, M. Tysklind, J. la Cour Jansen, and H. Andersen, Determination of sorption of seventy-five pharmaceuticals in sewage sludge, *Water Research,* vol. 45, 2011, pp. 4470-82.

[87] R. Rosal, A. Rodríguez, J. A. Perdigón-Melón, A. Petre, E. García-Calvo, M. J. Gómez, A. Agüera, and A. R. Fernández-Alba, Occurrence of emerging pollutants in urban wastewater and their removal through biological treatment followed by ozonation, *Water Research,* vol. 44, 2010, pp. 578-88.

[88] M. E. Casas, R. K. Chhetri, G. Ooi, K. M. Hansen, K. Litty, M. Christensson, C. Kragelund, H. Andersen, and K. Bester, Biodegradation of pharmaceuticals in hospital wastewater by staged Moving Bed Biofilm Reactors (MBBR), *Water Research,* vol. 83, 2015, pp. 293-302.

[89] L. J. Silva, A. M. Pereira, L. M. Meisel, C. M. Lino, and A. Pena, Reviewing the serotonin reuptake inhibitors (SSRIs) footprint in the aquatic biota: uptake, bioaccumulation and ecotoxicology, *Environmental Pollution,* vol. 197, 2015, pp. 127-43.

[90] J. Gelsleichter and N. J. Szabo, Uptake of human pharmaceuticals in bull sharks (*Carcharhinus leucas*) inhabiting a wastewater-impacted river, *Science of the Total Environment,* vol. 456-457, 2013, pp. 196-201.

[91] D. Alvarez-Munoz, B. Huerta, M. Fernandez-Tejedor, S. Rodríguez-Mozaz, and D. Barceló, Multi-residue method for the analysis of pharmaceuticals and some of their metabolites in bivalves, *Talanta,* vol. 136, 2015, pp. 174-82.

[92] A. Holmberg, J. Fogel, E. Albertsson, J. Fick, J. N. Brown, N. Paxéus, L. Förlin, J. I. Johnsson, and D. G. Joakim Larsson, Does waterborne citalopram affect the aggressive and sexual behaviour of rainbow trout and guppy?, *Journal of Hazardous Materials,* vol. 187, 2011, pp. 596-99.

[93] M. Christensen, S. Faaborg-Andersen, F. Ingerslev, and A. Baun, Mixture and single-substance toxicity of selective serotonin reuptake inhibitors toward algae and crustaceans, *Environmental Toxicology and Chemistry,* vol. 26, 2007, pp. 85–91.

[94] L. S. Clesceri, A. E. Greenberg and A. D. Eaton, eds., Standard Methods for the Examination of Water and Wastewater, 20th edition, *American Public Health Association/American Water Works Association/Water Environment Federation,* Washington, DC, 1998.

[95] S. Kern, R. Baumgartner, D. E. Helbling, J. Hollender, H. Singer, M. J. Loos, R. P. Schwarzenbach, and K. Fenner, A tiered procedure for assessing the formation of biotransformation products of pharmaceuticals and biocides during activated sludge treatment, *Journal of Environmental Monitoring,* vol. 12, 2010, pp. 2100-11.

[96] *https://test.eawag-bbd.ethz.ch/rxnmulti/* (accessed on August 20, 2015).

[97] B. Raman, B. A. Sharma, P. D. Ghugare, P. P. Karmuse, and A. Kumar, Semi-preparative isolation and structural elucidation of an impurity in citalopram by LC/MS/MS, *Journal of Pharmaceutical and Biomedical Analysis,* vol. 50, 2009, pp. 377-83.

[98] T. Jiang, Z. Rong, L. Peng, B. Chen, Y. Xie, C. Chen, *J. Sun*, Y. Xu, Y. Lu, and H. Chen, Simultaneous determination of citalopram and its metabolite in human plasma by LC-MS/MS applied to pharmacokinetic study, *Journal of Chromatography B,* vol. 878, 2010, pp. 615-19.